# STATE OF SEBASTIAN INLET REPORT: 2018

## An Assessment of Inlet Morphologic Processes, Shoreline Changes, Sediment Budget, and Beach Fill Performance

*by*

*Gary A. Zarillo, Irene M. Watts, Leaf Erickson, Kristen L. Hall, Sara Ramos*

**Department of Ocean Engineering**
**and**
**Marine Sciences**
**Florida Institute of Technology**
**150 University Blvd.**
**Melbourne, FL 32901**

July 11, 2018

**Executive Summary**

The annual update of the State of Sebastian Inlet includes five major areas of work; 1) an update of the analysis of volume contained in the sand reservoirs of the inlet system, 2) analysis of morphologic changes within the inlet system, 3) analysis of the sand budget based on the results of the sand volume analysis, 4) an update of the shoreline change analysis, and 5) numerical modeling analysis of hurricane impacts and infilling patterns of the sand trap. The volumetric analysis includes the major sand reservoirs within the immediate inlet system and sand volumes within the extended sand budget cells to the north and south of Sebastian Inlet. The volume analysis for each inlet sand reservoir extends from 2006 to 2018. Similar to the volumetric analysis described in previous state of the inlet reports, most inlet sand reservoirs are in a long-term dynamic equilibrium characterized by occasional large seasonal changes in volume superimposed on longer term trends of a lower order of magnitude. An examination of coastal sea level changes and sand volume between 2006 and 2018 revealed two important processes. First, the Sebastian Inlet sand reservoirs and the beach and shoreface areas to the north and to the south of the inlet undergo periods of regional sand volume losses and periods of sand volume gains. These gains and losses cover the entire region rather than being inversely linked to gains or losses in adjacent subsections. Examples are sand volume gains that peaked in 2010 and again in 2016. Periods of regional sand volume loss occurred in the years preceding the sand volume gains.

Secondly, from an examination of the sea level record measured at Sebastian Inlet over the 12-year period between 2006 and 2018, it can be demonstrated that periods of sand volume gains and decreasing cumulative sand volume losses, correspond to periods of falling sea level. Likewise, periods of rising sea level correspond to periods of increasing cumulative sand volume losses. Further, the sea level record for late 2017 and the first five months of 2018 indicates that another period of rising sea level is beginning. This indicates the potential for an upcoming period of increased loss of sand volume.

The dynamic equilibrium and trends of sand volume change within the inlet sand reservoirs associated with Sebastian Inlet are also reflected in sediment budget calculations. In this report, the sand budget for the Sebastian Inlet region is reported at three-time scales, including a longer time scale of 10 years, a time scale of 5 years, and a shorter time scale of 3 years. The most useful time scale is considered to be 10 years since it integrates over seasonal sand volume changes that masks shorter term trends. During the time period of 2000 to 2018, the benefits of sand by-passing from the sand trap and beach fill placement to the south of the inlet, can be shown to directly offset sand volume gains within the inlet. The impacts of rising and falling sea level are more apparent in the 5-year and 3-year sand budgets presented in this report.

Similar to the sand volume analysis, the results of shoreline mapping from survey data and aerial imagery vary considerably by time scale. Over the 10-year time scale from 2008 to 2017, shoreline changes south of the inlet reflect the position of beach fill placement in 2007, 2011, 2012 and 2014. These beach nourishment projects provided sections of advancing or stable shoreline. The influence of sand placement from the sand trap excavation during the spring of 2014, along with the benefits of a recent 2-year period of falling sea level can be seen in the shoreline accretion between 2013 and 2017 and in the comparison of the 2016-2017 shoreline positions.

The Sebastian Inlet Coastal Processes Model was applied to examine the impacts of the 2016 and 2017 hurricanes and sand trap infilling process. Model results are presented in a series of graphics and associated discussion. The model was applied to examine and evaluate the effect of Hurricanes Matthew and Irma on the inlet system. The movement and exchange of material between the sediment reservoirs during and after the storm are be examined, as well as the hydrodynamic conditions during the storm. Calculated channel infilling within the sand trap area is also presented. The model was run using the post 2014 dredge as an initial condition to examine the response of the system to the dredging event.

**Table of Contents**

**List of Figures**

List of Tables

## 1.0 Introduction and Previous Work

This report extends the analysis of the State of Sebastian Inlet from the publication of the 2016 report through the winter and spring months of 2018. In the original 2007 report, sand volume changes, sand budget, and morphological changes between 1989 and 2007 were examined (Zarillo et al. 2007). In addition, shoreline changes were documented between 1958 and 2007 using aerial images and between 1990 and 2007 using field survey data. In the 2013 report, much of the long-term analysis presented in the 2007 report was summarized in the main body of the text and re-stated in a series of appendices. This effort was to present a long-term analysis of inlet evolution and associated management strategies that have been applied over the years. The 2016 report emphasized the sand volume calculation within the sand reservoirs and sand budget cells of the Sebastian inlet area. At this time, the major sand budget cells and sand reservoirs were more or less stable in terms of longer-term trends outside of seasonal fluctuations. The 2016 state of the inlet analysis also presented a model-based evaluation of littoral transport rates.

In the present report, the morphological analysis, sand budget analysis and the shoreline analysis are updated to 2017. The movement and exchange of material between the sediment reservoirs during and after the storm are be examined as well as the hydrodynamic conditions during the storm. The Sebastian Inlet coastal processes model was applied to examine and evaluate the effect of Hurricane Matthew on the inlet system and the infilling process of the sand trap after dredging. Recommendations are made for applying the results of State of the Inlet Analysis to the ongoing Sebastian Inlet Management Plan.

## 2.0 Sand Volume Analysis and Sediment Budget

This section of the report provides an update of the sand budget around the inlet based on semiannual surveys of topography and changes in the sand volume contained in the various shoals associated with Sebastian Inlet. Much of the information in this report can be found in a series of annual “State of the Inlet” reports issued since 2007. The body and appendices of these reports provides detailed analyses of morphological and physical processes that control the dynamic equilibrium of the Sebastian Inlet system. In this section of the 2018 Inlet report details of sand volume and sediment budget exchanges around the inlet are provided to verify and update the Sebastian Inlet Sand Budget

The sandy shoals and veneers of sand within the Sebastian Inlet system are considered sand volume reservoirs that can gain, retain, and export sand throughout the system. A conceptual model of inlet sand reservoirs is given in a paper by Kraus and Zarillo, (2003). The concepts presented in this paper are the conceptual basis of littoral sand budgets in the vicinity of tidal inlets. Figure 1 shows the concepts of exchanges among tidal inlet sand reservoirs, including bypassing of sand across the inlet entrance to nourish adjoining shoreface and beaches. The visual concepts included in Figure 1 are the basis of terms used in sediment budget calculations (Rosati et al 1999).

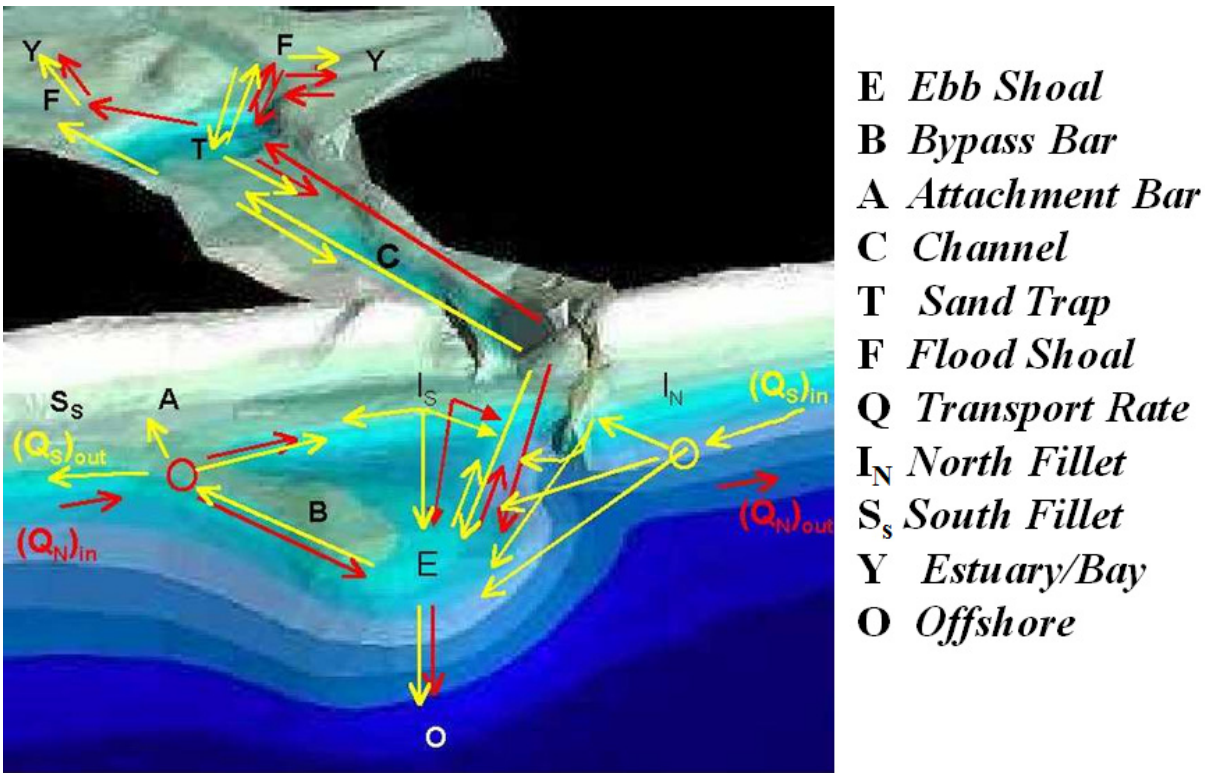


**Figure 1. Schematic vector diagram of sediment transport pathways among sand reservoirs at Sebastian Inlet (From Kraus and Zarillo, 2003).**

After a review of the sand volume changes within Sebastian Inlet shoals and sand budget cells over a 10-year period, the annualized sand budget in the inlet region is quantified. Sand budgets are presented as annualized terms but calculated over intermediate to longer term time periods. It will be noted in the summary and conclusions that the magnitude of the budget terms, including sand volume retained or exported by the inlet can change according to time scale

(Zarillo, 2010). Time scales of 5 years and longer, provide fewer variable terms and more consistency for management.

### 2.1 Sand Volume Analysis Methods

Certified hydrographic surveys of the inlet system and the surrounding shoreface and beaches have been conducted for the by Sebastian Inlet Tax District (SITD) since the summer of 1989. Table 1 lists the surveys completed in the past decade. Starting in winter 1991, surveys have been performed on a semiannual basis. Offshore elevation data are gathered by conventional boat/fathometer surveying methods from -4 ft. to -40 ft. in accordance with the Engineering Manual for Hydrographic Surveys (USACE, 1994).

Figure 2 shows the survey area including the entire inlet system (ebb shoal, throat, sand trap and flood shoal, etc.), and the adjacent barrier island system as well. The survey area extends approximately 30,000 ft. north (Brevard County) and 30,000 ft. south (Indian River County) of the inlet. Beach profiles taken about every 500 ft. Since 2011, survey methods have included multi-beam swath on the south side of the inlet entrance. The multibeam data provides high spatial resolution in areas where reef rock outcrops occur. The dredged channel extension between the inlet and the Intercoastal Waterway (ICW) to the west has been surveyed semi-annually since it was constructed in 2007.

This comprehensive dataset provides excellent support for volumetric calculations of inlet shoal and morphologic features, as well as for the analysis of changes in shoreline position through a “zero contour” extraction technique. Datasets used for this report are complete though the winter of 2018.

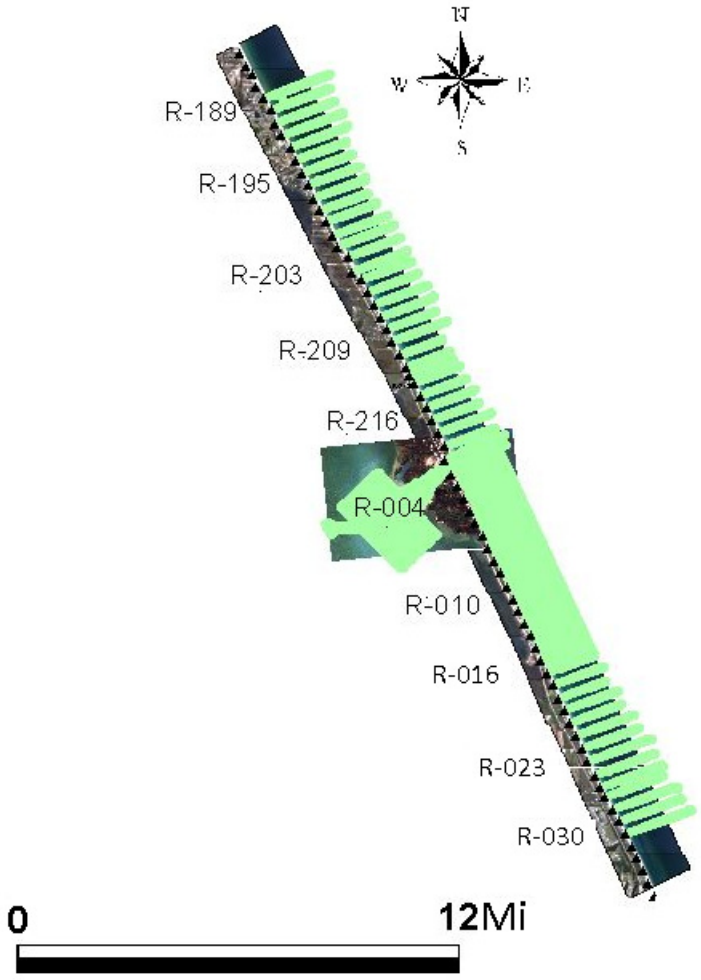


**Figure 2. Extent of hydrographic survey (2018 winter).**

**Table 1. Summary of Hydrographic Surveys (Source: Sebastian Inlet Tax District).**

| Survey Date | Ebb shoal | Channel | Sand trap | Channel Extension | Flood shoal | North beach (ft) | South beach (ft) |
|---|---|---|---|---|---|---|---|
| Jan-05 | x | x | x | | | 30,000 | 30,000 |
| Jul-05 | x | x | x | | | 30,000 | 30,000 |
| Jan-06 | x | x | x | | x | 30,000 | 30,000 |
| Jul-06 | x | x | x | | x | 30,000 | 30,000 |
| Jan-07 | x | x | x | | x | 30,000 | 30,000 |
| Jul-07 | x | x | x | | x | 30,000 | 30,000 |
| Jan-08 | x | x | x | | x | 30,000 | 20,000 |
| Jul-08 | x | x | x | x | x | 30,000 | 30,000 |
| Jan-09 | x | x | x | x | x | 30,000 | 30,000 |
| Jul-09 * | x | x | x | x | x | 30,000 | 30,000 |
| Jan-10 * | x | x | x | x | x | 30,000 | 30,000 |
| Jul-10 * | x | x | x | x | x | 30,000 | 30,000 |
| Jan-11 * | x | x | x | x | x | 30,000 | 30,000 |
| Jul-11 * | x | x | x | x | x | 30,000 | 30,000 |
| Jan-12 * | x | x | x | x | x | 30,000 | 30,000 |
| Jul-12 * | x | x | x | x | x | 30,000 | 30,000 |
| Jan-13 * | x | x | x | x | x | 30,000 | 30,000 |
| Jul-13 * | x | x | x | x | x | 30,000 | 30,000 |
| Jan-14 * | x | x | x | x | x | 30,000 | 30,000 |
| Jul-14 * | x | x | x | x | x | 30,000 | 30,000 |
| Jan-15 * | x | x | x | x | x | 30,000 | 30,000 |
| Jul-15* | x | x | x | x | x | 30,000 | 30,000 |
| Winter 2016* | x | x | x | x | x | 30,000 | 30,000 |
| Summer 2016* | x | x | x | x | x | 30,000 | 30,000 |
| winter 2017* | x | x | x | x | x | 30,000 | 30,000 |
| Summer 2017* | x | x | x | x | x | 30,000 | 30,000 |
| Winter 2018* | x | x | x | x | x | 30,000 | 30,000 |

* Multibeam data

Once each hydrographic survey is complete, volumetric data are added to the series of volume changes and volume changes from one survey to another are calculated. For consistent comparison from survey to survey, the Sebastian Inlet region is divided into subsections representing either a sand budget cell or sand reservoir. Figure 3 shows the sand budget cells used to calculate the changes in sediment volume associated with littoral transport rates over time. The N4 and N3 cells are north of the inlet entrance. N4 is bounded by FDEP R-Markers R189 and R195 in south Brevard County whereas the N3 sand budget cell is bounded between R195 and R203. The N2 and N 3 cells are placed between R203 and R-216. The inlet cell includes all of the sand reservoirs shown in Figure 4 and are bounded to the north by R-216 and to the south in Indian River County by R-4. On the south side of Sebastian Inlet sand budget cells are designated as S1, S2, S3 and S4. The S1 cell begins at R-4 and is bounded to the south by R-10 followed by the S2 cell bounded between R-10 and R16. Sand budget cell S3 extend from R-16 to R-23 followed by cell S4, which terminates at R30. All of the cells extend seaward to an approximate depth of -25 feet, NAVD88, which is considered beyond the depth of closure for changes in topography.

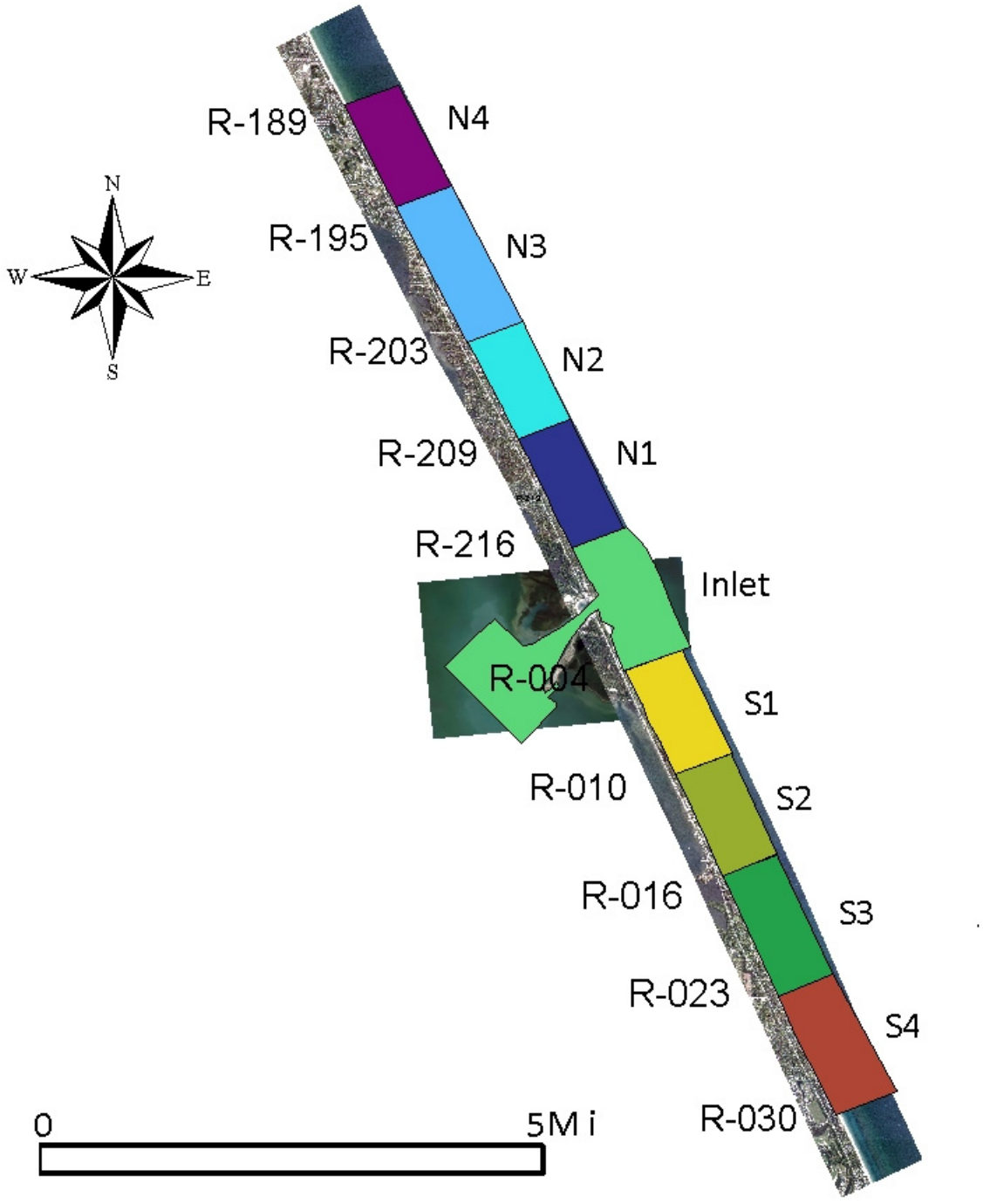


**Figure 3. Sand budget cells.**

Within the Inlet sand budget cell (Figure 3), further subdivisions are made to characterize sand reservoirs that exchange sand under the influence of strong tidal currents and waves. These subdivisions are shown and identified in Figure 4. Two of the sand reservoirs, the flood shoal and the ebb shoal are volumetrically large and control the magnitude of the topographic changes and sand bypassing within the Sebastian Inlet. The major reservoirs include the ebb shoal, flood shoal, and the sand trap. The sand trap, first excavated in 1962, re-established in 1972 and expanded in 2014 also influences the volume of the sand budget when it is periodically dredged. Other sand reservoirs contain lower sand volume relative to the ebb and flood shoal but may exert influence over sand transfer as exchange locations as shown in Figure 4. The attachment bar on the south side of the inlet serves this role.

The raw survey data in Easting, Northing, and elevations are imported into the ArcGIS software platform. Using 3D analysis and spatial analysis capabilities of GIS, the total volume of sediment in each cell or reservoir is calculated relative to a base elevation. These volumes are then compared between survey dates.

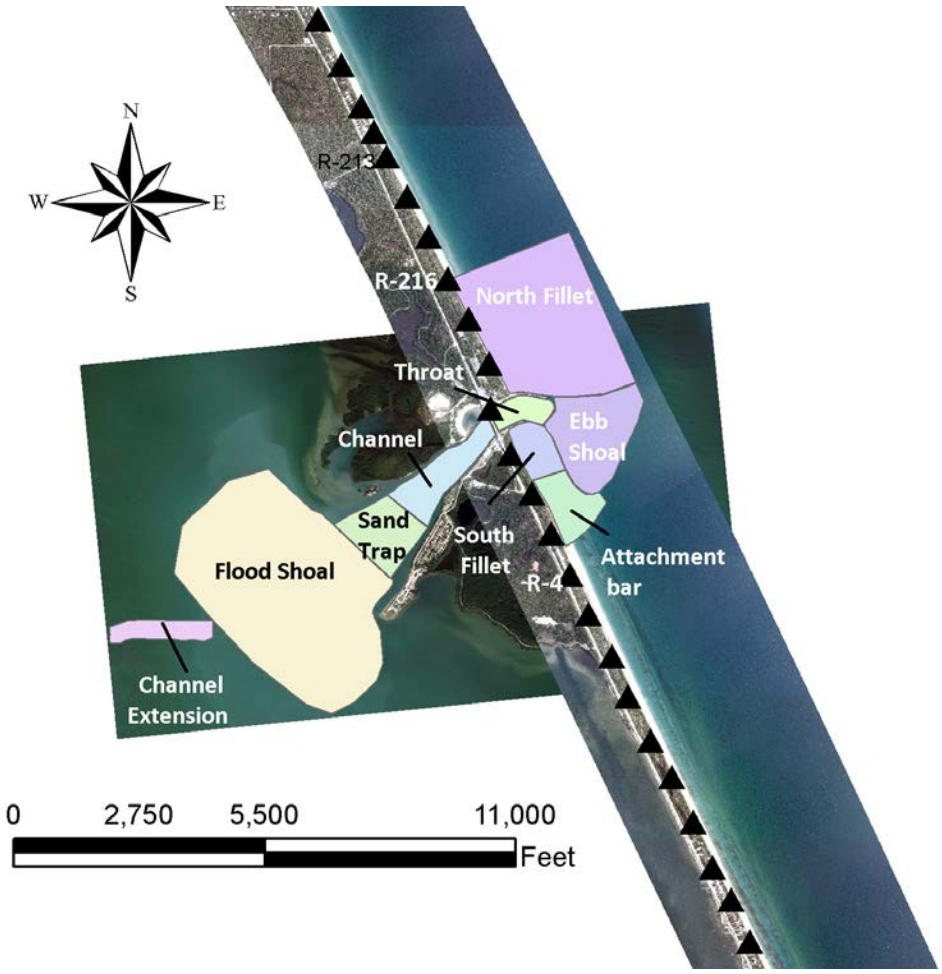


**Figure 4. Morphologic features forming the inlet sand reservoirs.**

## 3.0 Sand Reservoir Volume Analysis

The sand reservoirs are contained within the inlet sand budget cell (Figures 3 and 4). In order to fully understand the sand budget process, it is important to examine volume adjustments of each sand reservoir over time and in terms of variability and volume magnitude. Along with the sand reservoirs within the inlet, it is also useful to examine sand volume changes in sand budget cells contained within the barrier island system to the north and south of Sebastian Inlet. By considering the volume and variability of budget terms over shorter and longer time periods, the sand budget analysis can be more effectively applied to managing the regional sand resources. Thus, before presenting the sand budget for the Sebastian Inlet region, the volume evolution is reviewed for the major inlet sand reservoirs and for the cells within the sand budget calculation

Results presented in the volumetric analysis are divided into two subsections. Section 3.1 presents the volumetric evolution of the largest sand reservoirs within the inlet sand budget cell (Figure 4) with plots of net seasonal and cumulative volume change over time. Section 3.2 presents the volumetric evolution of the inlet littoral cells used for the sand budget computation. The calculated net seasonal volume changes ($\Delta V$) serve as inputs to the sand fluxes ($\Delta Q$) for the budget calculations discussed in Section 4. When reviewing the time series plots of volume changes in sand reservoirs and sand budget cells, the range of the vertical scale should be noted for each. Smaller sand bodies having less total volume have a much smaller range in volumetric changes compared to large sand bodies such as the flood shoal.

### 3.1 Individual Inlet Sand Reservoirs

The volumetric evolution of the ebb shoal from 2005 to 2018 is illustrated in Figure 5. Volume gains and losses that integrate over time to provide net volume change occur on short time scales that are usually on the order of 6 to 12 months. Volume gains or losses are most often followed by counter balancing volume losses or gains. For instance, 12 months of sand volume gains totaling about 89,000 cubic yards on the ebb shoal from July 2013 to July 2014 were followed by about a 50,000 cubic yard sand volume loss from July 2014 to winter 2015. This was followed by approximately 85,000 cubic yards of volume gain though the summer months

of 2016 (Figure 5). Little net change occurred from the summer of 2016 to the latest survey completed in March of 2018. Although seasonal and annual changes on the ebb shoal can reach and exceed 50,000 cubic yards it is important to recognize trends of volume change that occur over longer segments of time and can contribute to the overall sand budget of Sebastian Inlet. In Figure 3, a trend of increasing ebb shoal sand volume occurred over an approximate 5-year period between 2005 and 2010 that totaled about 150,000 cubic yards. This was followed by a 3-year period of stability between 2010 and 2013 that bounded a small net loss of 20,000 cubic yards of sand. Between the winter 2013 and winter 2018 survey the ebb shoal gained approximately 100,000 cubic yards. The total record for the ebb shoal shown in Figure 5 include about 227,000 cubic yards of volume increase. This along with volume changes in the flood shoal and sand excavations from the sand trap dominate the sand budget changes limited to the inlet. These interactions are discussed under Section 4 of the report.

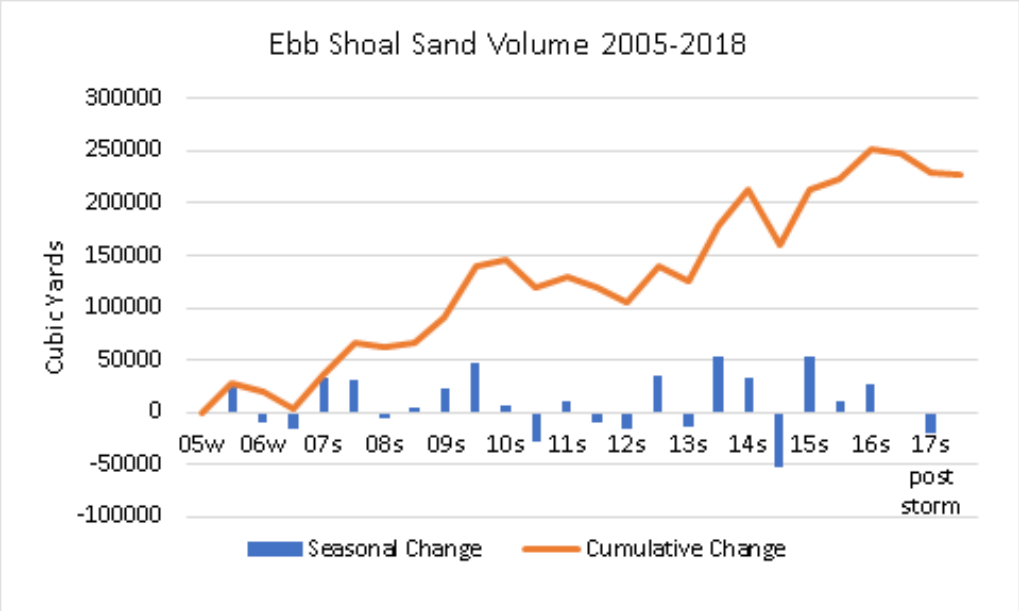


**Figure 5. Volumetric evolution of the ebb shoal from summer 2004 to summer 2015.**

The sand volume changes of the attachment bar are small due to its role as a sediment redistribution zone rather than an accumulation or storage zone (Zarillo et al., 1997). As seen in Figure 6, volume changes alternate between positive and negative on a seasonal basis. Increases in sand volume usually occur during the winter season of higher wave energy, whereas volume losses from the attachment bar usually occur during the summer season. It is likely that the

winter sand volume increases are due to sand bypassing around the inlet entrance by higher energy winter wave conditions. Losses in the summer months are likely due to the movement of sand further south or back to the inlet entrance during the lower energy conditions of the summer season and north directed littoral sand transport by wave energy from the southeast in the summer.

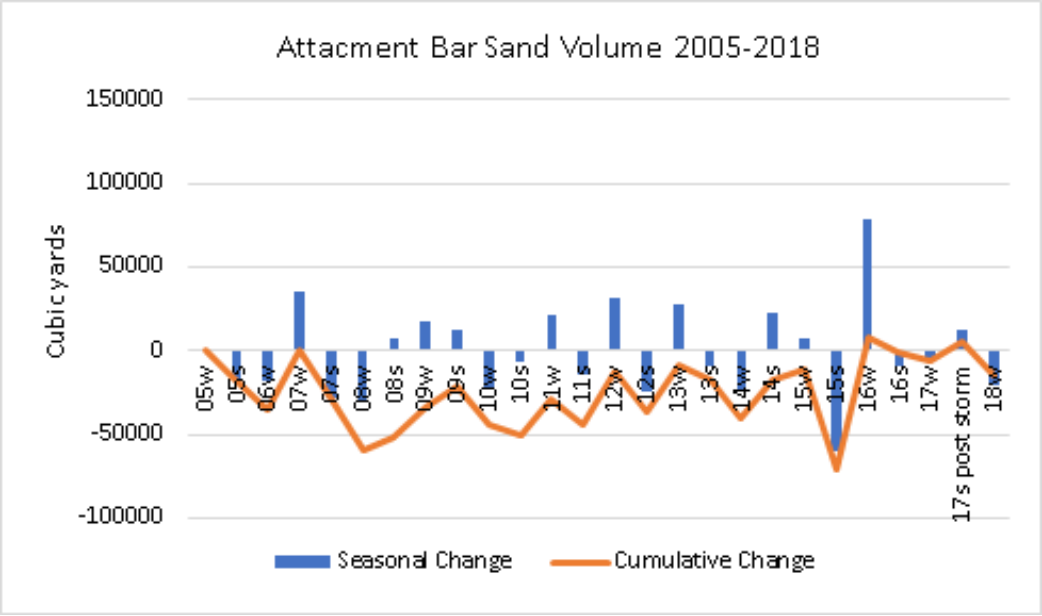


**Figure 6. Volumetric evolution of the attachment bar from summer 2004 to winter 2015.**

The volumetric evolution of the sand trap is presented in Figure 7. The trends and patterns of volume change are dominated by excavation from the sand trap in 2007, 2012 and 2014. Post dredge annual sand volume gains are on the order of 30,000 to 40,000 cubic yards averaging 15,000 to 20,000 cubic yards every 6 months. The pattern in Figure 6 shows that the highest rate of sand volume gains occurs in the first 6 months after dredging followed by smaller gains or small loss of volume thereafter until the next dredging cycle. The record from January, 2012 to July, 2014 clearly marks the recent dredging projects to bypass and expand the sand trap in 2014. The figure illustrates the mechanical bypassing of spring 2012 with the removal of

approximately 122,000 cubic yards of sand from the sand trap. In the winter to spring of 2014, approximately 160,000 cubic yards of material were removed as the trap was expanded. About 120,000 cubic yards of this material was placed to the south of Sebastian Inlet between R4 and R10. Since the 2014 sand trap expansion sand volume gains have totaled about 115,000 cubic yards. The gains include about 43,000 cubic yards in the first six months after dredging followed by smaller gains of less than about 6,000 cubic yards per year through the winter of 2016. Analysis of surveys in summer 2016 and winter 2017 indicate a total gain of about 37,000 cubic yards of sand. Sand volume gains in the second half of 2017 were minimal but followed by a gain of about 28,000 cubic yards by the winter survey of 2018.

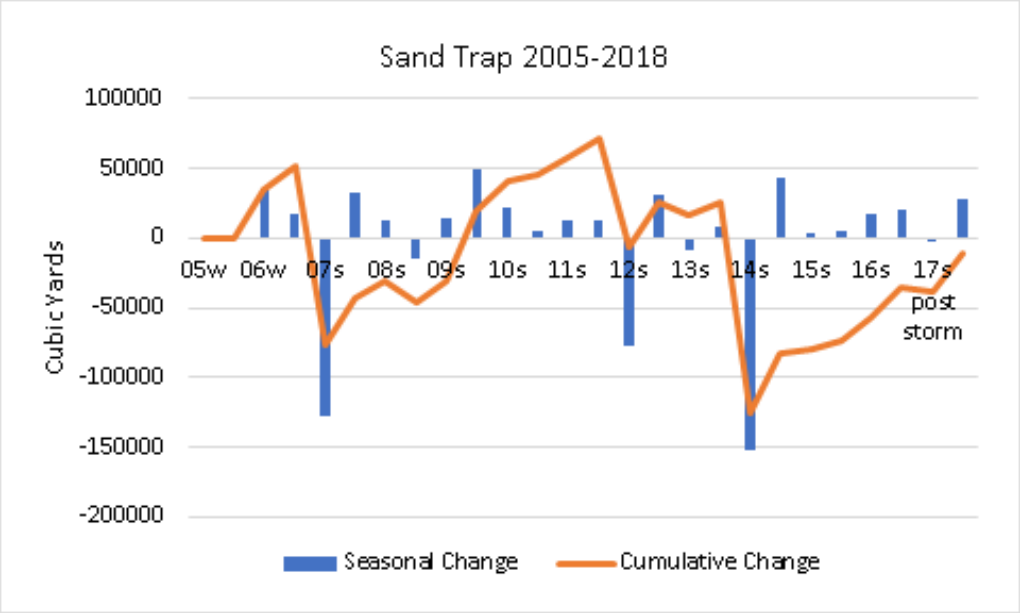


**Figure 7. Volumetric evolution of the sand trap from winter 2005 to winter 2018.**

Volumetric changes for the flood shoal (Figure 8)can be as more than 100,000 cubic yards on a seasonal basis. Temporary loss of sand volume from the flood shoal is associated with sand trap dredging, which temporarily limits the supply of sand reaching the shoal. The pattern of recovery can be seen after the sand trap excavation in 2007 when the flood shoal

recovered and increased its volume by summer of 2008. A period of continuing relatively large sand volume loss began in January, 2012 and continuing through 2014 when the sand trap was expanded. After expansion of the sand trap in 2014, the flood shoal entered a period of recovery and expansion, which is now complete as seen in Figure 8. Net volume change of the flood shoal in the 13-year period since 2006 is an approximate a gain of 35,000 cubic yards, although intra-annual sand volume fluctuations of more than 200,000 cubic yards can occur.

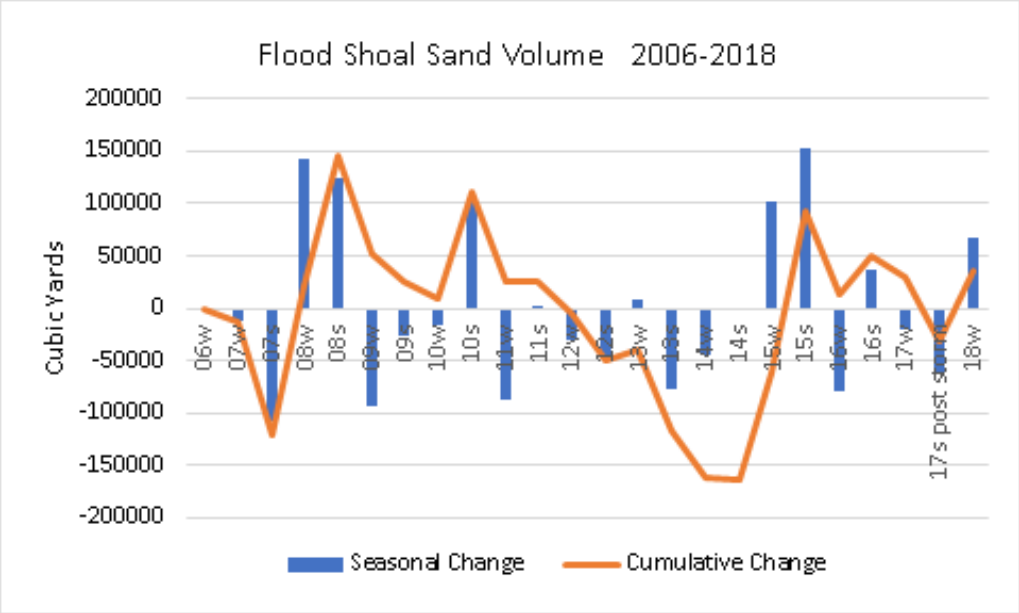


**Figure 8. Volumetric evolution of the flood shoal from winter 2006 to winter 2018.**

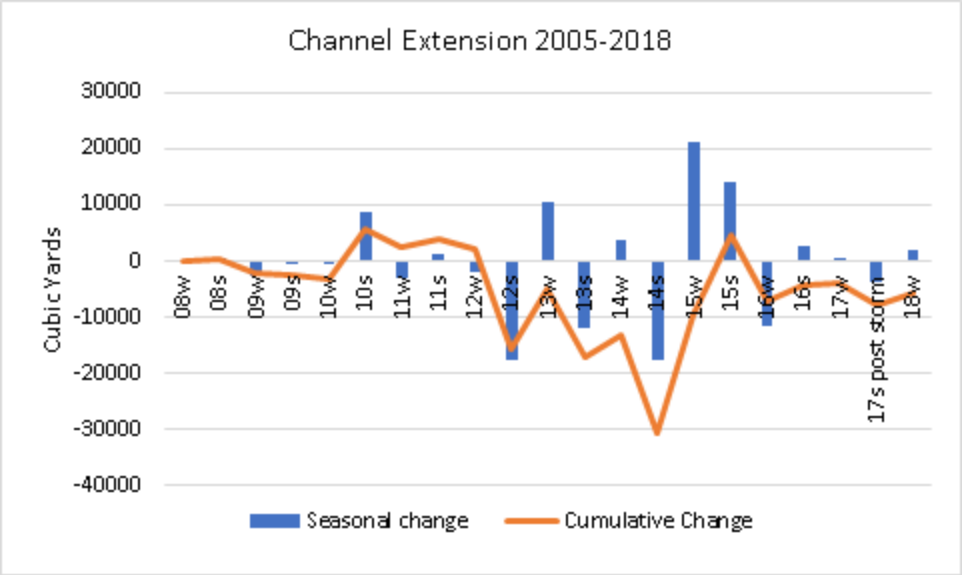


**Figure 9. Volumetric evolution of the channel from winter 2008 to winter 2018.**

### 3.2 Sand Budget Cells

The sediment budget calculations discussed in this report depend on the analysis of individual sand budget cells. The sand budget computational cells are shown in Figure 3. The inlet sand budget cell encompassing the nearshore zone from R216 in Brevard County to R4 in Indian River County, includes the ebb shoal, flood shoal, attachment bar and all other reservoirs shown in Figure 4. Annualized volume changes ($\Delta V$) for each cell, calculated over different time periods, were added to the sand budget equation to calculate the annual net littoral sand transport in and out of each cell. Annualized placement and removal volume data are also included to account for dredging/mechanical bypassing and beach fill activities in the cells concerned. Time series of volumetric change since 2006 for the eight littoral sand budget cells shown in Figure 4 are shown in Figure 10 through Figure 18, ranging from the northernmost to the southernmost distal cells.

Volume changes for the N4 cell, the section between R189 and R195, are presented in Figure 10. Results indicate small net change in volume from 2006 to 2018. However, large fluctuations in sand volume have occurred on a seasonal basis and sometimes exceed 200,000 cubic yards of either gains or loses. Particularly large variations occurred 2007 to 2008 and then again in the 2016-2017 period. Recent gains of sand volume from the summer of 2016 to the

post storm period of 2017 recovered about 400,000 cubic yards and have offset accumulated losses since the winter of 2016.

Volume changes in the N2 cell, (R195 - R203,Figure 3), are presented in Figure 11. Similar to the N2 cell, large volume changes in N2 are usually seasonal; characterized by gains in the winter months and volume losses in the summer months. This cycle is related to the stronger south directed littoral drift under winter conditions sending more sand into the N4 and N2 cells from the beach and shoreface to the north in Brevard County. Over the course of eleven years the sand volume in this budget cell accumulated by as much as 400,000 cubic yards in a season and then returned to lower volumes over the 6 to 18 months period. The total volume buildup in this sand budget cell in 2017 may be attributed to increased south directed littoral transport in the winter months and then again due to Hurricane Irma that sent large waves towards the Florida coast as it passed by offshore. The net sand volume change of the 2006 to 2018 period is a loss of about 200,000 cubic yards of sand. The volume changes found in the N2 sand budget cell (Figure 12) are similar in magnitude and pattern to those recorded in the N3 cell. Large volume changes occurred seasonally during the winter months followed by balancing volume losses over one or more seasons. The 12-year net volume change in N2 was about 85,000 cubic yards. Net sand volume change in the N1 Cell (R209-R216) followed the pattern of the N3 and N3 cell with the exception of large sand volume gain of about 250,000 cubic yards recorded in the summer 2016 survey. The N4, N3, and N2 budget cells were characterized by sand volume losses of 100,000 to more than 250,000 cubic yards during this period, which possibly result in accumulation in the N1 cell down the net littoral drift pathway. The 2016 sand volume gains in N1 were then largely erased by losses that occurred in the post-Irma period of late 2017 and the winter of 2018.

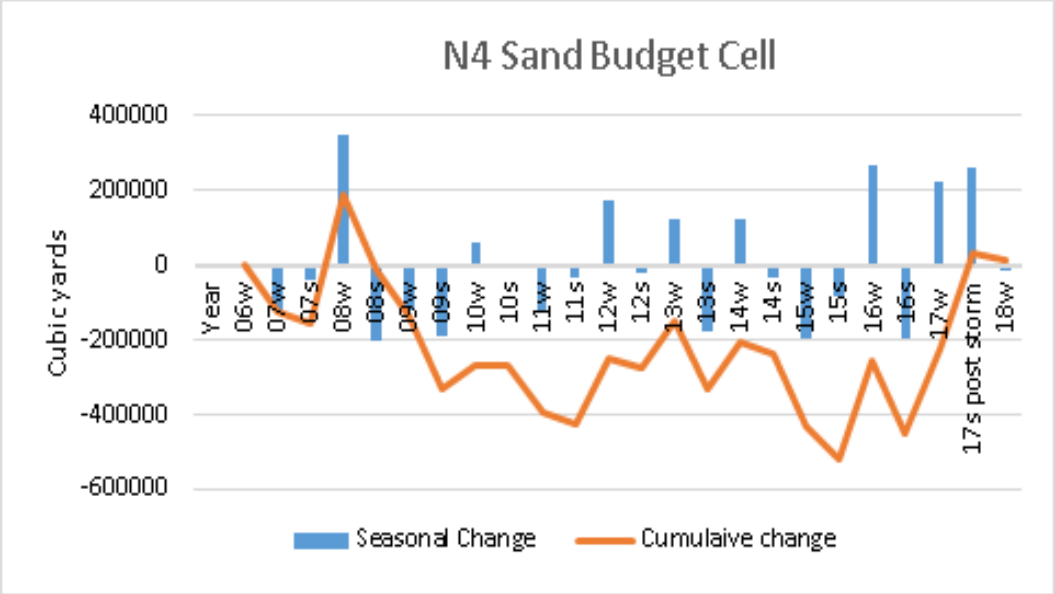


**Figure 10. Recent volumetric evolution of the N4 sand budget cell.**

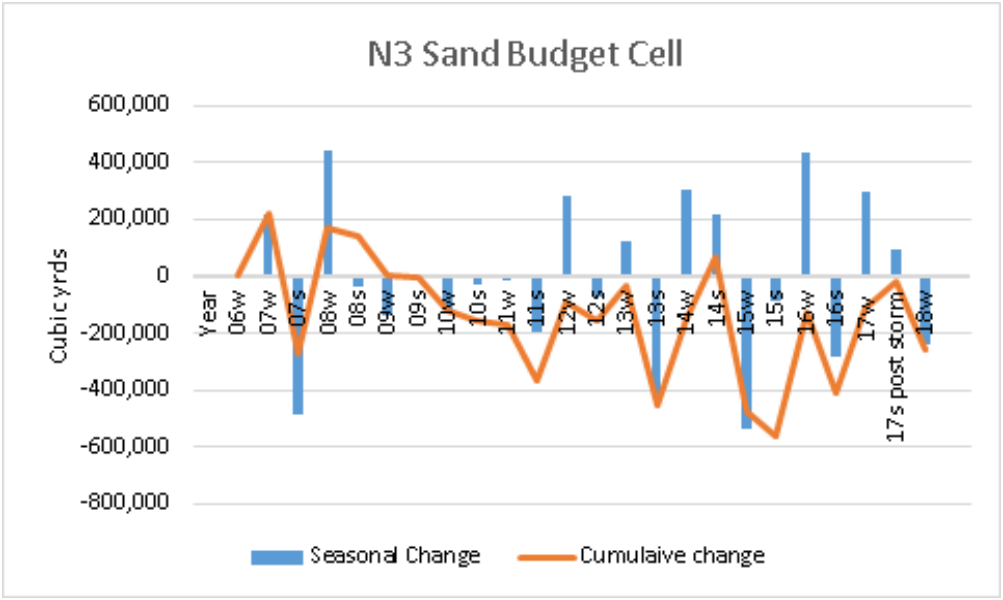


**Figure 11. Recent volumetric evolution of the N3 sand budget cell.**

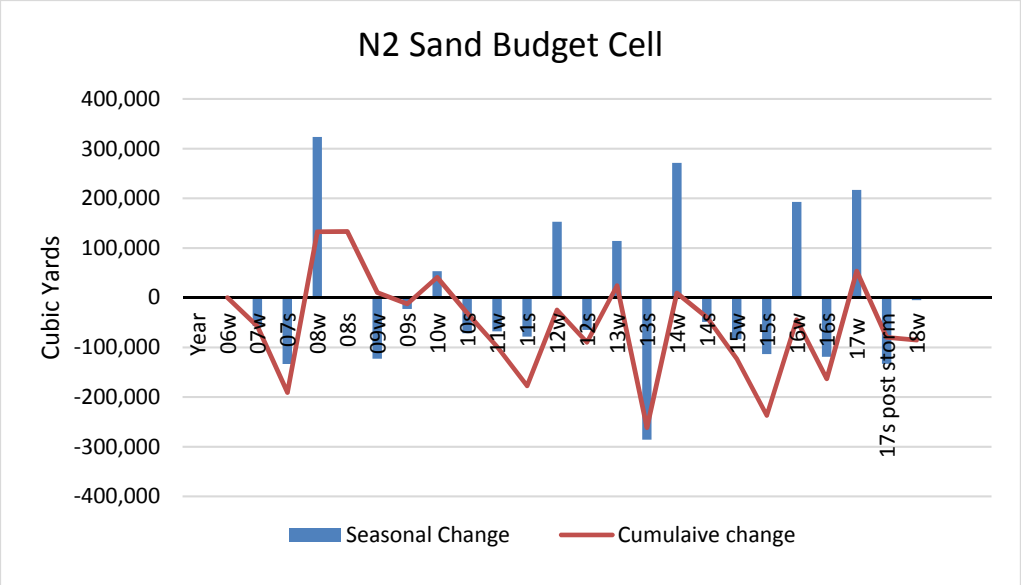


**Figure 12. Recent volumetric evolution of the N2 sand budget cell.**

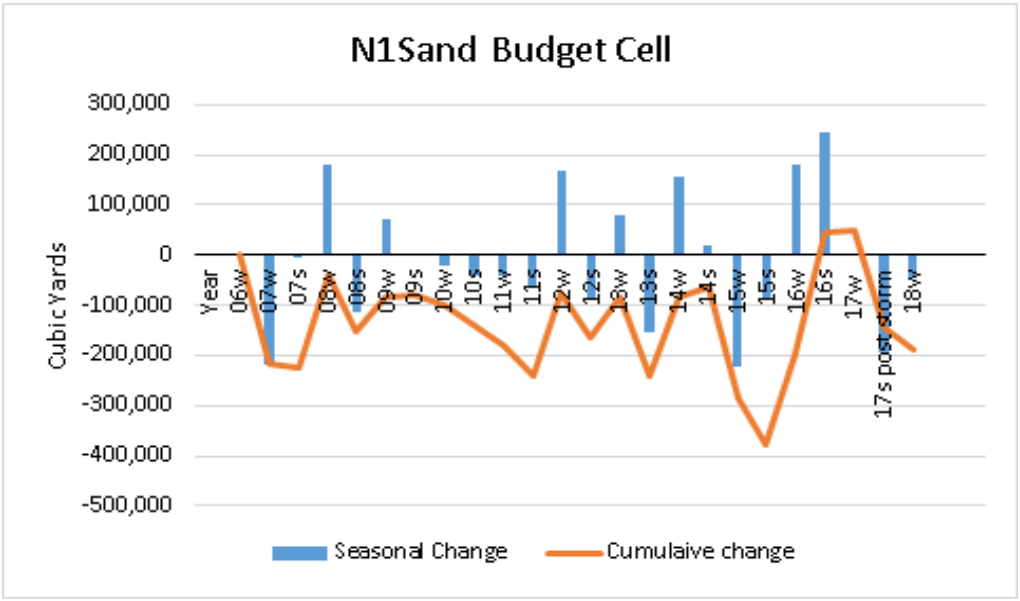


**Figure 13. Recent volumetric evolution of the N1 sand budget cell.**

Volume changes for the inlet sand budget cell (Figure 3) are shown in Figure 14. Sand volume in this budget cell is the combination of the ebb and flood shoals, as well as the sand trap. Thus, variations and trends of volume change in the ebb and flood shoal is reflected in the

sand volume patterns of the inlet budget cell. Sand is also stored in the channel and the fillet areas within about 4,000 feet of beach and shoreface to the north and south of the inlet entrance (Figure 4).

Sand volume seasonally fluctuates showing moderate gains in the higher energy winter months and moderate losses in the lower energy summer months. Divergence from this pattern occurs in association with major storms or in response to bypassing from the sand trap as can be seen in 2007 and again in 2012. This the cycle of abrupt sand loss followed by an extended period of sand volume gain is due to a combination of sand removal by dredging the sand trap and responding losses from the flood shoal followed by recovery of sand volume in the trap and rebound of the flood shoal. The influence of the ebb shoal sand volume within the inlet budget cell is considered to be independent of the sand trap excavation but more linked to accumulations of sand volume from the south directed littoral drift.

Over the past 12 years, net change in sand volume in this cell is about 400,000 cubic yards. However, this net accumulation has occurred largely within the last 3 years as seen in Figure 14. This volume gain is similar to the trend of increasing volume gain from 2007 to 2010 that occurred after the 2007 sand bypass project. In this period more than 600,000 cubic yards of sand accumulated within the inlet sand budget cell. However, in the next 3 years the inlet cell lost about 400,000 cubic yards of this accumulation. This volume loss was due to volume losses from the flood shoal and the ebb shoal as the inlet system rebounded from the dredging of the sand trap.

Inspecting the volume changes in the sand trap, flood shoal and ebb shoal, as well as volume losses in the N1 cell just to the north of the inlet cell, shows that the post sand bypass volume gains in the inlet are due to a combination of sand trap infilling, flood shoal rebound, and sand releases from the N1 cell to the inlet. The cycle of sand losses and gains within the inlet budget cell beginning with reach sand bypass from the sand trap is likely to be repeated as inlet system again responds to the sand bypass dredging event. Based on previous experience, the inlet budget cell gains since 2014 are likely to decline in rate and reverse to volume losses over the next few years. Sand released from the inlet budget cell is also likely to provide a benefit of increasing sand volume in the S1 to S4 budget cells to the south of the inlet as exemplified by volume gains in the S1 budget cell between 2008 and 2010 as seen in Figure 15.

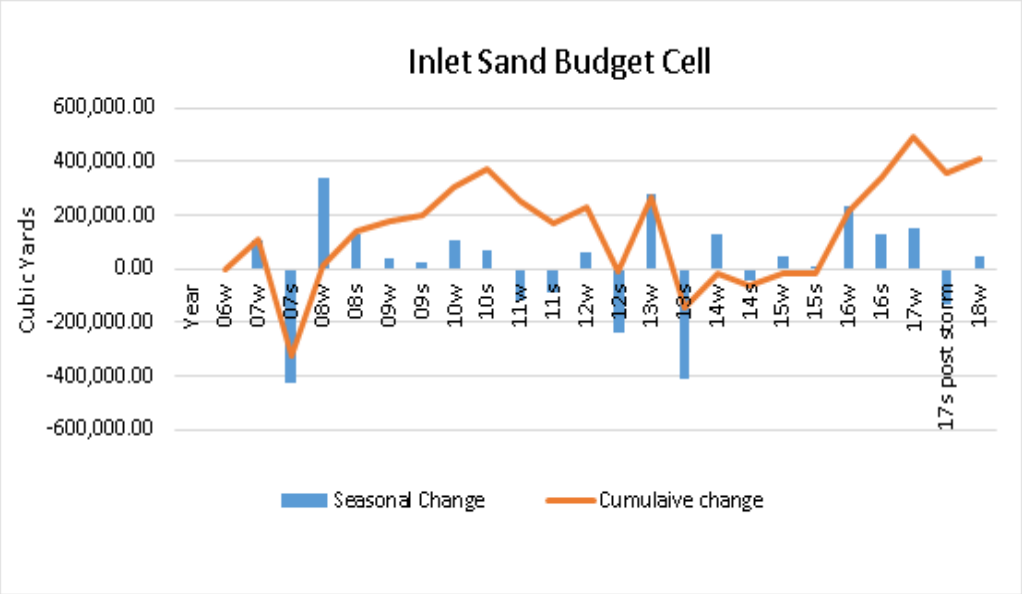


**Figure 14. Recent volumetric evolution of the Inlet sand budget cell.**

The volumetric evolution of the S1 cell, situated immediately south of the inlet cell between R4 and R10, is presented in Figure 15. The normal volume change pattern in this cell is a seasonal variation marked by volume gain in the winter and volume loss in the summer as seen between July, 2007 and winter, 2010. Seasonal losses of about 100,000 cubic yards occurred in this cell though the summer of 2011 followed by a gain of about 150,000 cubic yards recorded in the winter survey of 2012 and another gain of about 50,000 cubic yards by the summer of 2012. These gains are, in part due to 122,000 cubic yards of sand placed within the budget cell from the Sebastian Inlet sand trap. The volume gains of 2013 then dissipated by the summer of 2013 followed by a large volume gain in 2014 in the cell, again in part, due to sand bypass from the inlet sand trap. Large sand volume gains in all sand budget cells observed in the winter survey of 2014 indicate that there was a regional depositional event in this period that may be caused by onshore movement of sand from the lower shoreface. Sand volume gains of 2014 in the S1 cell were then passed to the S4 cell by the summer of 2015 as shown in Figure 18. Losses during this period from S2 and S3 also were passed to the S4 cell (Figure 16 and Figure 17). The S1 cell regained about 380,000 cubic yards of sand by the winter of 2018 due to large volume increases

recorded by the winter 2016 survey and the post Irma survey of 2017, which served as the summer survey. Similar to 2014, there was a regional depositional event during this period as seen I the records of all sand budget cells from N4 to S4. Net volume change in the S1 cell from 2006 to 2018 was an increase of about 80,000 cubic yards.

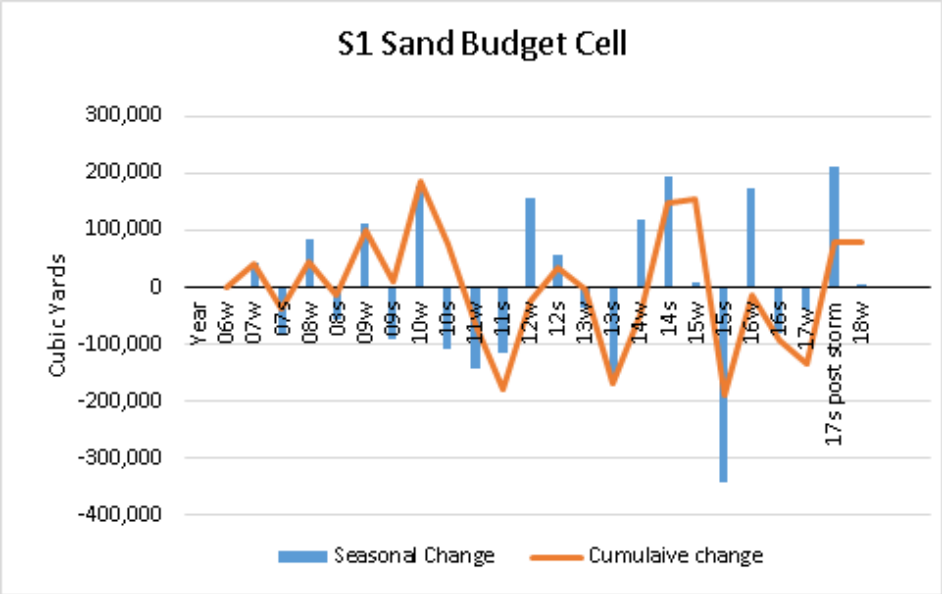


**Figure 15. Recent volumetric evolution of the S1 sand budget cell.**

Sand volume changes in the S2 cell (Figure 16, R-10 – R16) were generally similar to those of the S1 cell, being a combination of regional and littoral drift gains followed by sand volume losses that were shifted to the S3 and S4 cells. Gains the in 2010, 2014 and in 2016 are part of regional depositional events followed by sand volume losses over the following year. Over the 12-year period between 2006 and 2016 the net volume change in the S2 cell was a loss of about 29,000 cubic yards. During this period about 100,000 cubic yards of sand was placed in this cell.

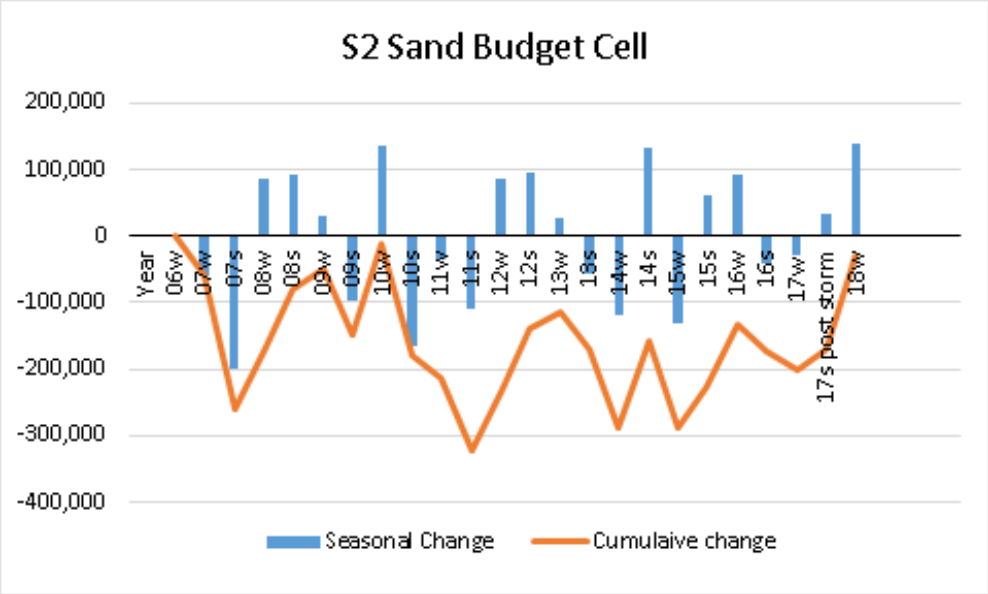


**Figure 16. Recent volumetric evolution of the S2 sand budget cell.**

Sand volume changes in the S3 cell (Figure 17) located between R16 and R23 have a more consistent seasonal pattern of gains followed by losses compared to other sand budget cells. However, gains are not always in the winter and losses in the summer. The regional sand volume gains of 2010, 2014, and 2016 are noted in the S3 record. Some of the gains in the S3 cell are offset by one season from a sand gain-loss cycle in cells father to the north indicating transfer of sand to the south by littoral drift. A net sand volume loss of about 318,000 cubic yards between 2006 and 2018 is attributed to a series of seasonal losses not completely balanced by sand volume gains in the following season. One of the larger seasonal losses occurring in the winter of 2015 of about 350,000 cubic yards was also noted in most of the other sand budget cell.

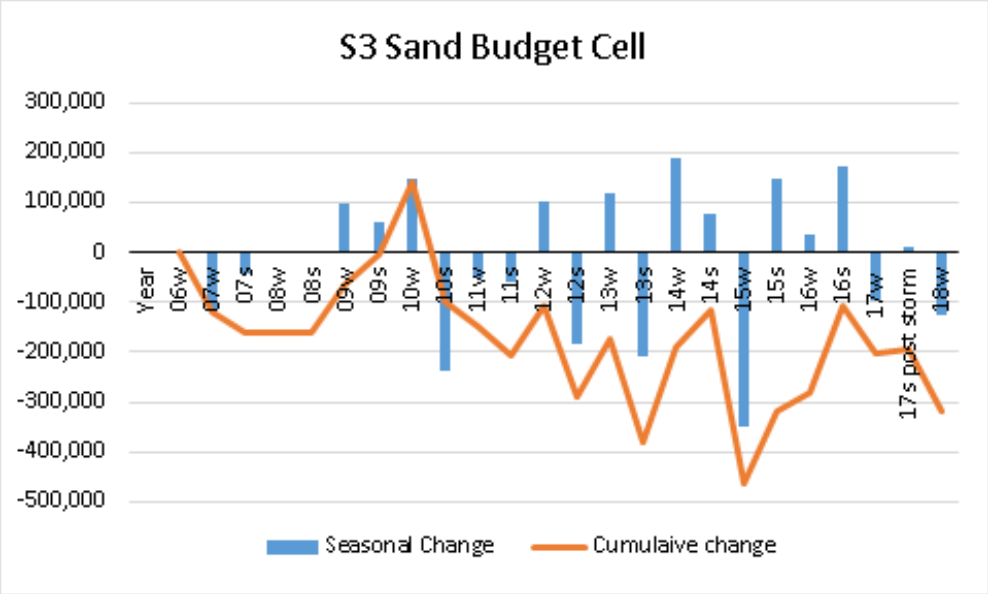


**Figure 17. Recent volumetric evolution of the S3 sand budget cell.**

The S2 sand budget cell (Figure 16, located between R23 and R30 (Figure 3) like S3 has an imbalance between seasonal gains and losses that add up to a net volume change of about 350,000 cubic yards between 2006 and 2018. The seasonal pattern of sequential gains and losses is not as consistent as seen in the S2 and S3 cell. The reginal sand volume gains of 2010, 2014, and 2016 persist in S4. Seasonal offsets between S4 and sand budget cells to the north indicate the role of sand movement in the littoral drift system. The interrelation of seasonal sand volume changes among the budget cells is examined in Section 3.3 of this report followed by the sand budget calculation in Section 3.4

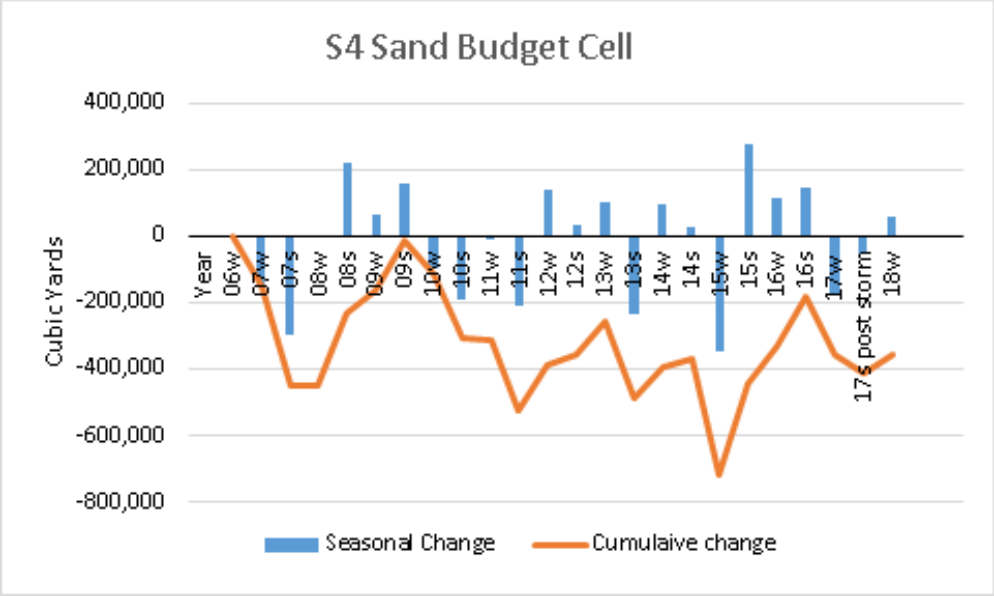


**Figure 18. Recent volumetric evolution of the S4 sand budget cell.**

### 3.3 Analysis of Sand Volume Changes, 2005 – 2018

Individual sand reservoirs and sand budget cells show short term changes that when integrated over time yield a net sediment budget when placed in an annualized format. Further, short-term changes can be spatially tracked though the barrier island-inlet system to observe how sand is moved from one compartment to another. Thus, in order to formulate a regional sand budget based on these data, it is important to consider temporal interrelation among the sand volume components of the Sebastian Inlet system. The time scale of a sediment budget should consider the dynamics of sand volume adjustments. Establishing a sediment budget on a very short time scale could reflect only abrupt changes from seasonal storms and not account for ongoing trends. To view the interrelation and exchanges among of the sediment budget cells Figure 19 compares sand volume changes all five of the sediment budget cells (N1, N2, Inlet, S1, S2) between 2006 and 2018. The figure shows the seasonal volume changes along with the cumulative volume change over this time period. Events of larger sand volume changes that correlate among the cells are shown and grouped on the plot.

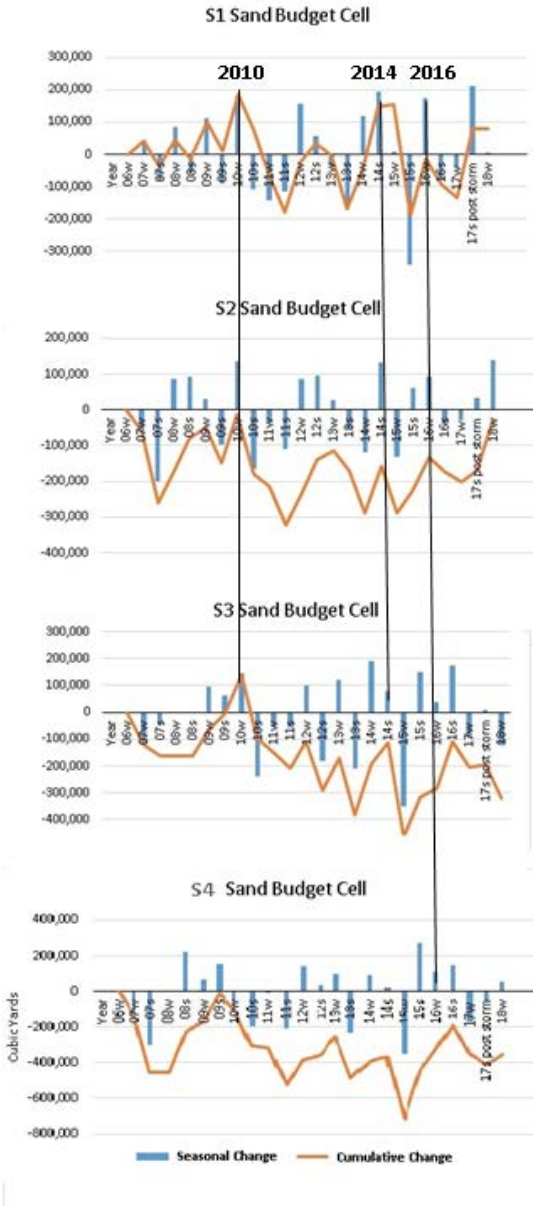


**Figure 19. Comparison of sand volume changes within the Sebastian Inlet sediment budget cells from 2006 to 2016. Groups of large seaonal volume changes that occurred in 2010, 2014, and 2016 are shown.**

Whereas volume changes that simultaneously affect several of the sand budget cells indicate regional gains, it is difficult to recognize volume changes that results from spatially progressive sand volume changes that are linked to changes in the rate littoral drift of sand and to progressive impoundment or release of sand from individual cells that influence adjacent sand budget cells over time. In order to view the relationship among sediment exchanges between the

sand budget cells Figure 20plots the cumulative volume change of all of the sand budget cells that occurred between 2006 and 2018.

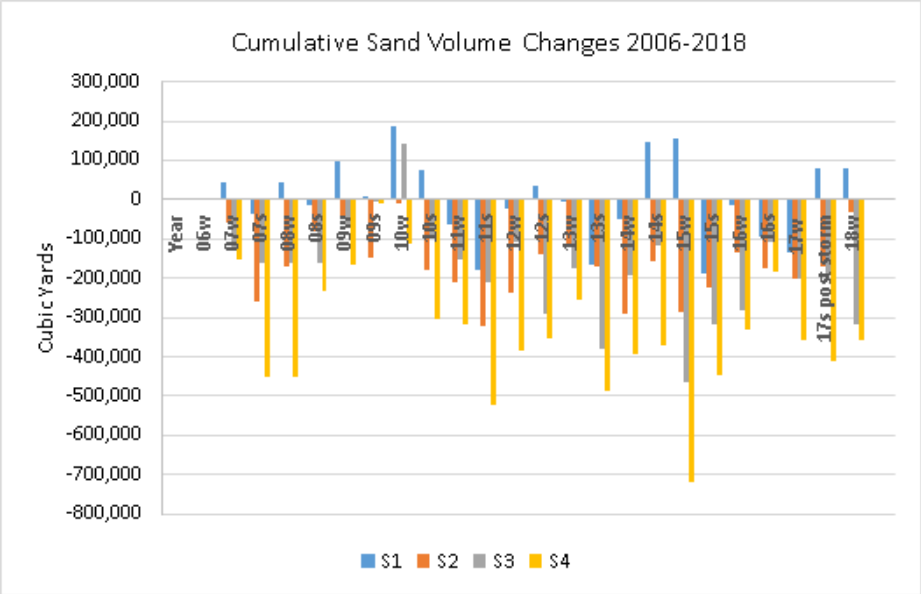


**Figure 20. Cumulative sand volume changes in the sediment budget cells south of Sebastian Inlet, 2006 to 2018.**

Figure 20shows that cumulative volume changes over the 12-year period between 2006 and 2018 have a pattern of progressively increasing loss of volume from north to south (S1 to S4). As the cumulative sand volume is viewed over time, the S1 cell shows episodic positive values of sand accumulation. The other budget cells show a spatial downdrift (south) increase in loss within each survey date with the exception of cell S2 which had a net accumulation of about 150,00 cubic yards at the winter 2010 survey along with a gain of nearly 200,000 cubic yards in the S1 cell and about 15,000 cubic yards in the S2 cell. At this time cumulative sand volume losses in the S3 and S4 cells were at the lowest within the 12-year analysis period.

Figure 21shows the same cumulative sand volume data as presented in Figure 20along with the cumulative volume changes within the inlet sediment budget cell from 2006 through 2018. If sand accumulation within the inlet budget cell is directly linked to sand volume losses to the south of the inlet, there should an inverse relationship between sand volume changes within the inlet and volume changes to the south of the inlet. However, over most of the 2006 to

2018 period, the inlet sand volume change and volume changes to the south have a positive correlation. Increased sand volume within the inlet corresponds with increased sand volume or declining volume losses in the sand budget cells to the south. For instance, increases in the cumulative sand volume gains within the inlet cell during the summer 2008 to summer 2010 period correspond to sand volume gains and declining sand volume losses in all of the sand budge cells to the south of the inlet. This corresponded to one of the regional depositional events described in Section 3, of this report. Declining sand volume gains and sand volume losses in the inlet budget cell from summer 2013 to summer 2015 corresponded to a period of increase and volume losses in cells S2, S3, and S4. Gains in cell S1 were attributed to sand bypassing projects from the trap. The most recent period of increasing sand volume gains in the inlet cell from winter 2016 to summer 2017 correspond to a period of increasing send volume loss om cells S2 to S4.

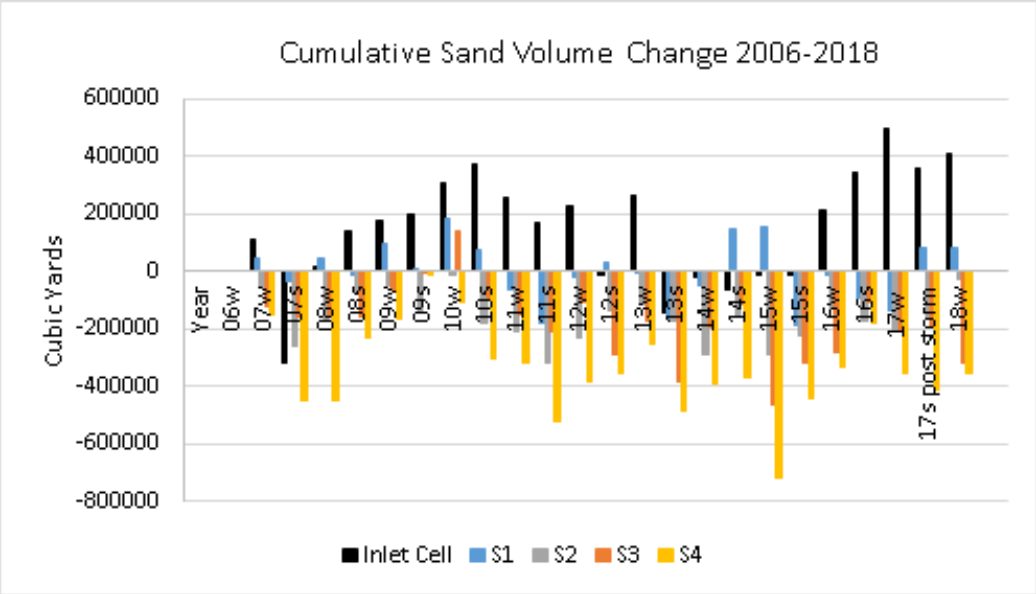


**Figure 21. Cumulative sand volume changes in the sediment budget cell in comparison of cumulative volume changes in the S1 to S4 cells south of Sebastian Inlet, 2006 to 2018.**

Figure 22compares volume changes in the S1 to S4 budget cells with sea level changes from 2006 to 2018. Periods of declining decreasing cumulative sand volume losses or gains correspond to periods of sea level drop Periods of higher sea level correspond to periods of increasing sand volume losses.

The sea level record for late 2017 and the first 5 months of 2018 may indicate that a period of rising sea level is beginning. This potentially indicates an upcoming period of increased loss of sand volume.

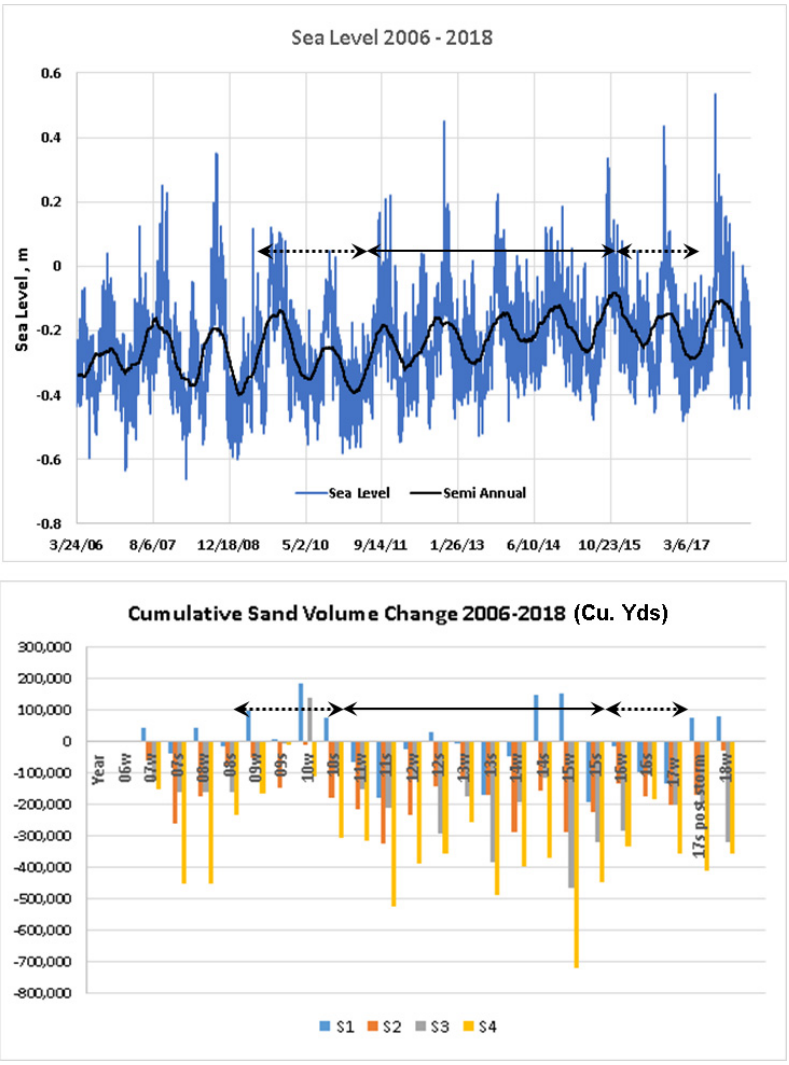


**Figure 22. Comparison of sand volume changes in the S1 to S4 budget cells with sea level changes from 2006 to 2018. Solid arrows indicate periods of declining sea level and decreasing cumulative sand volume losses or gains. Solid arrow indicates periods of sea level rise and increasing cumulative sand volume losses**

## 4.0 Sand Budget: Sebastian Inlet and Surrounding Barrier Segments

### 4.1 Methods

A sediment budget uses the conservation of mass to quantify sediment sources, sinks, and pathways in a littoral cell environment. It is used to quantify the effects of a changing sediment supply on the coastal system and to understand the large-scale morphological responses of the coastal system. The sediment budget equation is expressed as:

$$\sum Q_{source} - \sum Q_{\sin k} - \Delta V + P - R = residual \qquad \text{Equation 1}$$

The sources (Qsource) and sinks (Qsink) in the sediment budget together with net volume change within the cell (ΔV) and the amounts of material placed in (P) and removed from (R) the cell are calculated to determine the residual volume. For a completely balanced cell the residual would equal zero (Rosati and Kraus, 1999). +Figure 23schematically shows how calculations are made within each cell of the sediment budget model.

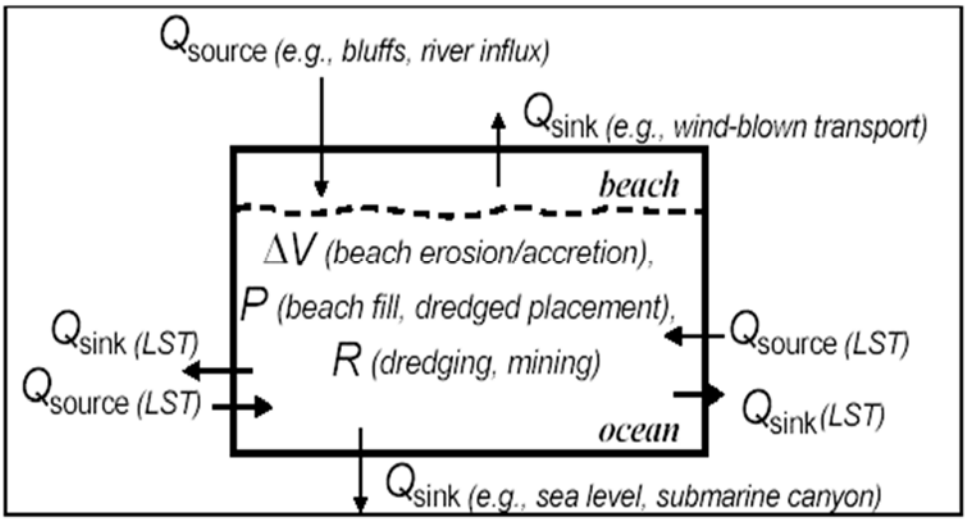


**+Figure 23. Schematics of a littoral sediment budget analysis (from Rosati and Kraus, 1999).**

Determination of net volume change for the local sediment budgets for Sebastian Inlet was based on volumetric analysis masks presented in section 3.0. The sediment budget encompasses the area between monuments R189 in Brevard County to monument R30 in Indian River County.

Since variability of the seasonal sand volume changes can be larger than the average range of values in the sediment budget, the temporal scale of the calculations is based on several time periods ranging from three to ten years between 2006 and 2018. The computational cells (masks) that were used to establish the local sediment budget are schematically shown in the volumetric section (see Figure 3). Volume changes for each mask were determined according to the methods described above in the net topographic changes section and input into the Sediment Budget Analysis System (S.B.A.S) program, provided by the Coastal Inlet Research Program. Details of these procedures can be found in the technical report by Rosati et al. 2001. Based on super regional sediment budget calculations described in Zarillo et al, 2007, an initial input value (Qsource) of 150,000 yd3/yr. was chosen. However, for some time periods the initial input value was increased to 200,000 yd3/yr. to accommodate periods of larger transport rates bounded by winter seasons. The placement values (P) correspond to the beach fill projects that were included in the calculations. Most of this placement is to the south of Sebastian inlet in the S2 and S3 sand budget cell from either the Sebastian Inlet sand trap or from upland sources accessed by Indian River County. However, beginning in 2016, placement in the N4 and N3 cells are associated with post-hurricane repair of beaches in south Brevard County. Removal of sand (R) through mechanical bypassing was included to account for the 2012, and the 2014 dredging projects within the sand trap. However, removal of sand (R) through offshore losses was assumed to be zero for all cells since the boundaries of the masks extend beyond the depth of closure. Placement and removal values are annualized and presented in Table 2.

Table 2. Annualized placement and removal volumes for sand budget calculations. Units are in cubic yards per year

| Time Period | Season | N4 | N3 | N2 | N1 | Inlet | S1 | S2 | S3 | S4 |
|---|---|---|---|---|---|---|---|---|---|---|
| 2007–17 | Winter | 810 | 1067 | 770 | 527 | -36754 | 32904 | 11748 | 7480 | 15925 |
| 2007–17 | Summer | 810 | 1067 | 770 | 527 | -36754 | 28620 | 10320 | 7480 | 15925 |
| 2013 –18 | Winter | 3144 | 4140 | 2987 | 3406 | -56508 | 23760 | 16100 | 7300 | 12040 |
| 2012–17 | Summer | 1620 | 2007 | 1539 | 1755 | -56508 | 48160 | 16100 | 10420 | 15680 |
| 2010-13 | Winter | 0 | 0 | 0 | 0 | -40667 | 43200 | 2522 | 12800 | 40617 |
| 2013-16 | Summer | 2700 | 3555 | 2565 | 1755 | -53513 | 37067 | 15600 | 3100 | 11000 |

### 4.1 Sand Budget Results

The sand budget is presented on three distinct time scales ranging from a longer-term budget for the past 10-years to short term budgets that examines volume changes and sand flux over 5 and 3-year year periods. The budget uses calculated annualized volume change per cell as inputs (see Figure 3). Annualized beach fill material is accounted for in the N4 to N21 cell on the north side of Sebastian Inlet, the inlet cell, and the S1 to S4 cells a shown in Figure 3.

Interpretation of the fluxes, especially those leaving the southernmost cell (S2, R16-R30) must consider that the sand budget assumes a fixed input of either +150,000 or 200,000 cy/yd. entering the first north cell (N4). Sand transport was assumed to flow north to south. indicate a reversal of sediment transport to the next cell north. The components of the long-term sand budget are listed in

Table **3** and covers the period from 2007 through 2017. A comparison is made between winter and summer-based budgets.

**Table 3. Annualized volume changes per cell and flux (2007 – 2017).**

| Time Period | Winter 2007 – Winter 2007 Qin=150,000 cy/yr | | Summer 2007 - Summer 2017 Qin=150,000 cy/yr | |
|---|---|---|---|---|
| **Sediment Budget Cell** | **ΔV (cy/yr.)** | **Q (cy/yr.)** | **ΔV (cy/yr.)** | **Q (cy/yr.)** |
| **North 4** | -10,301 | 161,111 | 19,224 | 131,586 |
| **North 3** | -10,337 | 172,515 | 2,287 | 129,300 |
| **North 2** | 1,1052 | 162,233 | 11,089 | 118,981 |
| **North 1** | 26,800 | 135,960 | 7,961 | 111,547 |
| **Inlet** | 36,750 | 99,210 | 68,046 | 43,501 |
| **South 1** | -17,715 | 113,075 | 11,597 | 60,524 |
| **South 2** | -14,195 | 139,018 | 8,980 | 25,110 |
| **South 3** | -8,363 | 154,861 | -3,165 | 35,755 |
| **South 4** | -20,438 | 191,224 | 4,121 | 47,559 |

Figure 24 is a visual representation of the data listed in

Table **3**. Shown are the locations of the sand budget cells and the annualized volume changes, and sand fluxes calculated from the survey data. Refer to Figure 10through Figure 18 for plots of sand volume changes in each of the sand budget cells. For each of these records the volume changes are annualized over the sand budget period and listed in

Table **3**. The analysis results for the 10-year sand budget based on a winter to winter period show that all but three cells lost sand volume between 2007 and 2017. All four cells located to the south of Sebastian Inlet lost sand volume, but the annualized losses were relatively small due to the placement from the sand trap and other sources and large littoral drift rates moving sand from north to south. The inlet cell gained an annual average of about 39,000 cubic

yards of sand per year. When the 2007, 2012 and 2014 sand trap excavations are combined, the annualized rate of sand removal from the inlet cell is about 27,000 cubic yards per year.

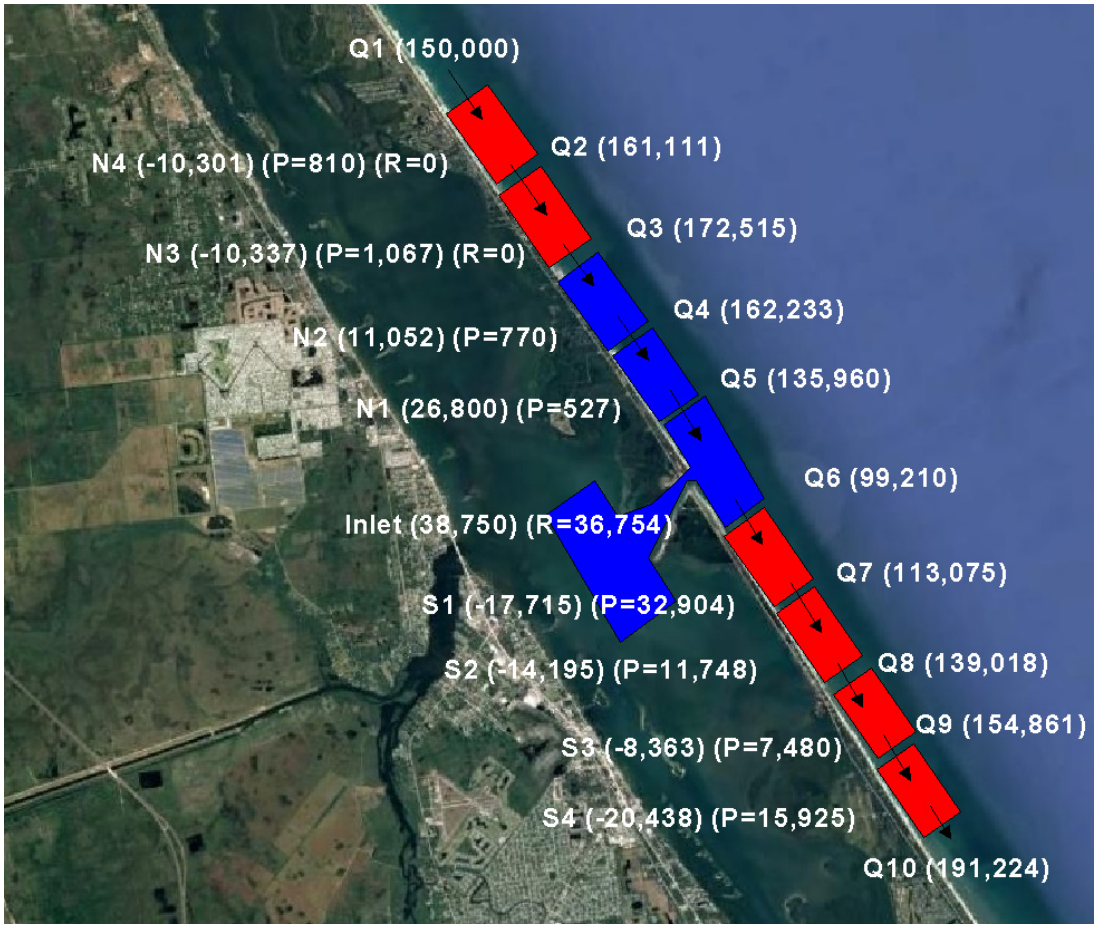


**Figure 24. Annualized sediment budget for the winter 2007 to winter 2017 time period. Values on the west of the barrier island indicate sand volume changes and values on the east indicate calculated sand flux rate in cubic yards per year. P= annualized placement quantities and R = annualized value of sand removed from the sand trap. Blue cells indicate sand volume increase whereas red cells indicate sand volume loss.**

Figure 25is the visualization of the summer to summer 10-year (2007 to 2017) sand budget. In this summer to summer analysis, all of the sand budget cells had volume gains except for S3. The magnitude of the annualized sand volume changes was smaller than the winter to winter changes and generally less than 10,000 cubic yards. Sand volume in the S1 to S4 cells were again aided by sand placement from the Sebastian Inlet sand trap and from upland sources used by Indian River County. The small annualized volumes of sand placed in the N4 to N2 cells

is derived from placement of about 30,000 cubic yards of sand on the beaches by Brevard County in the post storm period of 2017. The annualized gain of sand volume within the inlet budget cell for this period is about 68,000 cubic yards. This is largely offset by sand placement from the sand trap and upland sources in the S1 to S4 cells. Over the 10-year period between 2007 and 2017 a total of 666,000 cubic tards of sand was placed in these cells for an annual average of 66,000 cubic yards.

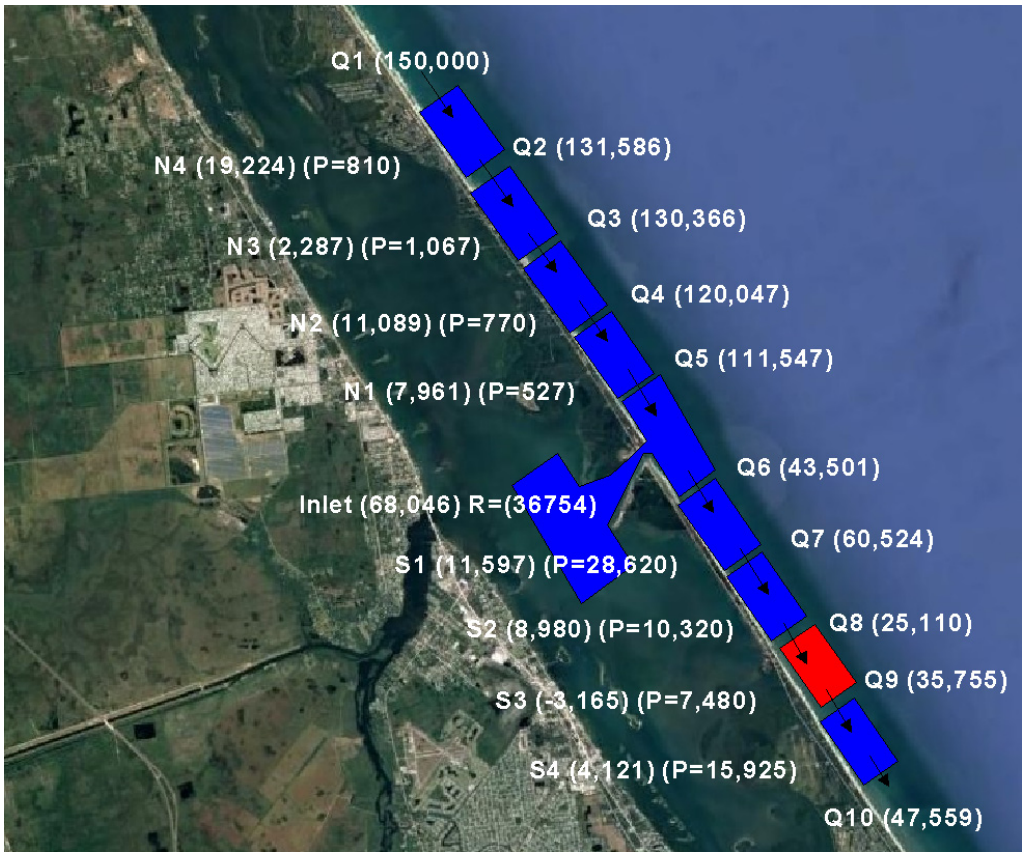


**Figure 25. Annualized sediment budget for the summer 2007 to summer 2017 time period. Values on the west of the barrier island indicate sand volume changes and values on the east indicates calculated sand flux rate in cubic yards per year. P= annualized placement quantities and R = annualized value of sand removed from the sand trap. Blue cells indicate sand volume increase whereas red cells indicate sand volume loss.**

A 5-year sand budget was calculated to compliment the longer term 10-year calculation. Table 4 lists the results for the winter 2013 to winter 2018 and summer 2012 to summer 2017 five-year calculation. The winter sand budget begins with an annualized input of 150,000 cubic yards at the north sand budget cell N4. Similar to the 10-year winter to winter sand budget (

**Table 3**, Figure 24) the calculated littoral drift sand transport rates are higher compared to the companion summer to summer sand budget. Within the individual cells, there is a mix of annualized volume gains and losses among the budget cells (Figure 26). The annualized sand volume gain of about 28,000 cubic yards of sand within the inlet cells is more than offset by sand placement in the S1 to S4 cell from the sand trap and sources proved by Indian River County that totaled about 296,000 cubic yards or about 59,000 cubic yards per year.

**Table 4. Five-year sand budget annualized volume changes per cell and flux**

| **Time Period** | **Winter 2013 – Winter 2018 Qin=150,000 cy/yr.** | | **Summer 2012 - Summer 2017 Qin=200,000 cy/yr.** | |
|---|---|---|---|---|
| **Sediment Budget Cell** | **∆V (cy/yr.)** | **Q (cy/yr.)** | **∆V (cy/yr.)** | **Q (cy/yr.)** |
| **North 4** | 33288 | 119856 | 61584 | 140036 |
| **North 3** | -43974 | 167970 | 28199 | 113844 |
| **North 2** | -21913 | 192870 | 1948 | 113435 |
| **North 1** | -20695 | 216971 | 3961 | 111229 |
| **Inlet** | 28234 | 175060 | 70355 | 40874 |
| **South 1** | 17112 | 181708 | 9020 | 80014 |
| **South 2** | 1361 | 196447 | -5841 | 102055 |
| **South 3** | -29198 | 232945 | 19468 | 93007 |
| **South 4** | -20181 | 265,166 | -11412 | 120.099 |

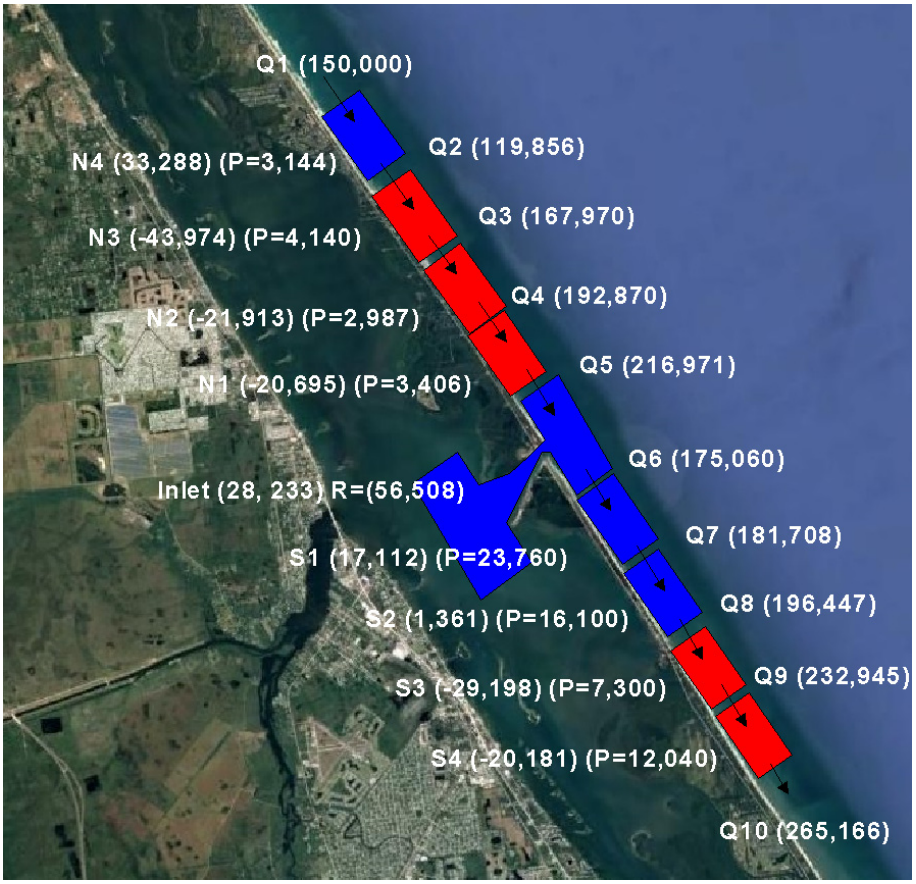


**Figure 26. Annualized sediment budget for the winter 2013 to winter 2018 time period. Values shown to the west of the barrier island indicate sand volume changes and values on the east indicates calculated sand flux rate in cubic yards per year. P= annualized placement quantities and R = annualized value of sand removed from the sand trap. Blue cells indicate sand volume increase whereas red cells indicate sand volume loss.**

The five-year summer to summer sand budget listed in Table 4 and illustrated in Figure 27is largely depositional on an annualized basis. The 2012 to 2017 time period corresponds to a period of sand volume gains or lower sand volume losses across the entire sand budget domain. As seen in Figure 27, the summer to summer 5-year sand budget includes the period of declining sand volume losses in the S1 to S4 cells even as the cumulative sand volume increased within the inlet sand budget cell.

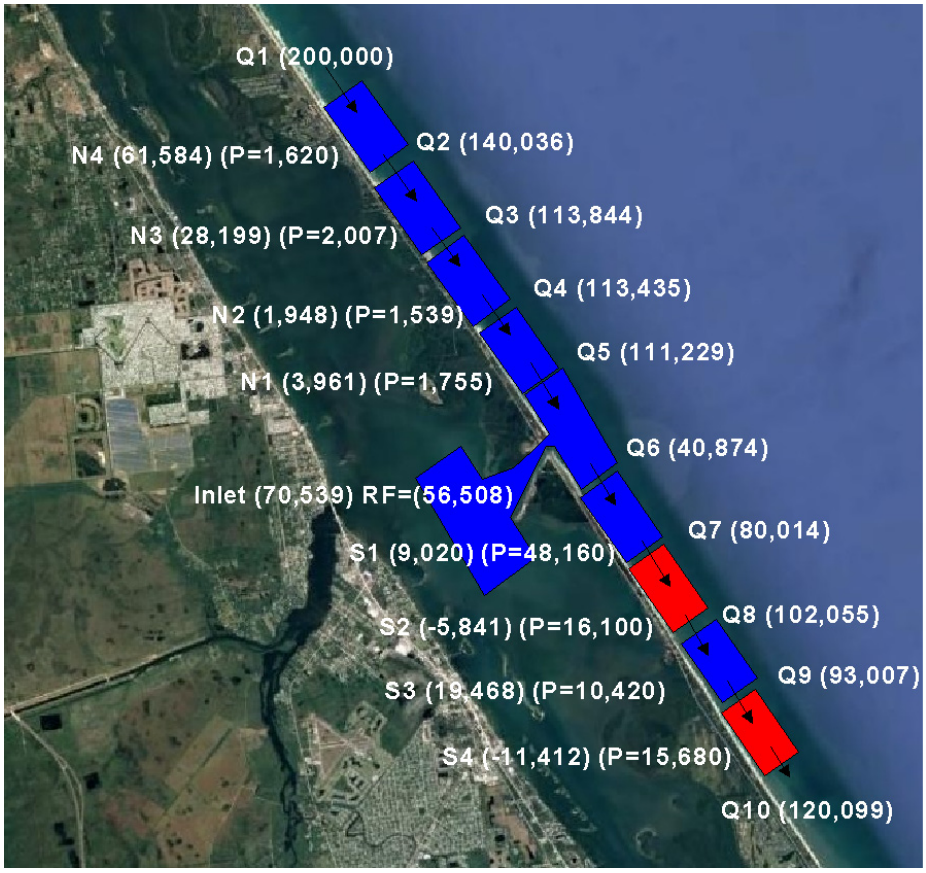


**Figure 27. Annualized sediment budget for the summer 2012 to summer 2017 time period. Values on the west of the barrier island indicate sand volume changes and values on the east indicates calculated sand flux rate in cubic yards per year. P= annualized placement quantities and R = annualized value of sand removed from the sand trap. Blue cells indicate sand volume increase whereas red cells indicate sand volume loss.**

Two 3-year sand budgets ae calculated to contrast sand exchanges among the budget cells during a time of stable or decreasing volume of the ebb shoal and during a time of increasing ebb shoal volume. Although short-term 3-year sand budget is not useful for regional sand management over longer periods, it provides insight on the role of the ebb shoal on the sand budget. As seen in Figure 5, the Sebastian Inlet ebb shoal has increased in volume by approximately 250,000 cubic yards between 2006 and 2018. However, the increase has not been continuous and is the integrated result of a series of seasonal sand volume losses and gains of about 50,000 cubic yards or less.

Figure 28 displays the results of calculating 3-year sand budgets from summer 2010 to summer 2013 when the volume of the ebb shoal remained stable (see Figure 5). The second 3-year period shown in Figure 29 is from summer 2013 to summer 2016 when the ebb shoal volume increased by about 120,000 cubic yards. In both, 3-year time periods additional sand fluxes were required to balance the sand budget and keep annualized longshore transport rates at reasonable levels. In the 2010 to 2013 period, the input sand flux at the north boundary of the sand budget cells was specified at 150,000 cubic yards per year. Annualized sand volume loss rates in all but one of the cells required offshore losses beyond the seaward boundary of the cells. Thus, an annualized loss of 25,000 cubic yards was specified for each cell. Even with his offshore loss, the calculated annualized littoral drift out of the S4 cell at the south boundary increased to about 390,000 cubic yards. Thus, it is likely that offshore sand losses were higher than specified.

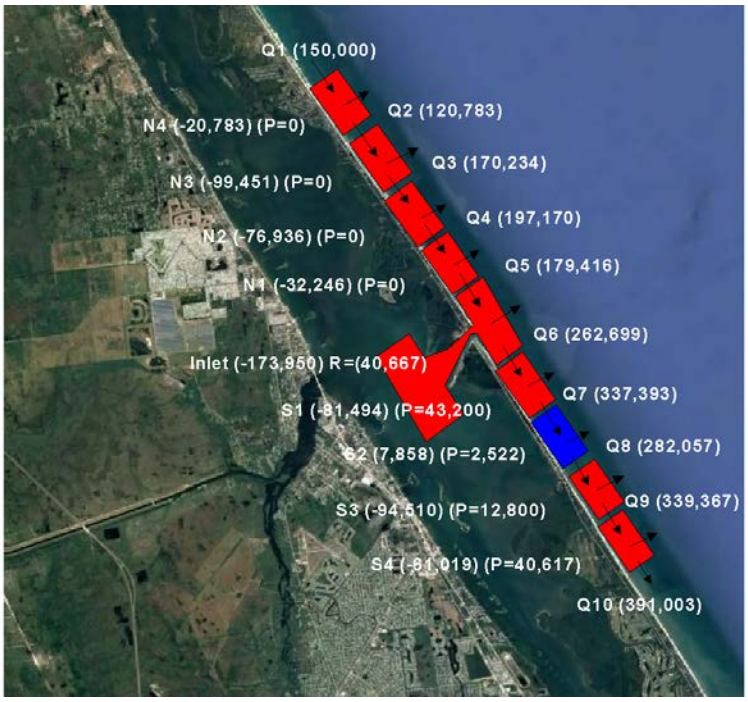


**Figure 28. Annualized sediment budget for the summer 2010 to summer 2013 time period. Values on the west of the barrier island indicate sand volume changes and values on the east indicates calculated sand flux rate in cubic yards per year. P= annualized placement quantities and R = annualized value of sand removed from the sand trap. Blue cells indicate sand volume increase whereas red cells indicate sand volume loss. Offshore transport from each of the cells was required to balance the sand budget.**

The 3-year sand budget, although not useful for long term planning and sand management, illustrates that depositional and erosional events can overwhelm the local to regional sand budget on a short-term basis.

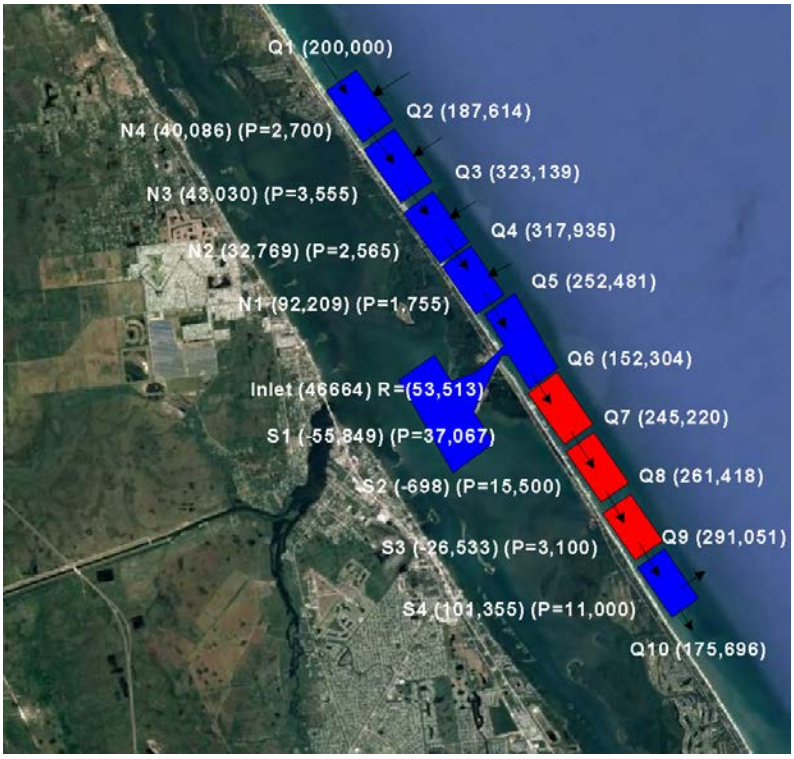


**Figure 29. Annualized sediment budget for the summer 2013 to summer 2016 time period. Values on the west of the barrier island indicate sand volume changes and values on the east indicates calculated sand flux rate in cubic yards per year. P= annualized placement quantities and R = annualized value of sand removed from the sand trap. Blue cells indicate sand volume increase whereas red cells indicate sand volume loss. Onshore transport from cells N1 to N4 was required to balance the sand budget.**

## 5.0 Morphologic Changes

### 5.1 Methods

The analysis uses the same dataset and overall methodology as the sand volume analysis and sand budget analysis described Sections 3 and 4. The morphologic change section is subdivided according to the time period of analysis. The time interval covered in this report

includes a longer time period of 2010 to either 2017 or 2018 and a shorter interval covering approximately 1 year to 18 months. The net morphologic changes over 5-year and 20-year periods are presented in the series of earlier report (Zarillo et al, 2007, 2012, 2013, 2016).

In the color convention for figures depicting topographic change; blue represents erosion, whereas red indicates deposition. Topographic changes were combined with results from shoreline changes and sand budget calculations for a better understanding of the sedimentation processes.

### 5.2 Topographic Changes

Figure 30 shows net topographic changes in the vicinity of Sebastian Inlet for the longest time period examined based on the winter 2010 and winter 2018 topographic surveys. As seen in Figures 5 and 8 in Section 2 of this report the net sand volume change of the flood shoal was minimal and the accumulation of sand within the ebb shoal area was about 100,00 cubic yards, which can be seen in Figure 31 as areas of 1 to 3 feet of shoaling. Sand accumulation within the S1 budget cell can be seen in the southeast section of the plot and correlates with sand volume accumulation of about 20,000 cubic yards seen in Figure 15, Section 3.2 of this report. The summer 2010 to winter 2018 comparison shown in Figure 31 is similar to the winter to winter comparison shown in Figure 30. However, deeper blue patterns indicate more sand volume loss with the footprint of the inlet budget cell, which us deemed the signature of the winter season.

Both plots show the signature of the sand trap in terms of a slight topographic low as the sand trap continues to recover from excavation in 2014.

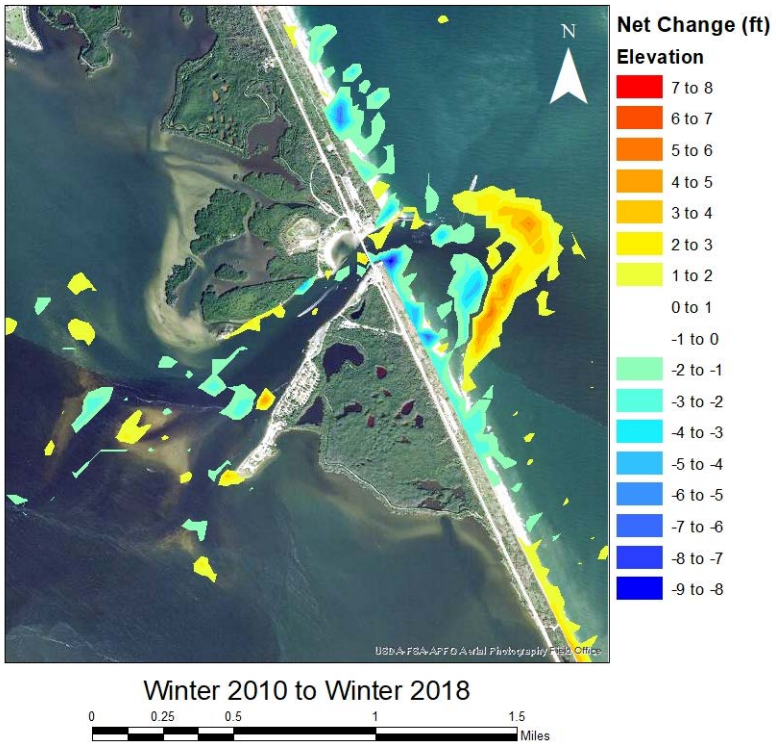


**Figure 30. Topographic changes in the vicinity of Sebastian Inlet between the winter 2010 and winter 2018.**

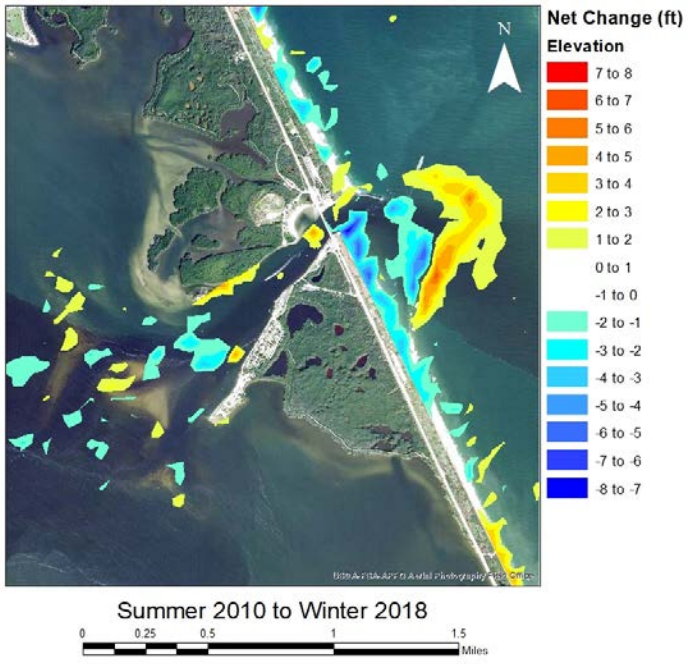


**Figure 31. Topographic changes in the vicinity of Sebastian Inlet between the winter 2010 and winter 2018.**

The effects of sand volume accumulation from 2013 to a peak accumulation in 2016 are represented in Figure 32 which shows net topographic changes in between the summer survey of 2012 and 2016. Likewise Figure 33 shows topographic gains in the winter to winter survey comparisons between 2012 and 2016. During this period most, sand budget cells included sand volume increases or small volume losses as shown by Figure 10 to Figure 18 in Section 3 of this report. This consistent with the sand budget calculations shown in Figure 29, which required onshore sand transport to balance the budget in a realistic way.

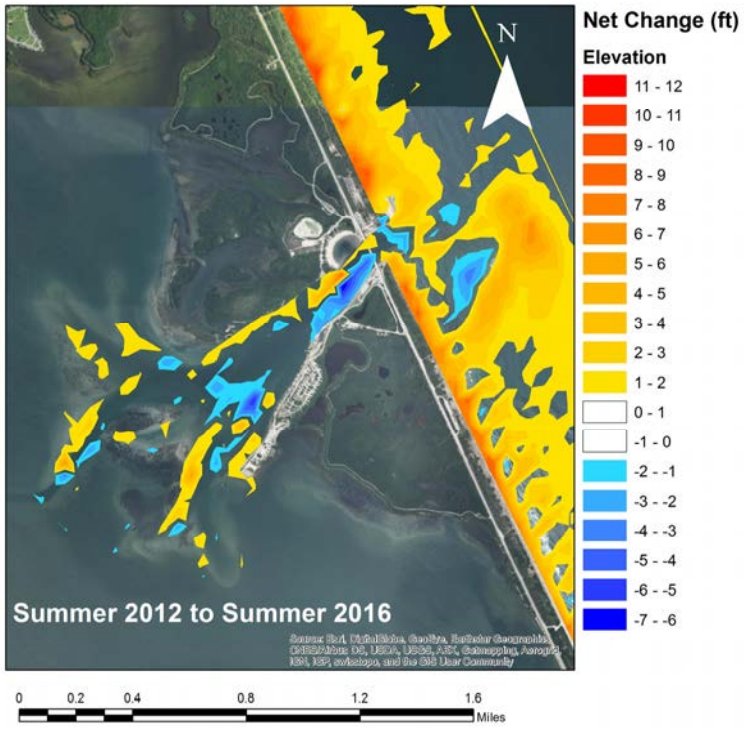


**Figure 32. Topographic changes in the vicinity of Sebastian Inlet between summer 2012 and winter 2016.**

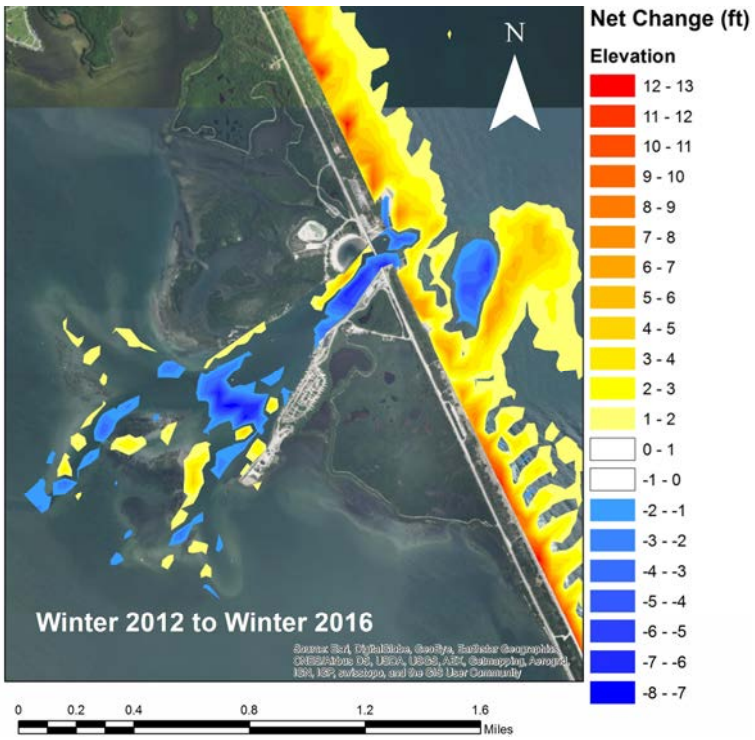


**Figure 33. Topographic changes in the vicinity of Sebastian Inlet between winter 2012 and winter 2016.**

Topographic changes over the 18-month period between the summer topographic survey of 2016 and the winter survey of 2018 are shown in a sequence of Figure 34, Figure 35 and Figure 36. This period is characterized moderate to large sand volume gains over most of the region. However, sand volume losses in the S3 and S4 cells were on the order of 170,000 to 200,000 cubic yards. The seasonal frequency of Figures 34 to 36 also shows the winter-summer seasonal cycle in which sand volume losses depicted by blue colors are more prominent in the summer to summer transition. This is contrasted with the warmer colors I nth immediate vicinity of the inlet (Figure 35) in the winter to summer transition. The signature of topographic change in the sand trap area at the west end of the inlet channel indicates continued infilling.

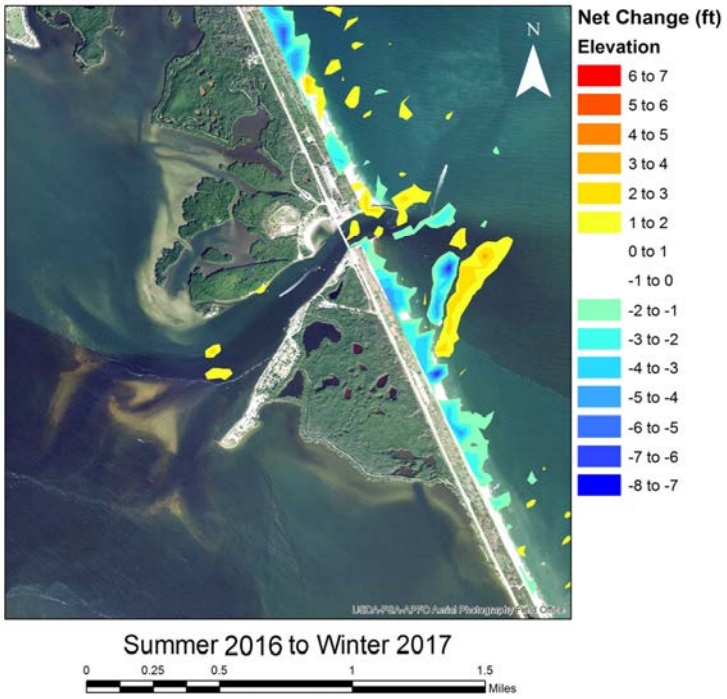


**Figure 34. Topographic changes in the vicinity of Sebastian Inlet between summer 2016 and winter 2017.**

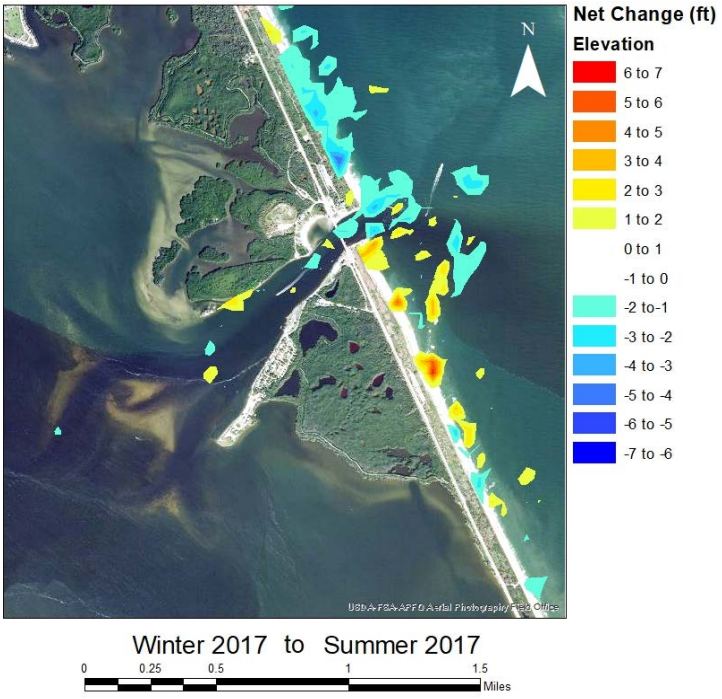


**Figure 35. Topographic changes in the vicinity of Sebastian Inlet between winter 2017 and summer 2017.**

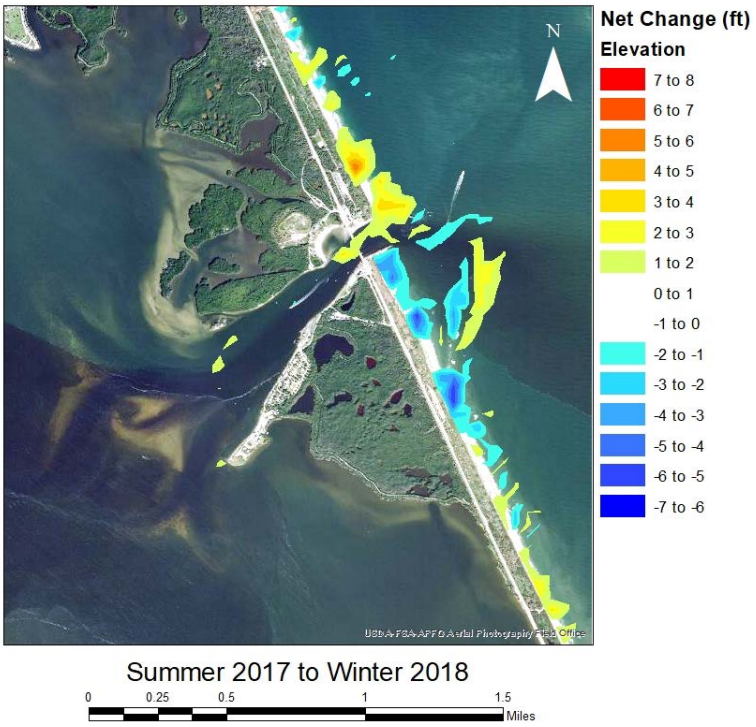


**Figure 36. Topographic changes in the vicinity of Sebastian Inlet between summer 2017 and winter 2018.**

## 6.0 Shoreline Changes

Shoreline positions were digitized from the geo-referenced aerial imagery for a domain covering approximately 7 miles north to 7 miles south of Sebastian Inlet, FL (~75,000 ft, Table 1). Changes to the shoreline position were determined by comparing 30 time series of transects generated every 25 ft along the coast. Table 5 lists the number of transects included in each aerial image set beginning with the 1943 photo set. Table 6 indicates the extent of coverage for each of the time series used in the analysis according to the total number of transects and the alongshore distances. Table 6 shows the extent of coverage and the aerial image sub-cells (e.g. North1) used for analysis within the full domain. Transects were generated using the BeachTools© extension for ArcGIS © from a standardized baseline (~SR A1A) to the wet/dry line (low-tide terrace). The change in shoreline position was determined by subtracting the distances along each transect between time-series of interest. Shoreline change rates were calculated using both the End Point Rate (EPR) and Linear Regression (LR) methods (Crowell et al., 1993; Morton et al., 2002). For details on the methodology the reader is referred to the previous report. In this version of the report, long-term changes and rates of change have been updated for the time spans of 1958-2017 (historical) and an intermediate term analysis covered the years 2008-2017. Additional short-term analyses are included to account for the changes occurring since the previous report, spanning from 2016-2017, as well as those changes occurring during the 2014 - 2017-time span.

## Table 5. Summary of transect coverage.

| Year | Extent of Coverage | | | | | North | | | | | South | | | | |
|---|---|---|---|---|---|---|---|---|---|---|---|---|---|---|---|
| | # | Distance | | Transects | | # | Distance | | Transects | | # | Distance | | Transects | |
| | Transects | feet | miles | start | end | Transects | feet | miles | start | end | Transects | feet | miles | start | end |
| **1943** | 2442 | 61050 | 11.6 | 531 | 2972 | 950 | 23750 | 4.5 | 531 | 1480 | 1465 | 36625 | 6.9 | 1508 | 2972 |
| **1958** | 2300 | 57500 | 10.9 | 0 | 2299 | 1481 | 37025 | 7.0 | 0 | 1480 | 792 | 19800 | 3.8 | 1508 | 2299 |
| **1968** | 1853 | 46325 | 8.8 | 1118 | 2970 | 363 | 9075 | 1.7 | 1118 | 1480 | 1463 | 36575 | 6.9 | 1508 | 2970 |
| **1970** | 405 | 10125 | 1.9 | 1369 | 1773 | 112 | 2800 | 0.5 | 1369 | 1480 | 266 | 6650 | 1.3 | 1508 | 1773 |
| **1972** | 1349 | 33725 | 6.4 | 501 | 1895 | 934 | *23350 | 4.4 | 501 | *1480 | 388 | 9700 | 1.8 | 1508 | 1895 |
| **1974** | 2144 | 53600 | 10.2 | 831 | 2974 | 650 | 16250 | 3.1 | 831 | 1480 | 1467 | 36675 | 6.9 | 1508 | 2974 |
| **1978** | 2038 | 50950 | 9.6 | 935 | 2972 | 546 | 13650 | 2.6 | 935 | 1480 | 1465 | 36625 | 6.9 | 1508 | 2972 |
| **1980** | 1943 | 48575 | 9.2 | 1 | 1943 | 1480 | 37000 | 7.0 | 1 | 1480 | 436 | 10900 | 2.1 | 1508 | 1943 |
| **1981** | 2011 | 50275 | 9.5 | 964 | 2974 | 517 | 12925 | 2.4 | 964 | 1480 | 1467 | 36675 | 6.9 | 1508 | 2974 |
| **1983** | 1621 | 40525 | 7.7 | 25 | 1645 | 1456 | 36400 | 6.9 | 25 | 1480 | 138 | 3450 | 0.7 | 1508 | 1645 |
| **1984** | 1818 | 45450 | 8.6 | 1153 | 2970 | 328 | 8200 | 1.6 | 1153 | 1480 | 1463 | 36575 | 6.9 | 1508 | 2970 |
| **1986** | 1251 | 31275 | 5.9 | 536 | 1786 | 945 | 23625 | 4.5 | 536 | 1480 | 279 | 6975 | 1.3 | 1508 | 1786 |
| **1988** | 1777 | 44425 | 8.4 | 1124 | 2971 | 357 | 8925 | 1.7 | 1124 | 1480 | 1393 | *34825 | 6.6 | 1508 | *2971 |
| **1989** | 1757 | 43925 | 8.3 | 199 | 1955 | 1282 | 32050 | 6.1 | 199 | 1480 | 448 | 11200 | 2.1 | 1508 | 1955 |
| **1992** | 1989 | 49725 | 9.4 | 958 | 2946 | 523 | 13075 | 2.5 | 958 | 1480 | 1439 | 35975 | 6.8 | 1508 | 2946 |
| **1993** | 1891 | 47275 | 9.0 | 91 | 1981 | 1390 | 34750 | 6.6 | 91 | 1480 | 474 | 11850 | 2.2 | 1508 | 1981 |
| **1995** | 2975 | 74375 | 14.1 | 0 | 2974 | 1481 | 37025 | 7.0 | 0 | 1480 | 1467 | 36675 | 6.9 | 1508 | 2974 |
| **1996** | 1070 | 26750 | 5.1 | 1305 | 2374 | 176 | 4400 | 0.8 | 1305 | 1480 | 867 | 21675 | 4.1 | 1508 | 2374 |
| **1997** | 987 | 24675 | 4.7 | 1315 | 2301 | 166 | 4150 | 0.8 | 1315 | 1480 | 794 | 19850 | 3.8 | 1508 | 2301 |
| **1998** | 943 | 23575 | 4.5 | 1405 | 2347 | 76 | 1900 | 0.4 | 1405 | 1480 | 840 | 21000 | 4.0 | 1508 | 2347 |
| **1999** | 963 | 24075 | 4.6 | 1382 | 2344 | 99 | 2475 | 0.5 | 1382 | 1480 | 837 | 20925 | 4.0 | 1508 | 2344 |
| **2002** | 2973 | 74325 | 14.1 | 2 | 2974 | 1479 | 36975 | 7.0 | 2 | 1480 | 1467 | 36675 | 6.9 | 1508 | 2974 |
| **2004** | 2965 | 74125 | 14.0 | 10 | 2974 | 1471 | 36775 | 7.0 | 10 | 1480 | 1467 | 36675 | 6.9 | 1508 | 2974 |
| **2006** | 2972 | 74300 | 14.1 | 3 | 2974 | 1478 | 36950 | 7.0 | 3 | 1480 | 1467 | 36675 | 6.9 | 1508 | 2974 |
| **2007** | 2678 | 66950 | 12.7 | 176 | 2853 | 1305 | 32625 | 6.2 | 176 | 1480 | 1346 | 33650 | 6.4 | 1508 | 2853 |
| **2008** | 2693 | 67325 | 12.8 | 159 | 2851 | 1323 | 33075 | 6.3 | 159 | 1480 | 1345 | 33625 | 6.3 | 1508 | 2851 |
| **2009** | 2678 | 66950 | 12.7 | 153 | 2846 | 1329 | 32225 | 6.3 | 153 | 1480 | 1339 | 33475 | 6.4 | 1508 | 2846 |
| **2010** | 2678 | 66950 | 12.7 | 153 | 2846 | 1329 | 32225 | 6.3 | 153 | 1480 | 1339 | 33475 | 6.4 | 1508 | 2846 |
| **2011** | 2678 | 66950 | 12.7 | 153 | 2846 | 1329 | 32225 | 6.3 | 153 | 1480 | 1339 | 33475 | 6.4 | 1508 | 2846 |
| **2012** | 2678 | 66950 | 12.7 | 153 | 2846 | 1329 | 32225 | 6.3 | 153 | 1480 | 1339 | 33475 | 6.4 | 1508 | 2846 |
| **2013** | 2678 | 66950 | 12.7 | 153 | 2846 | 1329 | 32225 | 6.3 | 153 | 1480 | 1339 | 33475 | 6.4 | 1508 | 2846 |
| **2014** | 2678 | 66950 | 12.7 | 153 | 2846 | 1329 | 32225 | 6.3 | 153 | 1480 | 1339 | 33475 | 6.4 | 1508 | 2846 |
| **2015** | 2678 | 66950 | 12.7 | 153 | 2846 | 1329 | 32225 | 6.3 | 153 | 1480 | 1339 | 33475 | 6.4 | 1508 | 2846 |
| **2016** | 2678 | 66950 | 12.7 | 153 | 2846 | 1329 | 32225 | 6.3 | 153 | 1480 | 1339 | 33475 | 6.4 | 1508 | 2846 |
| **2017** | 2678 | 66950 | 12.7 | 153 | 2846 | 1329 | 32225 | 6.3 | 153 | 1480 | 1339 | 33475 | 6.4 | 1508 | 2846 |

* 1972: gap in North: 1150 ft, id 808-853

* 1988: gap in South: 1800 ft, id 2034-2104

### 6.1 Results

The fundamental results of mapping shorelines from aerial imagery are presented in Table 7.The results presented and discussed in this section on image-based shoreline change will focus on the linear regression method. However, results obtained through the use of the end-point-rate (EPR) method are also included despite its use being subject to several disadvantages. For example, if either shoreline is uncharacteristic, the resulting rate of change will be misleading; also, data between the endpoints that is ignored may produce rates that do not capture important trends or changes in trends, especially as temporal variation increases (Dolan et al. 1991). The reader is referred to the earlier version of the report for more information on both (the linear regression and end-point-rate) of method used.

**Table 6. Summary of transect coverage to extract shoreline data from aerial imagery**

| Domains | Transect ID | R Marker | Miles |
|---|---|---|---|
| **North** | 0-1480 | 180.5-219 | 7.0 |
| **South** | 1508-2974 | 0-37.5 | 6.9 |
| **N3** | 0-880 | 160.5-203 | 4.2 |
| **N2** | 880-1364 | 203-216 | 2.3 |
| **N1** | 1364-1480 | 216-219 | 0.6 |
| **Inlet** | 1365-1645 | BC216-IRC4 | 1.3 |
| **S1** | 1508-1627 | 0-3.5 | 0.6 |
| **S2** | 1627-212- | 3.5-16 | 2.3 |
| **S3** | 2120-2974 | 16-37.5 | 4.0 |

**Table 7. Average rate of change for EPR and LR methods (ft/yr.).**

| Extent | | Method | ('58-'17) | ('08-'17) | ('13-'17) | ('16-'17) |
|---|---|---|---|---|---|---|
| N-S | | EPR | 0.4286 | -0.2715 | 6.8030 | 25.0420 |
| | | LR | 0.3827 | -0.0658 | 4.7740 | 22.5955 |
| Brevard Co. | N | EPR | 1.1851 | -0.1813 | 7.1565 | 23.4202 |
| | | LR | 0.6514 | 0.0661 | 5.1154 | 20.9690 |
| Indian River | S | EPR | -0.3595 | -0.3595 | 6.4603 | 26.6530 |
| | | LR | -0.1978 | -0.1978 | 4.4345 | 24.2184 |
| Brevard Co. | R180.5 – 203 (N3) | EPR | 0.8031 | 0.4632 | 8.1233 | 24.9781 |
| | | LR | 0.5698 | 0.3856 | 5.4689 | 20.5835 |
| | R203 – 216 (N2) | EPR | 1.7286 | -0.5001 | 7.1979 | 22.9748 |
| | | LR | 0.7405 | -0.1734 | 5.7067 | 22.9748 |
| | R216 – 219 (N1) | EPR | 1.2894 | -2.8651 | 0.9801 | 15.6030 |
| | | LR | 0.8920 | -1.3672 | 0.0131 | 15.6030 |
| Indian River Co. | R1 – 3.5 (S1) | EPR | 3.7152 | -0.3827 | 17.8001 | 51.5266 |
| | | LR | 2.7424 | -0.3796 | 15.2919 | 51.0972 |
| | R3.5 – R16 (S2) | EPR | -0.7405 | -2.6315 | 5.3669 | 21.2469 |
| | | LR | -0.7751 | -1.4731 | 3.5537 | 21.2469 |
| | R16 – 37.5 (S3) | EPR | -0.6400 | 0.6159 | 5.3583 | 26.2887 |
| | | LR | -0.6381 | 0.5630 | 3.4323 | 22.1993 |
| Inlet | | EPR | 2.5671 | -0.4165 | 9.3721 | 33.4378 |
| | | LR | 1.8755 | -0.6644 | 7.6165 | 33.4378 |

In general, both methods yielded similar results with most of the values in the same order of magnitude and with either a positive or negative trend in concordance with each other the EPR and LR methods yielded similar trends in all domain within the selected time periods shown in Table 7.

Historical Period (1958-2016)

As seen in Figure 37, comparing the 1958 and 2017 shorelines, the distance from the baseline to the wet/dry shifted seaward by distances of up to 125 feet. A section of beach centered around Brevard R-marker 4 retreated by up to 35 feet between 1958 and 2017. South of Sebastian Inlet between Indian River (IRC) County R-markers 6 and 9 the shoreline shifted seaward by up to 225 feet. Further south to IRC R-marker 24 where the earlier aerial image coverage ends, the shoreline retreated over the 1958 to 2017-time scale. Table 8 lists shoreline change rates according to the LR method, the range of shoreline changes, and the percent of the shoreline in undergoing erosion or accretion with respect to position of the aerial image.

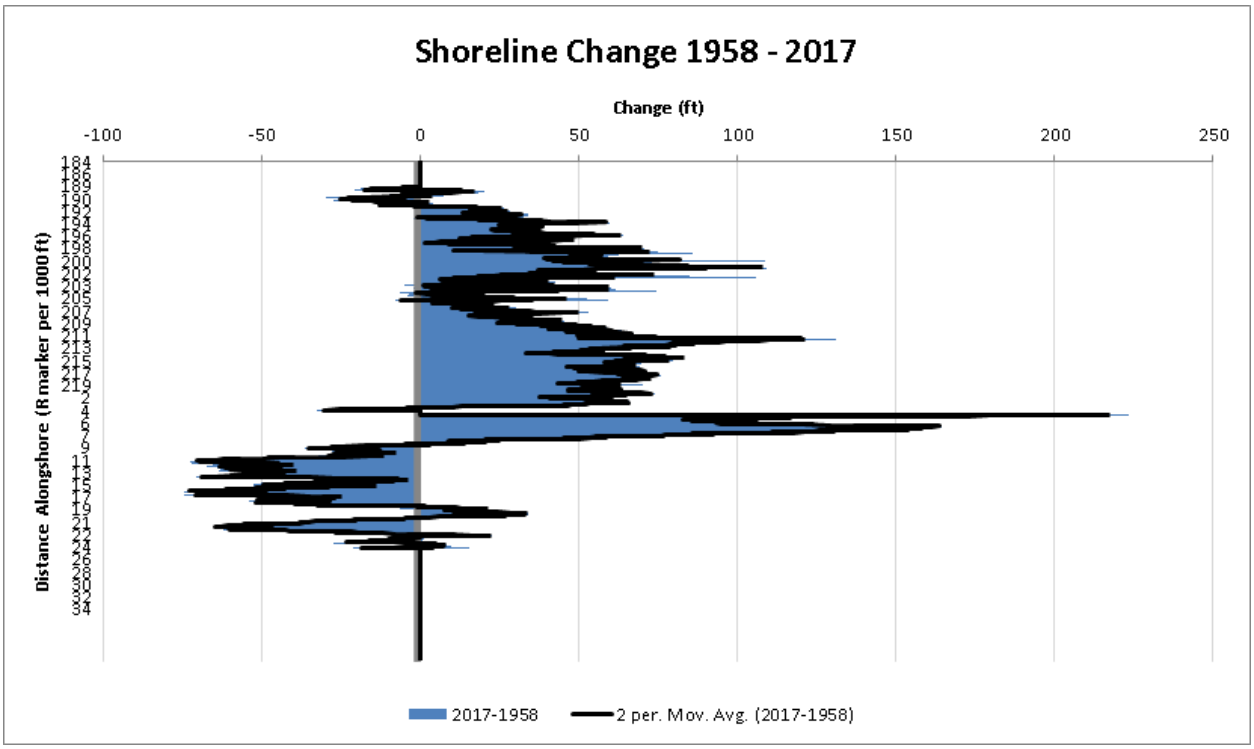


**Figure 37. Change (ft) in shoreline position from 1958-2015.**

**Table 8. Summary shoreline changes for the historical period (1958-2017).**

| Extent | Range(ft/yr.) | Average LR (ft/yr.) | Erosion % | Accretion % |
|---|---|---|---|---|
| **North to South** | -1.97 to +3.4205 | +0.2973 | 30.49 | 68.61 |
| **North** | -0.85 to 1.9074 | +0.5558 | 20.19 | 79.81 |
| **South** | -1.97 to 3.4205 | +0.0360 | 41.45 | 58.49 |
| **N3** | -0.85 to1.9074 | +0.4198 | 33.03 | 66.97 |
| **N2** | -0.08 to1.5442 | +0.7091 | 1.65 | 98.35 |
| **N1** | 0.63 to 1.2295 | +0.9408 | 0 | 100 |
| **Inlet** | 0.00 to +3.4205 | +1.8380 | 0 | 90.39 |
| **S1** | 0.00 to +3.4205 | +2.6264 | 0 | 99.17 |
| **S2** | -0.13 to 2.5024 | +0.7376 | 2.43 | 97.57 |
| **S3** | -1.97 to 0.7687 | -0.7293 | 69.71 | 30.29 |

The greatest area of accretion occurs just south of the inlet between the jetty and the attachment bar (S1) from R2 to R4 with a maximum of +3.48 ft/yr at an average of +2.64 ft/yr. In contrast, the region from R16 to R 37 (S3) is predominantly erosional with an average rate of change of -0.75 ft/yr including the maximum erosion rate of about -2.00 ft/yr for the entire domain of the study area (near R-26). The northern sub-domain is also predominantly accreting with only smaller regions showing erosional trends.

Intermediate Period (2008-2017)

Figure 38 and Table 9 list the results of the shoreline analysis results for the 2008 to 2017 period. The trend obtained by analyzing the time series of data representing the past 9 year the years of shoreline change indicates the beaches along the 14-mile domain are predominantly eroding. In this case both methods (EPR and LR) are in agreement that the majority of the study area is experiencing erosion (Table 9). Shoreline recession dominates in most of the shoreline segments area from north to south. However, the percentages are more or less subequal with

shoreline recession generally having the highest occurrence on a percentage basis. The average shoreline recession rate for the entire study area is low at rate of about 0.06 ft/yr.

The shoreline from about R-4 to R-9 shifted seaward to a maxim about +30 ft at R-6, while the entire north extent has receded to an average of -10.89 ft at -0.99 ft/yr. (Figure 38). South of R-9 in subdomain S2, shoreline recession dominates in this period. The southernmost region from R16-R37.5 (sub-cell S3) is the only area in which accretion is occurring at about 64 % with a rate of change of about 0.6 +ft/yr.

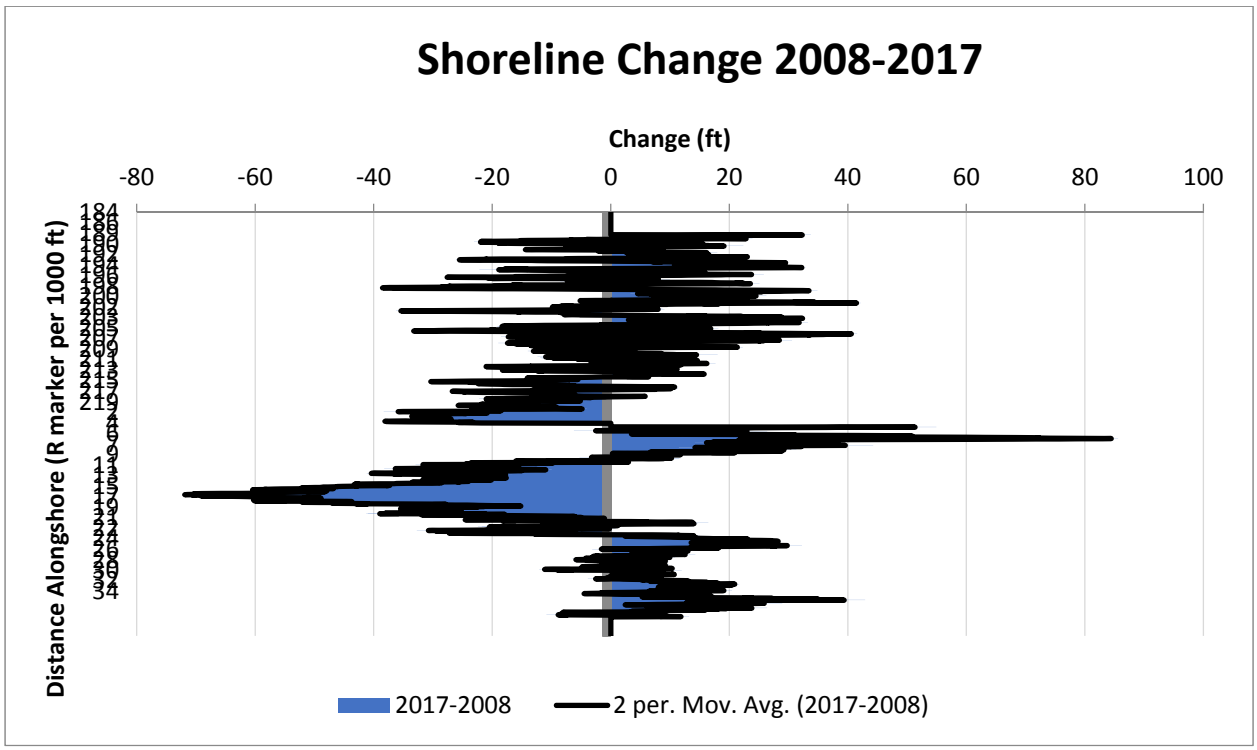


**Figure 38. Change (ft) in shoreline position from 2008-2017.**

**Table 9. Summary of short-term changes for the recent period (2008-2017).**

| Extent | Range (ft/yr) | Average LR (ft/yr) | Erosion % | Accretion % |
|---|---|---|---|---|
| **North to South** | -6.76 4.87 | -0.0658 | 39.93 | 49.34 |
| **North** | -2.85 3.54 | 0.066 | 42.47 | 46.79 |
| **South** | -6.76 to 4.87 | -0.20 | 38.04 | 52.83 |
| **N3** | -2.85 3.5439 | 0.38 | 25.99 | 55.96 |
| **N2** | -2.51 to 2.22 | -0.17 | 58.97 | 41.03 |
| **N1** | -2.72 0.31 | -1.3672 | 99.15 | 0.85 |
| **Inlet** | -4.14 to 4.87 | -0.6644 | 65.48 | 24.91 |
| **S1** | -4.14 to 4.87 | -0.3796 | 56.67 | 42.50 |
| **S2** | -6.76 to 3.84 | -1.47 | 65.38 | 34.62 |
| **S3** | -4.09 to 3.09 | 0.56 | 19.65 | 64.80 |

.

Recent Update (2013-2017)

As apparent in Figure 39 and Table 10the 2013-2017 period is one of shoreline accretion, which is consistent with the sand volume analysis results shown in Figures 10 to 18 of Section 3 of this report and in Figure 29, which shows a 3-year sand budget (2013-2016) requiring onshore sand transport for balance. As stated in the previous report Section describing the sand budget for the Sebastian Inlet area periods of sand volume accretion and as shown here, periods of shoreline accretion can dominate the entire region. The fundamental process that is likely to account for periods of stability and sand volume accumulation is periods of lower sea level sea level that can last two years or longer as seen in Figure 22.

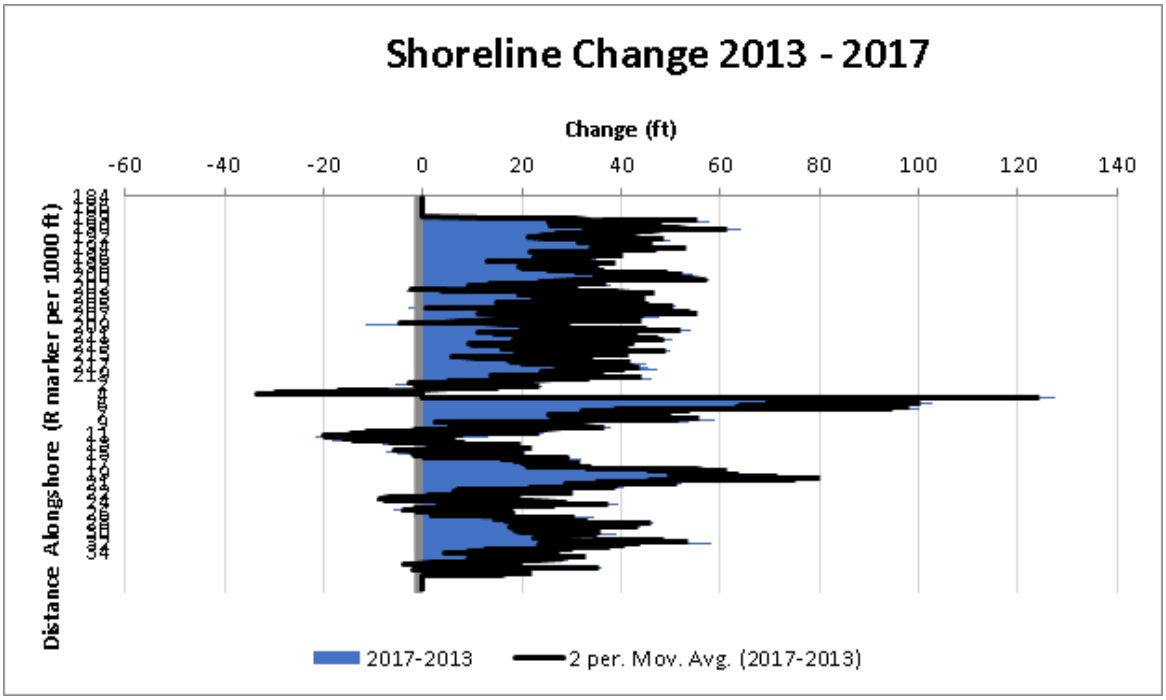


**Figure 39. Change (ft) in shoreline position from 2013-2017.**

**Table 10. Summary of short-term changes for the latest update (2013-2017)**

| Extent | Range (ft/yr) | Average LR (ft/yr) | Erosion % | Accretion % |
|---|---|---|---|---|
| North to South | -7.37 to 75.77 | 22.59 | 0.74 | 88.67 |
| North | -7.37 to 49.97 | 20.96 | 0.81 | 88.72 |
| South | -6.62 to 75.77 | 24.21 | 0.68 | 90.18 |
| N3 | -7.37 to 49.97 | 20.58 | 1.25 | 81.16 |
| N2 | 4.41 to 42.64 | 22.97 | 0 | 100.00 |
| N1 | -0.39 to 29.75 | 15.60 | 0.85 | 99.15 |
| Inlet | -0.39 to 75.77 | 33.43 | 0.36 | 90.04 |
| S1 | 0.00 to 75.77 | 51.09 | 0.00 | 99.17 |
| S2 | -6.62 to 52.52 | 21.24 | 2.02 | 97.98 |
| S3 | 0.00 to 46.52 | | 0.00 | 84.44 |

Annual Update (2016-2017)

Analysis of the most recent shoreline changes available from comparison of the 2016 to 2017 aerial imagery is shown in Figure 40.The overall region under study has an average shoreline change at a rate of about 22 ft/yr. (Table 11), The accretion trend is encountered throughout almost all of the entire 14-mile extent. The percentages of the shoreline analysis domains having a shoreline accretion trend range from more than 81 to 100 %. In addition to the beach fill places in selected areas to the north and south of the inlet, the main factor accounting for shoreline accretion is the period of sand volume accumulation linked to falling sea level in the 2015-2017 period.

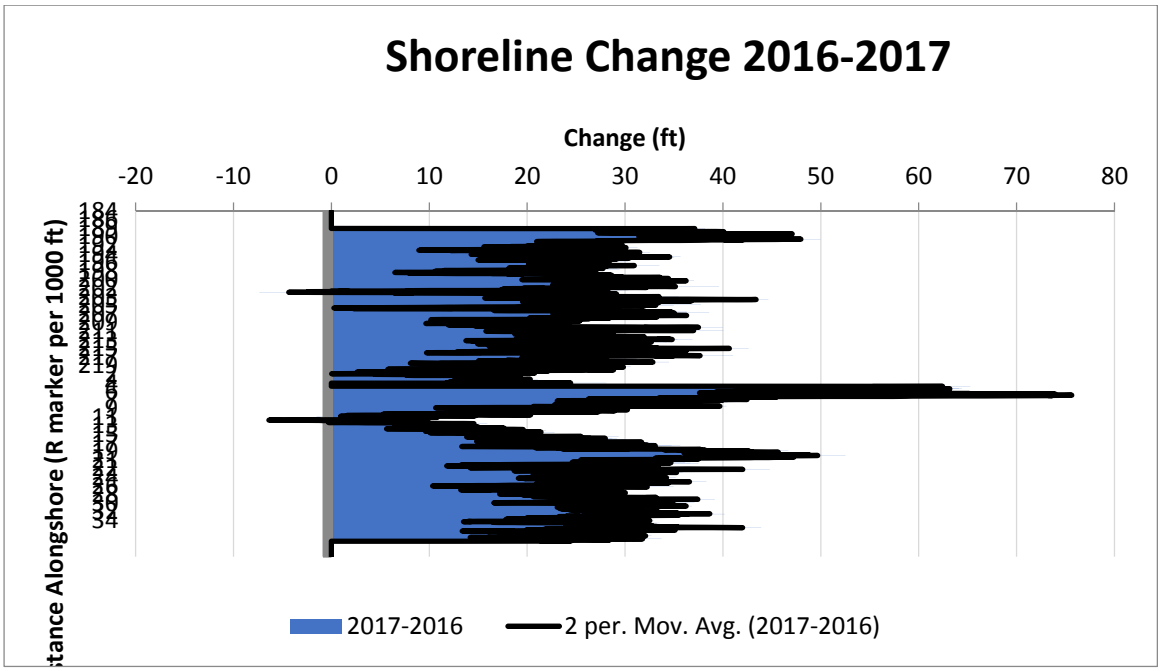


**Figure 40. Change (ft) in shoreline position from 2016-2017.**

Table 11 Summary of short-term changes for the recent period (2016-2017)

| **Extent** | **Range (ft/yr)** | **Average LR (ft/yr)** | **Erosion %** | **Accretion %** |
|---|---|---|---|---|
| North to South | -7.37 to 75.77 | 22.59 | 0.74 | 88.67 |
| North | -7.37 to 49.97 | 20.96 | 0.81 | 88.72 |
| South | -6.62 to 75.7700 | 24.22 | 0.68 | 90.18 |
| N3 | -7.37 to 49.97 | 20.58 | 1.25 | 81.16 |
| N2 | 4.41 to 42.64 | 22.97 | 0 | 100.00 |
| N1 | -0.39 to 29.75 | 15.60 | 0.85 | 99.15 |
| Inlet | -0.39 to 75.7 | 33.43 | 0.36 | 90.04 |
| S1 | 0.00 to 75.7700 | 51.09 | 0 | 99.17 |
| S2 | -6.62 to 52.52 | 21.24 | 2.02 | 97.98 |
| S3 | 0.00 to 46.52 | 22.20 | 0 | 84.44 |

## 7.0 Numerical Modeling 2016-2017: Hurricane Impacts

The primary goal of numerical modeling for the 2016 – 2017 effort is to simulate and evaluate the effect of Hurricane Matthew on the inlet. The movement and exchange of material between the sediment reservoirs during and after the storm will be examined as well as the hydrodynamic conditions during the storm. This section presents both the numerical modeling efforts with the measured field data during Hurricane Matthew.

### 7.1 Model Improvements and Development

*2016 LIDAR Data*

The bottom topography dataset greatly benefited from pre and post-storm Light Detection and Ranging (LIDAR) topography flown by the U.S. Army Corps of Engineers (USACE). Flights were performed in May – June 2016 and again after Hurricane Matthew on November 16$^{th}$, 2016. Areas within the model grid were refined and updated with the latest pre-storm bottom topography most notably along the channel banks and the tide pool. This refinement aids in better representation of the field as well as aid in model stability. The post storm lidar also provided coverage where the traditional survey omitted such as portions of the flood shoal and nearshore areas. Figure 41 presents the pre-Hurricane (panel a, left) and post-Hurricane (panel b, right) LIDAR coverage. Warmer colors indicate higher elevations while cooler colors indicate deeper water depths. These data are also used to produce difference plots to evaluate the performance of the model with regards to morphology change.

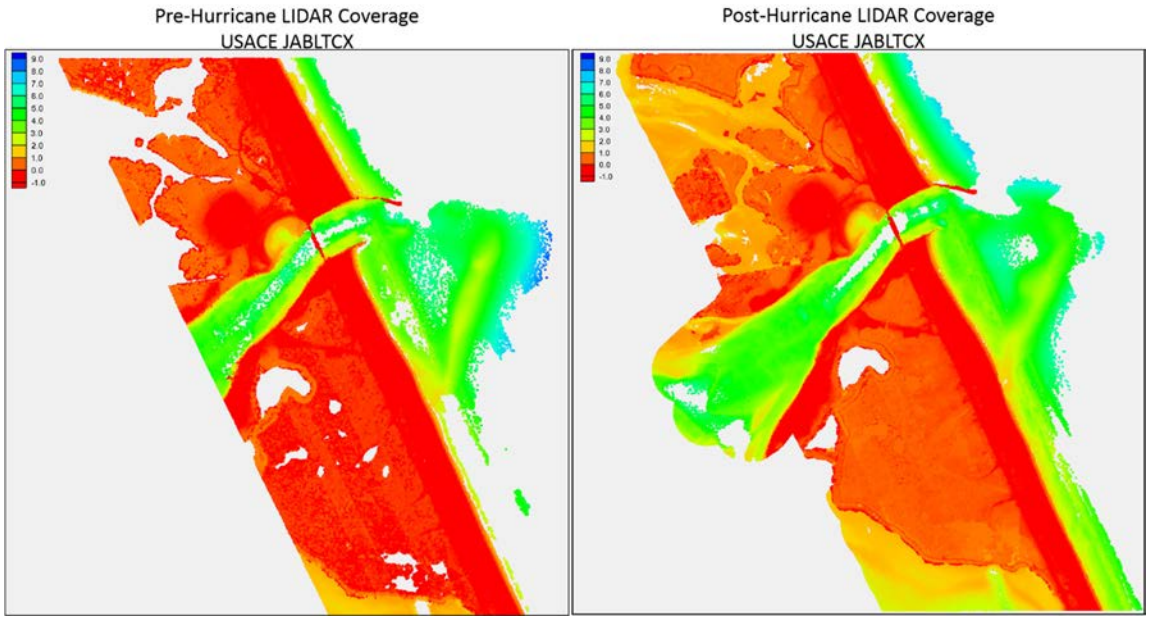


**Figure 41. Pre and Post Hurricane LIDAR Coverage.**

## 7.2 Model Description and Set Up

The Coastal Modeling System (CMS) developed and maintained by the Coastal Inlets Research Program (CIRP) which is a research group at the Coastal Hydraulics Laboratory (CHL), part of the USACE Engineer Research and Development Center (ERDC) located in Vicksburg, MS. The coastal processes included in the CMS model are diagramed in Figure 42.

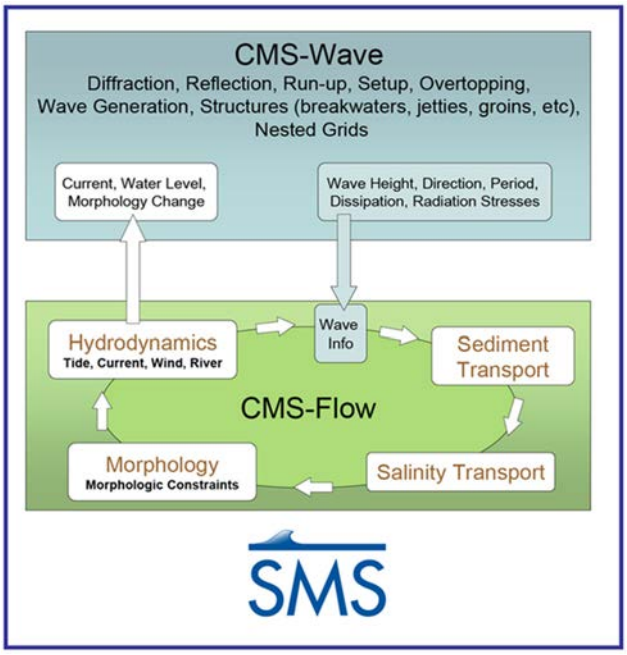


**Figure 42. CMS Components (CIRP, 2016).**

The model applied to the Sebastian Inlet includes three distinct components; a regional wave grid, local wave and flow grids. The regional wave grid which extends 40 km offshore and 18 km alongshore is used to bring in waves from the offshore using NOAA's Wave Watch III as a model input. The offshore boundary corresponds to water depths of 40 meters. The regional wave grid consists of approximately 71,000 computational cells. Calculated wave data from the regional grid is extracted and used as a model input for the local wave grid. Water level data is developed to include the seasonal high and low stands of sea level that fluctuates annually at this location. These variations are up to a meter and are an important process at this location.

The local model set up consists of both a wave and flow grid. The flow grid contains approximately 340,000 computational cells spanning alongshore approximately 18 km with the inlet located at the midpoint. The grid includes the Indian River Lagoon and extends offshore approximately 6 km to a water depth of 13 m. Figure 43 shows the local grid domain coverage and refinement. The refinement for the ocean cells range from 5 m x 5 m at the inlet mouth to 160 m x 160 m in the offshore. This telescoping quadtree approach optimizes computational time while increasing the ability for high levels of resolution in the nearshore and inlet areas.

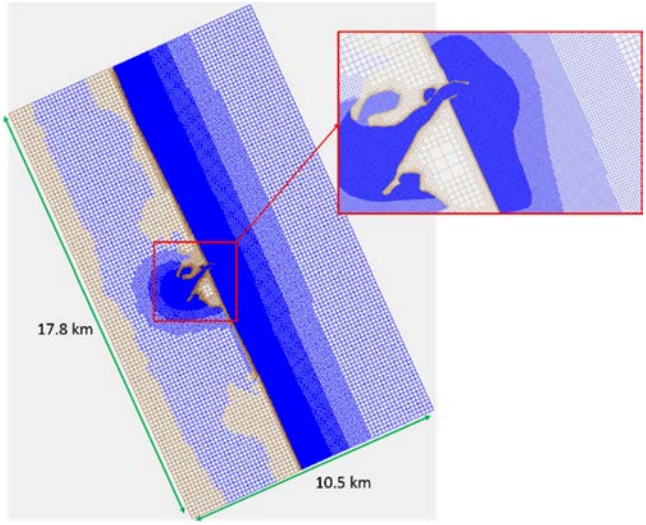


**Figure 43. CMS Local Flow Grid Domain and Refinement.**

The simulation for this year temporally spans August 1st, 2016 to December 31st, 2016 to include Hurricane Matthew and match the survey dates. A pre-storm survey was performed in September 2016 and a post-storm survey taken in December 2016.

### 7.3 Model Skill

Goodness of fit statistics were calculated using the measured field data and the computed results of the model to evaluate the performance of the model to replicate the study area. Due to the alongshore placement of the nearshore ADCPs as part of the ongoing monitoring program, the model skill can be evaluated at 2 different locations across the domain.

Table 12 presents the goodness of fit statistics determined for hydrodynamics. Sediment transport rates were not directly measured as part of the field campaign and is not included for this evaluation.

**Table 12. Goodness of Fit Statistics: Hydrodynamics.**

| Parameter | Mean Error (m) | Mean Absolute Error (m) | RMSE (m) | Normalized RMSE | Evaluation |
|---|---|---|---|---|---|
| **North Jetty ADCP Location** | | | | | |
| Water Surface Elevation | -0.007 | 0.293 | 0.451 | 16.71% | Underprediction |
| Wave Height | 0.23 | 0.22 | 0.42 | 11.97% | Overprediction |
| Wave Period | -0.06 | 2.30 | 1.35 | 12.57% | Underprediction |
| Current Magnitude | -0.07 | 0.07 | 0.23 | 15.62% | Underprediction |
| **South Station 2** | | | | | |
| Water Surface Elevation | -0.35 | 0.48 | 0.62 | 12.61% | Overprediction |
| Wave Height | 0.40 | 0.42 | 0.58 | 15.43% | Overprediction |
| Wave Period | -0.21 | 1.38 | 1.01 | 9.09% | Underprediction |
| Current Magnitude | -0.06 | 0.06 | 0.23 | 27.01% | Underprediction |

The water surface elevation showed good correlation with the measured data throughout the run except underpredicting the peak during Hurricane Matthew. Figure 44 shows a comparison between measured and calculated water surface elevation spanning 11 days of simulation time from 10/1/2016 – 10/11/2016 as extracted from the model at the legacy ADCP

location immediately north of the North Jetty. The calculated water surface elevation compares well with the measured water surface elevation during the majority of the model run but misses the peak by approximately 1m in water surface elevation. This underprediction during the storm could be caused by processes such as wind not being sufficiently represented in the model. It should also be noted that the comparison for water surface elevation was performed using the field measurements collected at the north jetty rather than the measurements via pressure gauge on the bottom mounted ADCP. This is performed for this dataset only because of the relative unknown height of the pressure transducer from the bottom. The comparison between measured and calculated water surface elevation at the South Station 2 gauge performed slightly better. Figure 45 presents the comparison between measured and calculated water surface elevation at the South Station 2-gauge location.

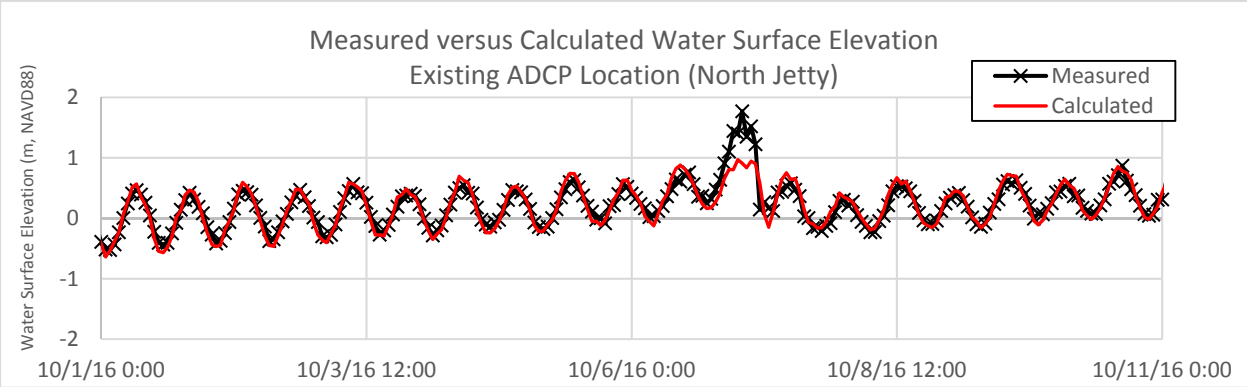


**Figure 44. Measured versus Calculated Water Surface Elevation (North Jetty).**

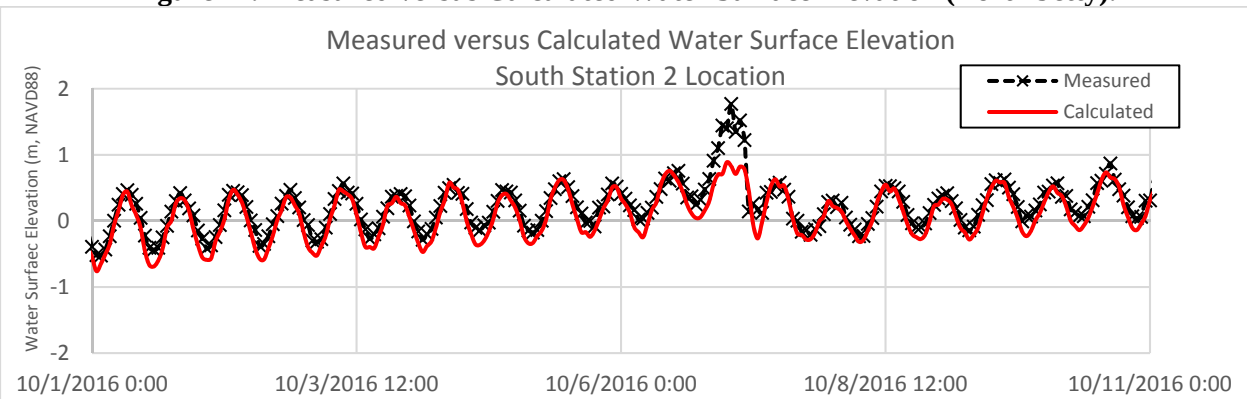


**Figure 45. Measured versus Calculated Water Surface Elevation (South Station 2).**

Figure 46 and Figure 47 compare the calculated and measured significant wave height for the North Jetty and South Station 2-gauge location respectively. For wave height fit statistics, the south station 2 location value is almost twice the values at the north jetty gauge. This is most likely due to the presence of reef near the south Station 2 gauge. This performance indicates there is not enough roughness added to the model. Roughness is represented in the CMS wave and flow model as Manning's N. In the wave model it is assumed constant but the flow model allows for spatially varying. Manning's N is adjusted where reef is present as well as coarser grain sizes. In the model near the South Station 2 location, the bottom is represented as fully erodible and the previous mapped locations of reef are inshore from the gauge location. Known reef rock locations may need to be updated and potentially expanded.

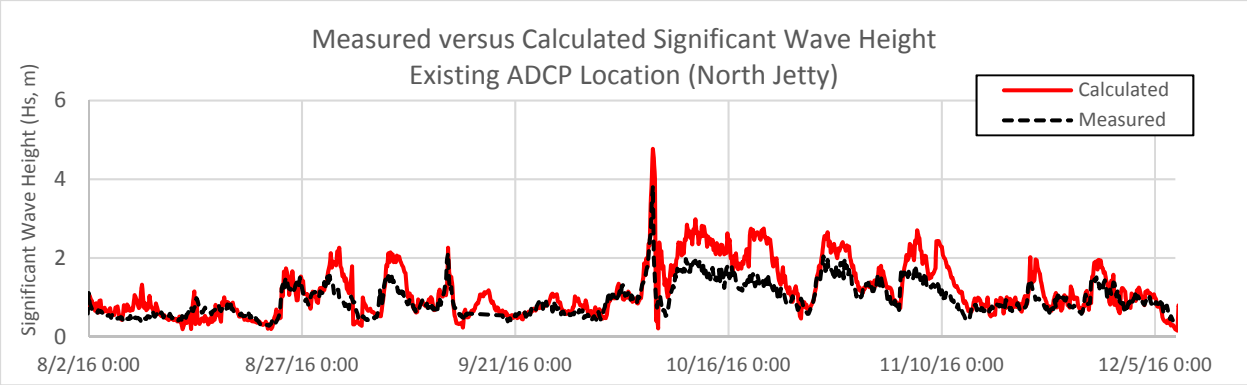


**Figure 46. Measured versus Calculated Significant Wave Height (North Jetty).**

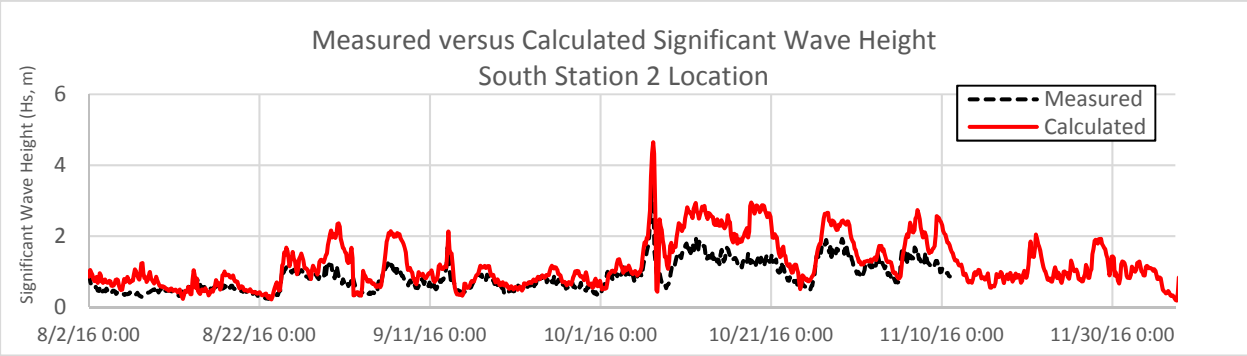


**Figure 47. Measured versus Calculated Significant Wave Height (South Station 2).**

Figure 48 and Figure 49 details the wave period comparison between measured and calculated.

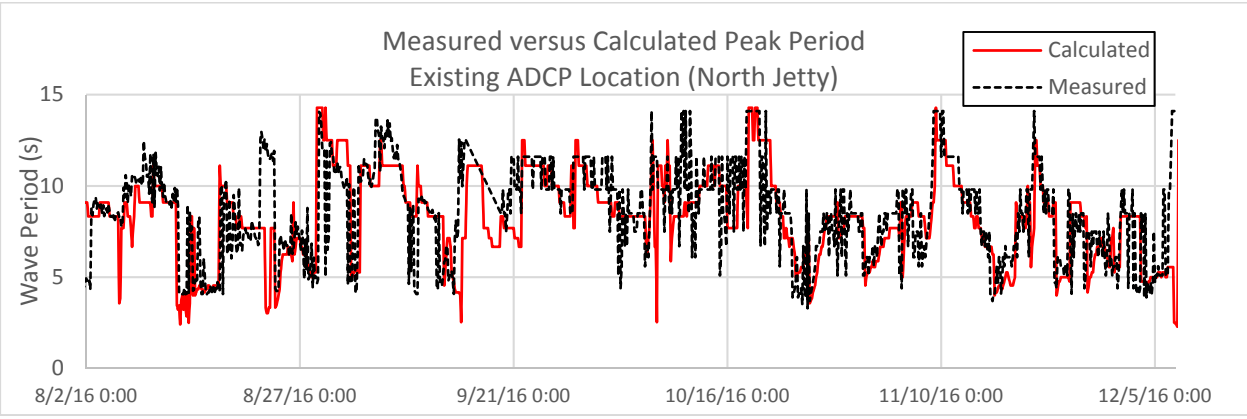


**Figure 48. Measured versus Calculated Peak Period (North Jetty).**

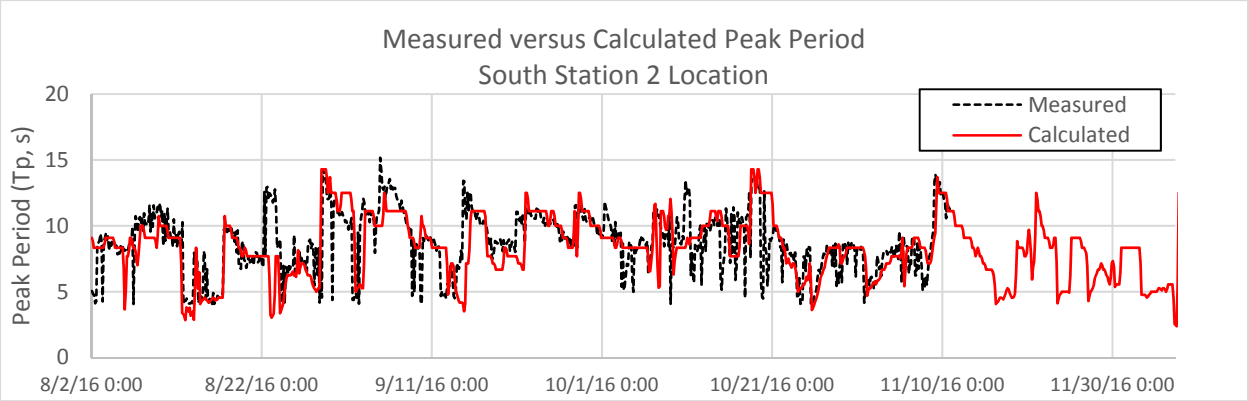


**Figure 49. Measured versus Calculated Peak Period (South Station 2).**

Current magnitude plots focusing on Hurricane Matthew are presented in Figure 50 and Figure 51. There is poor agreement between the measured and calculated data during the Hurricane and throughout the model run. The model is underpredicting the current magnitude. The calculated current magnitude signal looks to be primarily tide driven which indicates that the model is most likely not applying the winds correctly. Further research into improving the model performance for nearshore currents is ongoing.

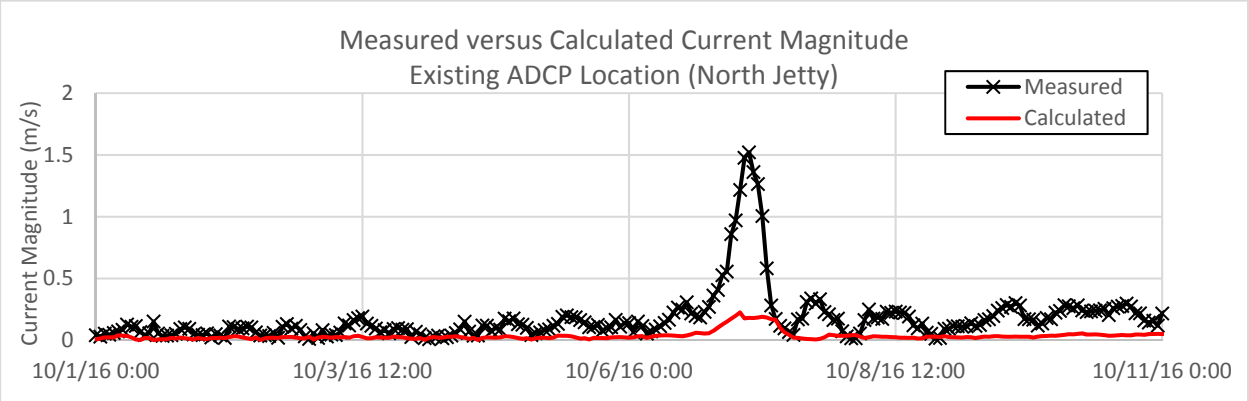


**Figure 50. Measured versus Calculated Current Magnitude (North Jetty).**

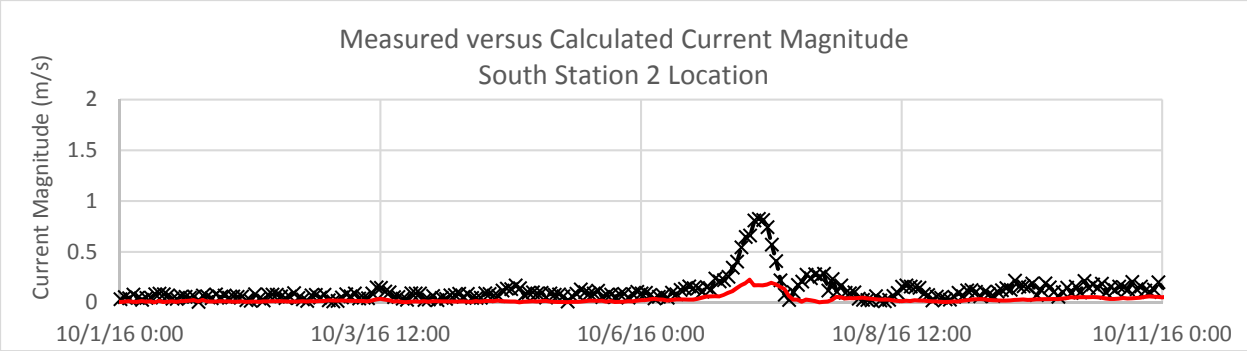


**Figure 51. Measured versus Calculated Current Magnitude (South Station 2).**

## 7.4 Model Results

Figure 52 presents a comparison between measured and calculated morphology change. The left panel (a) is measured morphology change which is a difference plot between the December 2016 and September 2016 surveys. Warmer colors indicate accretion while cooler colors indicate erosion. The color bars are identical in each panel. There is accretion on the crest of the ebb shoal and the southern nearshore areas. Erosion occurred on the outer lobe of the ebb shoal as well as areas near coconut point. The white area directly to the north of the inlet and immediately offshore of the ebb shoal indicates a gap in survey data from the post storm survey. The right panel (b) is the calculated morphology change from the CMS model over the same time period. The general patterns of erosion and accretion are replicated on the ebb shoal and the nearshore areas. However, much more material is shown to deposit in the sand trap than measured in panel a. There is some erosion calculated near coconut point but some of the finer areas of accretion in the channel are lost.

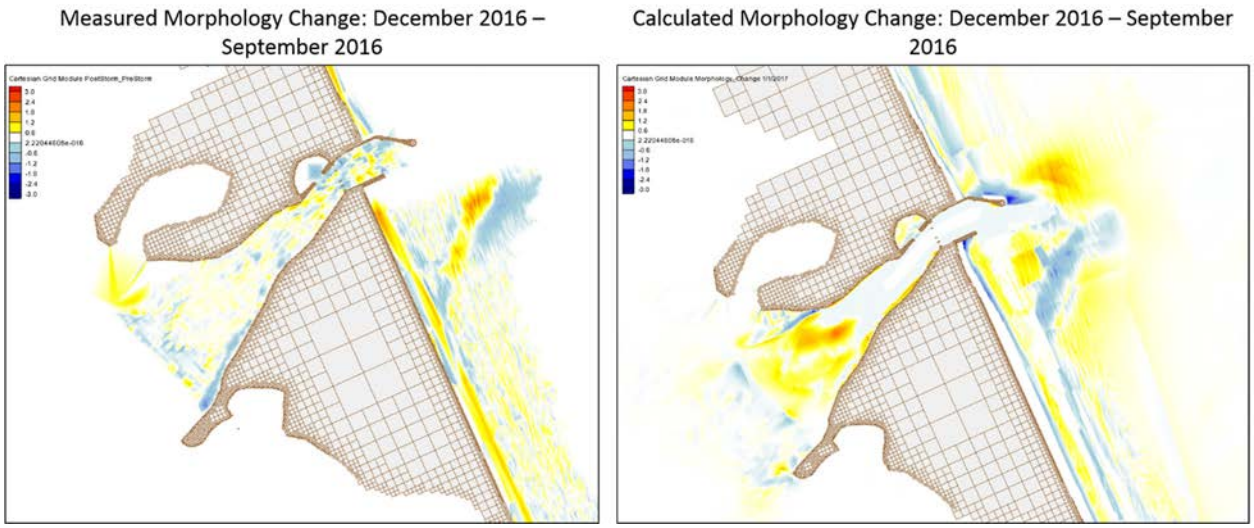


**Figure 52. Measured and Calculated Morphology Change Comparison.**

The poor performance of the model in the channel throat is most likely due to the model not reproducing the flow through the throat well. Field data is difficult to obtain in the channel preventing further tuning of the model in this area of the domain.

### 7.5 Discussion

The numerical model reproduced wave height, peak period and water surface elevation at two locations in the domain. Future improvements in the model will include an expanded reef outcrop to the south to better represent wave heights in the model. Model performance for water surface elevation was well throughout the time series but underpredicted the storm surge at both locations in the model. It should be noted that the comparison for water surface elevation is between the radar water level gauge and the measured location due to the imprecise elevation of the bottom mounted ADCP. Current magnitude was not well reproduced in the model Further investigation is needed as to why and how the model is providing poor performance for current magnitudes. Calculated morphology change compared well to measured qualitatively. The model was able to erode sand from the outer portion of the ebb shoal and deposit the bulk of the material on the nearshore attachment bar area. This model skill efforts using Hurricane Matthew field data provided insights into future model development.

## 7.6 Hurricane Matthew Observations

The established nearshore monitoring array was able to record the effects of Hurricane Matthew as it passed the inlet in October, 2016. The following section details the observations during Hurricane Matthew and compares the data from the two recovered gauges. Figure 53 shows the data recorded by the MET tower spanning October 7th through 9th.

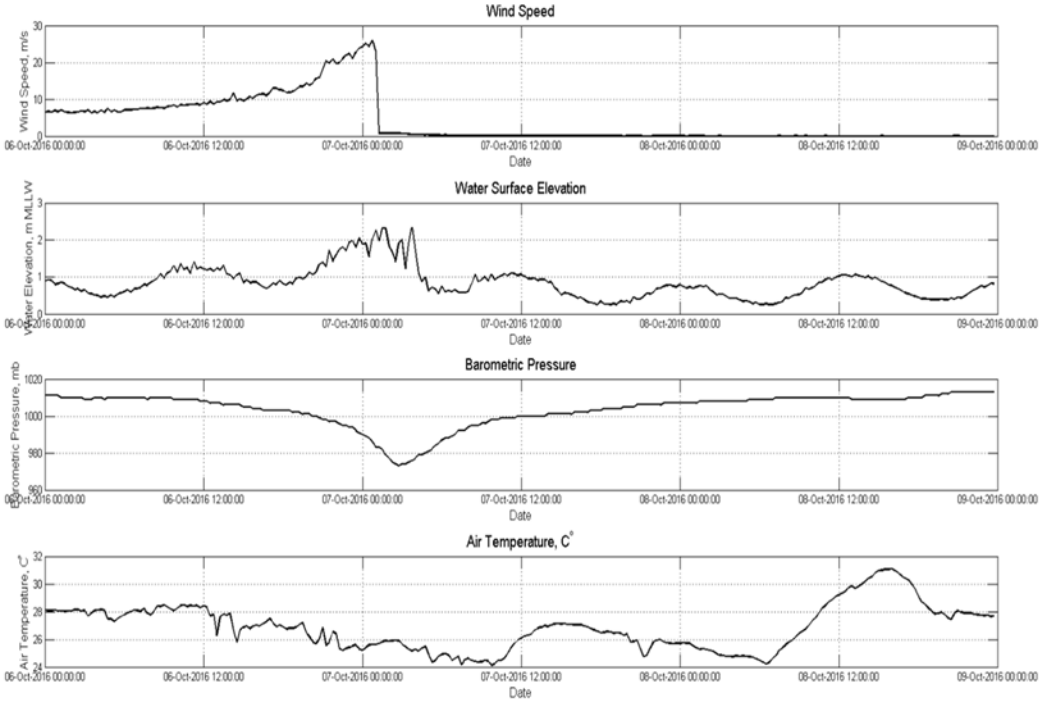


**Figure 53. Metrologic Observations during Hurricane Matthew.**

The recorded wind speed shown in the top panel peaks at 25 m/s (56 mph) and dropped rapidly as the blades of the impeller flew off during the storm. The anemometer has since been replaced and full monitoring capabilities of the MET tower restored. Storm surge recorded by the radar water level gauge during the storm was approximately 1 m (3.3 ft). Maximum wave height recoded during the storm was 4 m (13 ft) as shown in the timeseries provided in Figure 3. This wave height is smaller than waves recorded from NDBC buoy 41114 which peaked at 6.3 m (21 ft) before records ceased during the storm. It should be noted that the NDBC buoy is in deeper water (16 m or 54 ft) than compared with the Sebastian nearshore gauges that are deployed at a water depth of 8 m. Higher than average waves persisted (Figure 54) post storm as

low pressure systems continue to affect the region. Waves approximately 1 m higher than normal continued post storm.

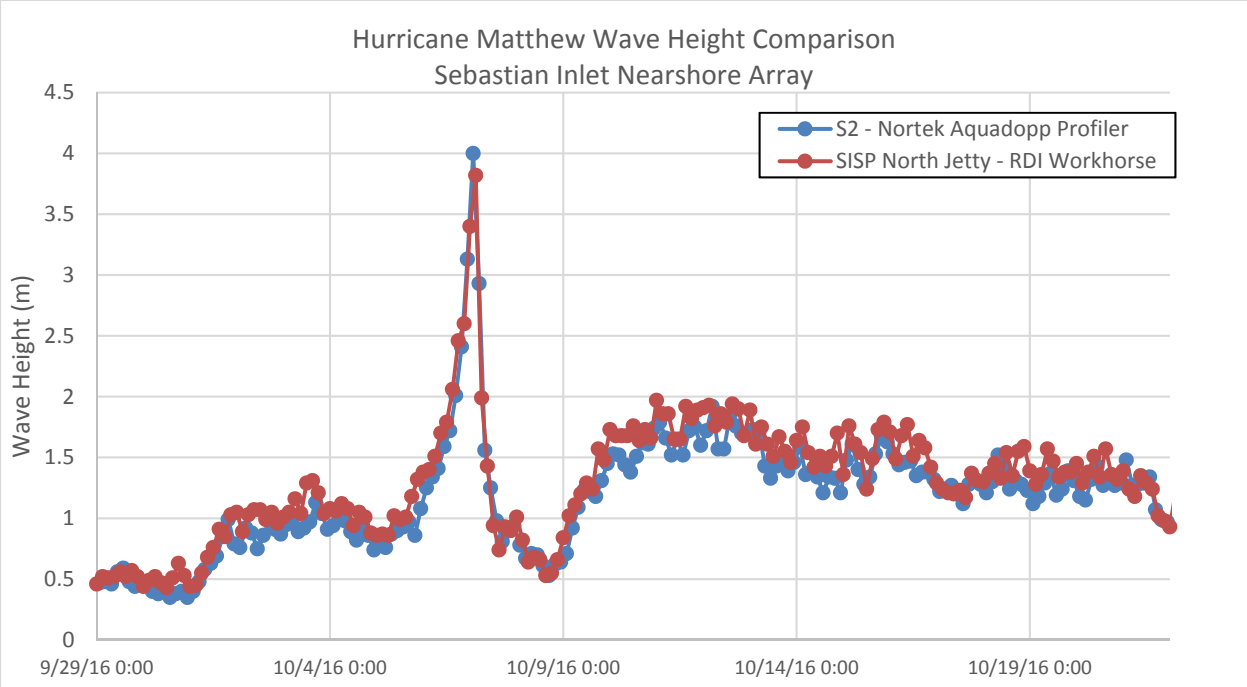


**Figure 54. Hurricane Matthew Wave Height Observations (North Jetty and South Station 2).**

Depth averaged current data recovered from the "Existing ADCP" and "South Station 2" gauges is presented as directional roses in Figure 55. The current roses are in oceanographic convention indicating the direction towards the current is flowing. The current speeds reached a maximum of 1.6 m/s at the "Existing ADCP" gauge in contrast to the 10-year average current speed of 0.1 m/s. The most important finding for ongoing monitoring is the bi-directionality of the currents at the southern portion of the model domain. The site of the existing ADCP location immediately north of the inlet was established in the mid 1990's and it has been theorized that this location is experiencing hydrodynamic effects of the inlet and clearly demonstrated in Figure 55.

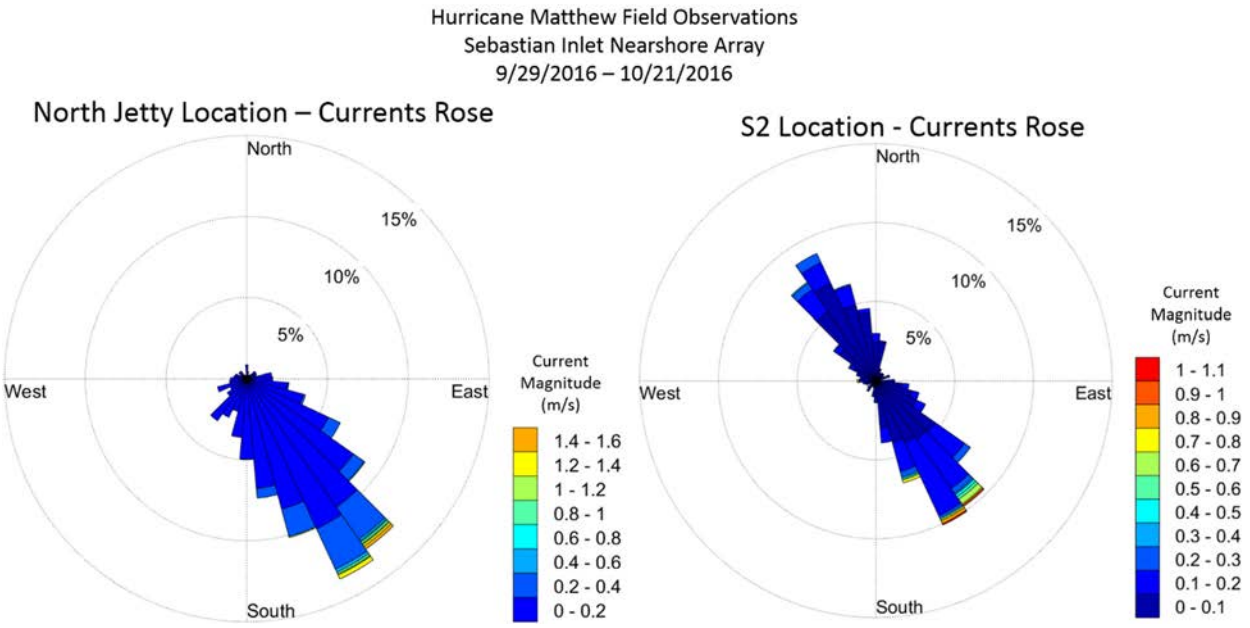


**Figure 55. Measured Current Roses during Hurricane Matthew (North Jetty and South Station 2).**

In particular interest is the response of the various sediment reservoirs to the storm and their post storm evolution. Measured morphology change was also examined across several sediment reservoirs. Bottom topography surfaces were generated using a combination of commercial survey and available Light Detection and Ranging (LIDAR) provided by USACE's Joint Airborne Lidar Bathymetry Technical Center of Expertise (JABLTCX) obtained through NOAA's Digital Coast. Morphology change was measured by taking the difference between the post storm surface and the pre-storm surface extrapolated onto a grid. All measurements and computations were performed in Aquaveo's Surface Water Modeling System (SMS). The sediment reservoirs evaluated for measured volume change include the ebb shoal, downdrift attachment/bypass bar, sand trap and channel throat. Table 1 provides the accretion, erosion and net volume change for each sediment reservoir. Most of the sediment reservoirs experienced a net loss of material except for the downdrift attachment bar area. Figure 56 presents the pre and post storm bottom topography of the ebb shoal of Sebastian Inlet. The crest of the ebb shoal deflects towards the inlet and the southern portion of the ebb shoal moves slightly offshore.

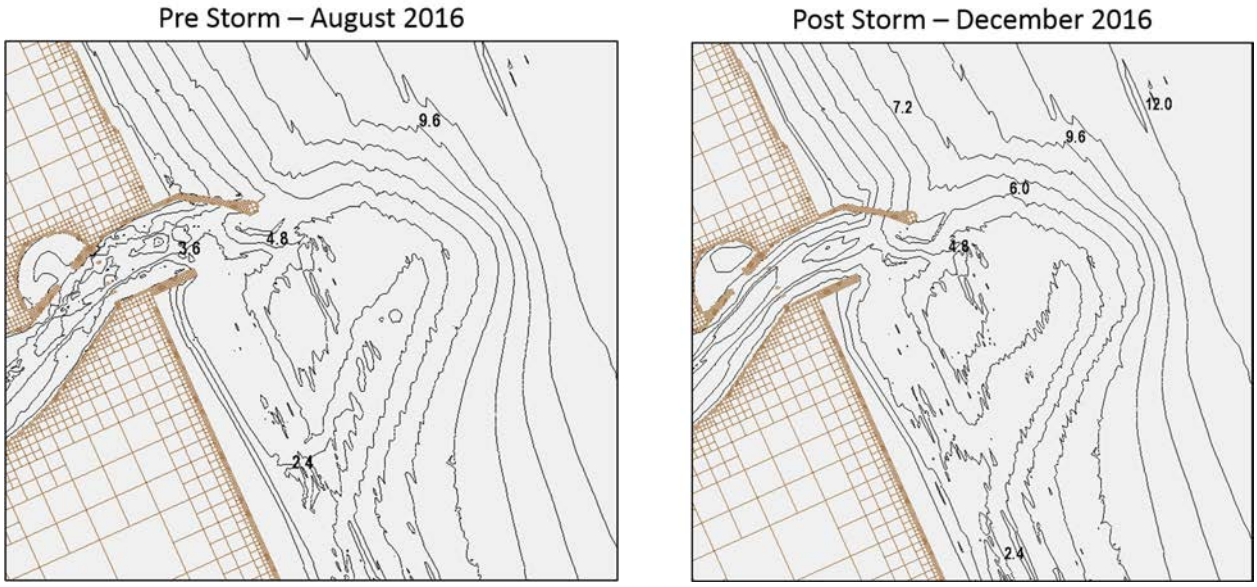


**Figure 56. Measured Bottom Topography Comparison pre and post Hurricane Matthew.**

## 8.0 Hydrodynamic, Sediment Transport and Morphological Numerical Modeling: 2017 – 2018

### 8.1 Purpose

The goals for this modeling work are to evaluate the following:

1. Evaluate model's ability to reproduce Hurricane Irma;
2. Evaluate different methodologies to represent the north jetty within the model environment;
3. Calculate channel infilling after sand trap dredging.

*Bottom Topography Development*

The motivation behind updating the nearshore areas is twofold;

1. better represent the topography above and below the waterline to present condition,
2. improve model stability and performance in nearshore areas and near the boundaries.

Surveys performed by Land and Sea Surveying Concepts, Inc have been incorporated for each season to generate a Winter 2017 and Summer 2017 condition Digital Elevation Model (DEM) to use for the numerical model grids and evaluate model performance to measured morphology change. The latest LIDAR datasets collected by USACE FEMA have also been incorporated to the shoreface and dune areas to better represent the nearshore areas. Specifically, the 2017 Post Irma flight performed in October, 2017 has been added to the Summer 2017 topography dataset. The 2016 Post Matthew flight performed in November, 2016 has been used for the Winter 2017 dataset.

The Indian River Lagoon portions of the merged topography has been updated with the latest survey data of the Intracoastal Waterway (ICW). The survey data was provided by USACE Jacksonville District (SAJ) and the Florida Inland Navigation District (FIND). The ICW datasets were combined with a 1995 survey of the entire Lagoon performed by Morgan and Eckland. The coverage of these datasets and resulting navigation channel and bay areas refinement are shown in Figure 57.

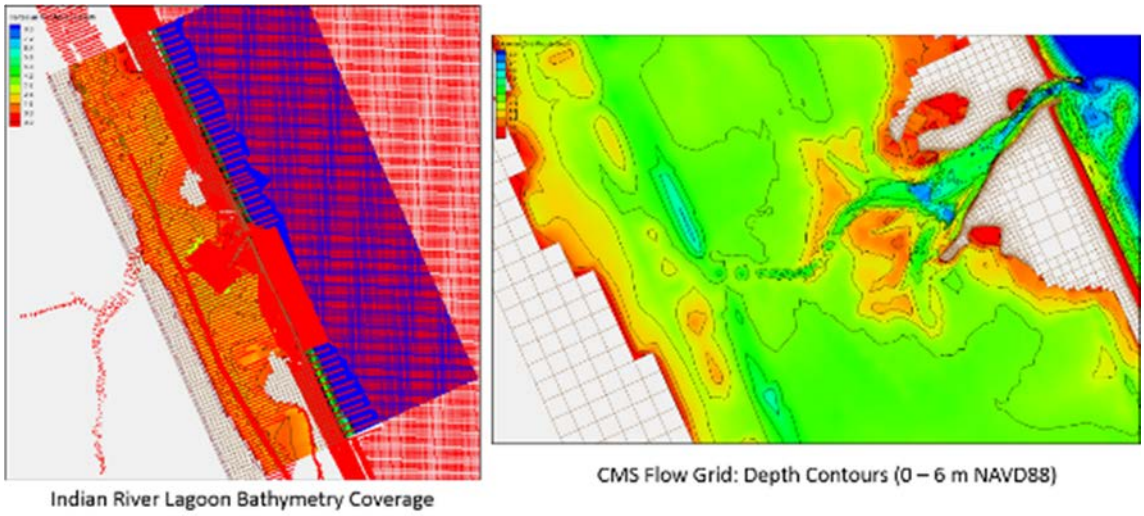


**Figure 57. Indian River Lagoon Refined Bathymetry.**

The merged topographic dataset is spatially referenced to NAD83 State Plane Florida East in meters and vertically to NAVD88 in meters.

## 8.2 Regional Wave Modeling

The regional wave modeling transforms offshore waves to the nearshore for use in the highly refined local model grids. To generate wave inputs for both the Winter and Summer time periods, this model configuration was run for 11 months spanning from January 2017 – October 2017. The structures are represented in the model as rubble mound structures which is defined in the model as a low permeable structure. A sensitivity analysis of the structure specification within the model will be performed in the Local Modeling efforts and described in later sections.

*Regional Model Input Parameters*

The model is driven with offshore waves and winds that are extracted from the NOAA Wave Watch III (WW3) 10 m grid. WW3 is hindcast data developed from global models for waves and winds (NOAA, 2018). Extracted data products include significant wave height, peak wave period, winds, and direction. The waves timeseries is presented in the top panel of Figure 58 and wave period follows in the lower panel. Wind speed timeseries is provided in Figure 59 and directional wave and wind plots are provided in Figure 60. Hurricane Irma can be observed in the timeseries for wave height and winds in early September. 2017 was an energetic year but compared well with 2016. Descriptive statistics of WW3 input data for this simulation year and previous years are presented in

Table 13.

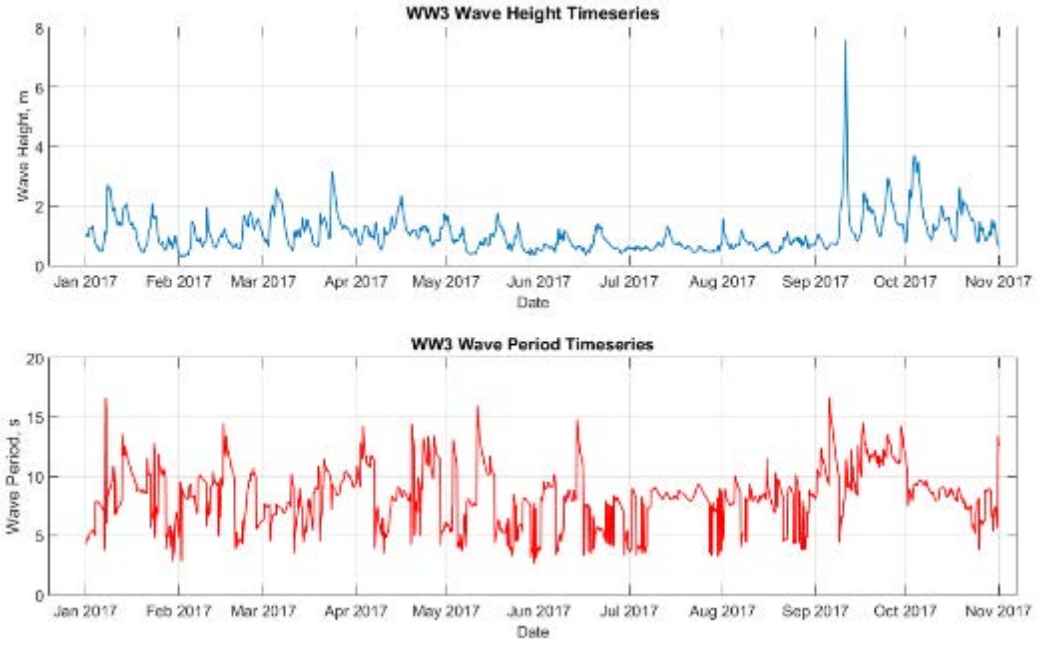


**Figure 58. WW3 Wave Height (a, top) and Period (b, bottom) Timeseries.**

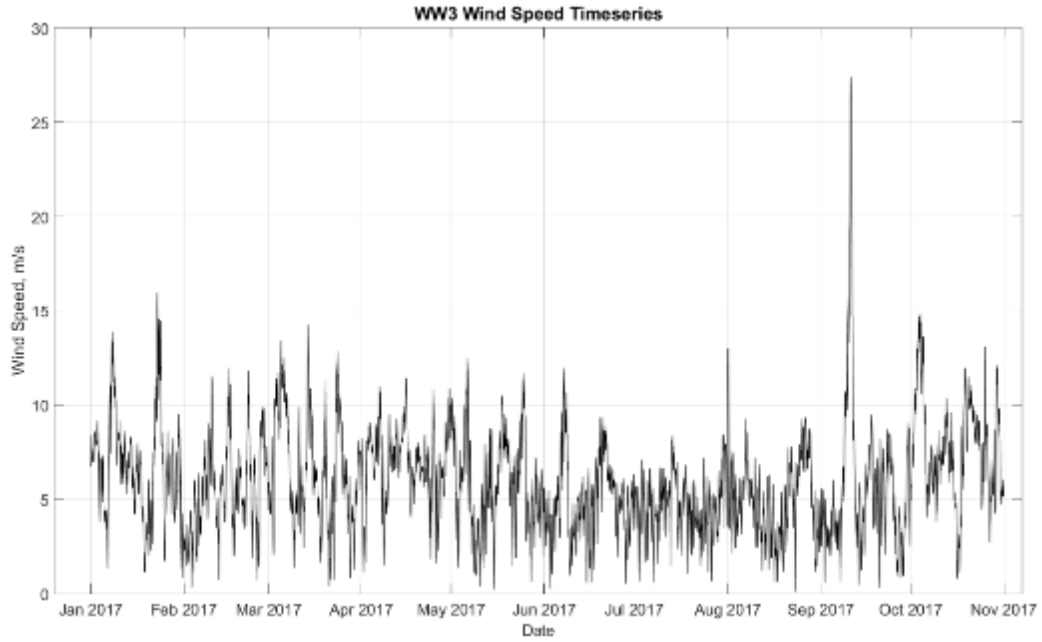


**Figure 59. WW3 Wind Speed Timeseries.**

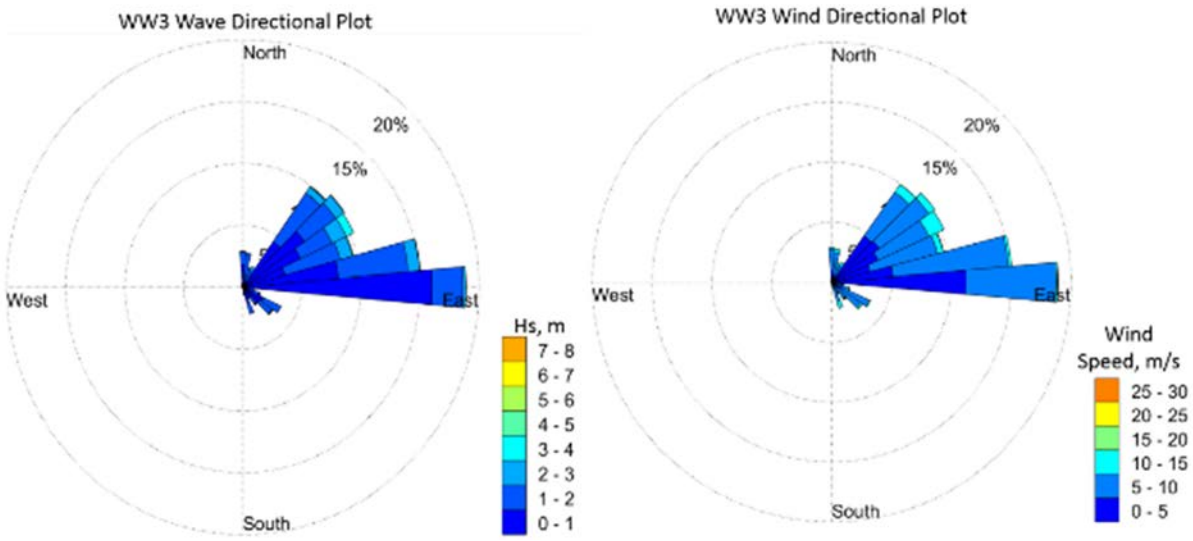


**Figure 60. WW3 Wave Directional Plot (a, left) and Wind Directional Plot (b, right).**

**Table 13. Wave Watch 3 Descriptive Statistics during Simulation Period.**

| Year | Max Hs (m) | Avg. Hs (m) | Max Tp (s) | Avg. Tp (s) | Max. Wind Speed (m/s) | Avg. Wind Speed (m/s) | Time Period |
|---|---|---|---|---|---|---|---|
| 2017 | 7.58 | 1.06 | 16.69 | 8.25 | 27.41 | 5.93 | 1/1/2017 – 11/1/2017 |
| 2016 | 7.93 | 1.14 | 15.68 | 8.34 | 32.05 | 5.89 | 8/1/2016 – 12/31/2016 |

*Local Refined Model Input Parameters*

Grid Configurations and Wave Input

Calculated wave information generated from the regional model run is used to drive the local, refined model set up. Data is extracted from the regional grid at the location corresponding to the offshore boundary condition of the local grid. Figure 61 depicts the spatial relationship between the regional and local grids.

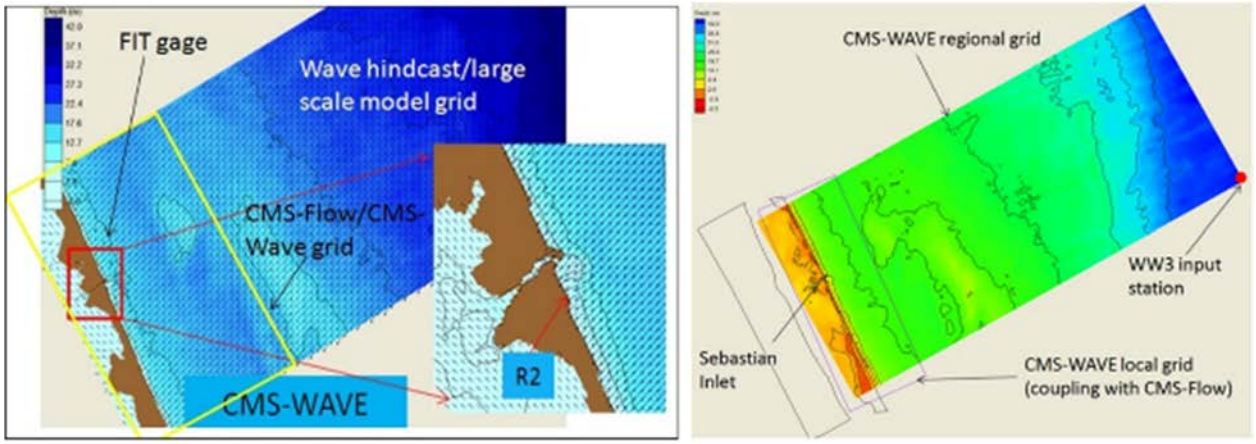


**Figure 61. Regional Grid and Local Grid Configuration.**

The local grid uses the telescoping grid approach and spans between 160x160 m grid cells to 5x5 m grid cells. The alongshore spatial coverage is nearly 18 km while the cross-shore distance is 105 km to a depth of 14 m at the offshore boundary.

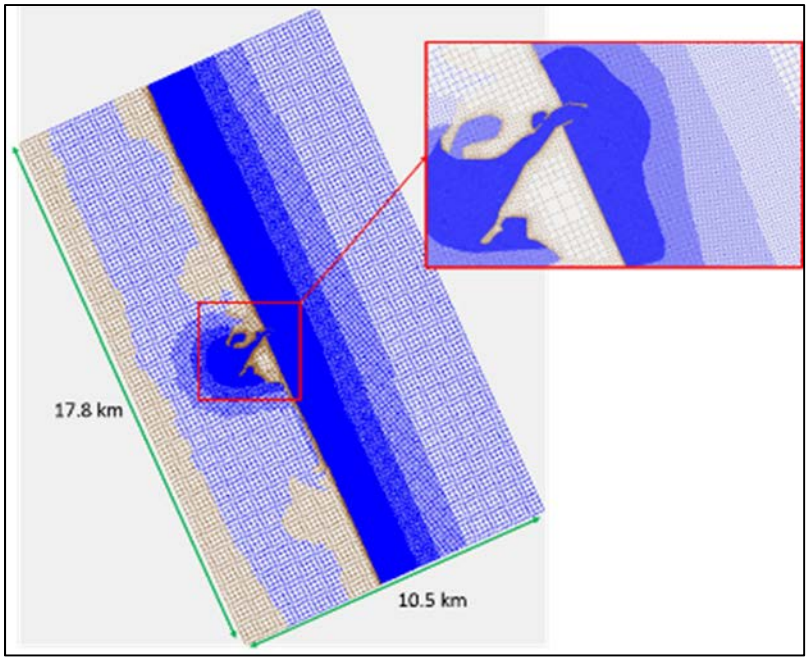


**Figure 62. Local Grid Refinement Telescoping.**

The telescoping flow grid contains ~160,000 of ocean cells and ~6,000 of land (non-computational cells) The nested wave grid for the local model configuration uses a rectilinear grid configuration using refine points to provide additional model resolution near the inlet and nearshore areas. The wave model includes “rubble mound” cells at the North Jetty, South Jetty and along the banks of the inlet throat to represent the presence of armor stone in these areas. The rubble mound structure selection assumes a low permeable structure

One of the research goals of this work is to investigate alternatives for representing the North Jetty within the model. Previously, the entire length of the jetty has been represented in the Flow model grid as non-computational cells with added roughness around the to represent the presence of the rocks. A model alternative was constructed to represent a more open configuration. The impermeable section closest to shore is represented as non-computational cells while the offshore portions of the north jetty are represented as 5x5 m ocean cells. This allows the cells to alternatively wet and dry with rise and fall of the tide and waves. Roughness factors are included over the appropriate portions of the jetty and expanded to include the new cells. This change added ~4,000 of cells which is a minimal addition compared to the previous north jetty configuration with active ocean cells at ~160,000 cells. These additional cells should not constitute a substantial increase in run time but add model stability since wetting and drying

can add instability in a numerical model. Figure 63 presents a comparison of closed jetty and open jetty flow grid configurations plotted with the 2017 aerial imagery. A more in-depth discussion of the jetty configuration is presented in Model Skill and Results.


**Figure 63. Solid (a, left) and Open Jetty (b, right) Grid Configuration (Aerial Imagery: Sebastian Inlet District, 2017).**

The closed jetty configuration was used to impose a post dredge bathymetry condition since the grid has been used previously with good, stable model performance. This model configuration was run with the 2017 model year forcing to observe channel and sand trap infilling immediately post-dredge. Results of this analysis is provided in the model results section of this report.

Wind Field

Due to storms and equipment outages, the local wind field is a combination between the Sebastian Inlet North Jetty weather station, Trident Station (NOAA Trident Pier, Port Canaveral, FL: 8721604) and Vero Beach Municipal Airport (VBO).

Water Surface Elevation

Water surface elevation is observed at the North Jetty Weather Station and is used as the offshore boundary condition.

*Model Skill and Results*

This section presents the model skill results as compared to the available field data. At the time of this report, the field gauge has not been recovered. Therefore, the comparison between calculated and measured is not available for the entire simulation time period. But it is sufficiently long to evaluate model performance over a variety of conditions.

**Table 14. Field Observations and Simulation Time Period.**

| | Start | End | Days |
|---|---|---|---|
| **Field Observation (North Jetty ADCP)** | 5/9/2017 | 9/4/2017 | 118 |
| **Simulation Period** | 5/1/2017 | 11/1/2017 | 184 |

| Parameter | RMSE (m) | NRMSE | MAE (m) | NMAE | Correlation Coefficient ($R^2$) | Bias |
|---|---|---|---|---|---|---|
| **WSEL** | 0.102 | 5.52% | 0.10 | 5.52% | 0.95 | 0.01 |
| **Wave Height (m)** | 0.39 | 27.84% | 0.40 | 27.84% | 0.35 | -0.37 |

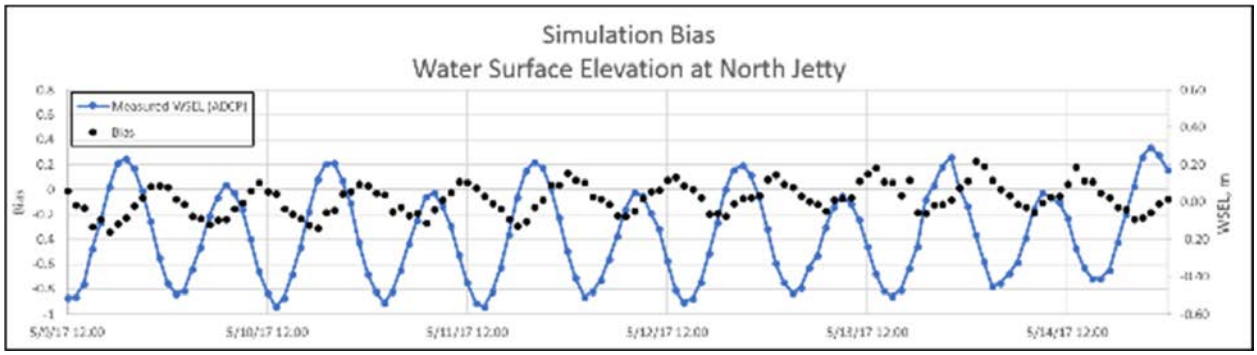


**Figure 64. Simulation Bias: Water Surface Elevation.**

Figure 65 compares the simulation bias to the measured wave heights from the ADCP located at the North Jetty to examine the model's ability to reproduce wave height with variations in forcing. Throughout the simulation, the model is underpredicting wave heights as indicated by a negative value for bias. This bias increases with peaks and troughs. Negative bias

occurs during times of higher wave heights while lower wave heights are indicating positive bias.

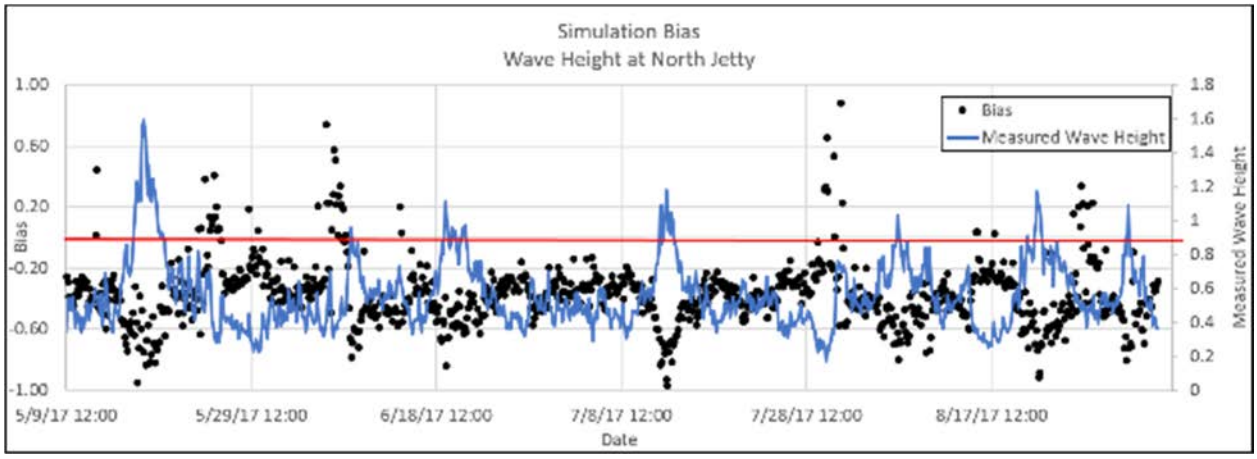


**Figure 65. Simulation Bias: Wave Height**

Channel Infilling

The Inlet District is interested in calculating the rate of infilling of the sand trap immediately post-dredge and examine the changes in current patterns as the trap begins to fill. These rates and morphology will be compared to a simulation run using the most recent bottom topography condition. The 2017 bottom topography is roughly 4 years into the dredging cycle and represents the latter half of the dredging cycle. The most recent sand trap dredging event took place in the Spring of 2014. Using 2014 merged bathymetry/topography data, the model was run with the present (2017) forcing conditions. The expectation is the immediate post dredge condition should yield higher rates of sedimentation and rates should slow in the 2017 bottom topography condition as the sand trap continues to fill. Additionally, the volumes in the existing condition should be larger than the 2014 post dredge condition. Morphology change will also be compared between the two runs to examine if patterns change through time and as the sand trap increases in volume. It should be noted that in order to represent immediately post dredge, the Spring 2014 dataset was used and some seasonal variability is to be expected as compared to the Winter 2017 dataset.

Channel infilling calculations were performed using the computed depth timeseries from CMS. A series of transects were constructed along the channel and a second series cross channel

to quantify the channel shoaling at different locations in the sand trap. These transects were generated after initial qualitative examination of the calculated morphology change. Calculated morphology change at the sand trap is shown in Figure 66. Preferential deposition of material on the eastern (Inlet) side of the observation area can be seen as well as on the northern portion of the sand trap area. Less material is observed to deposit southward. This non-uniform deposition behavior gives rise to the need to evaluate the channel infilling at multiple location both along channel and cross channel. Cross sections are presented in Figure 67 with a total of 6 transects shown; three along channel and three cross channels. This design allows for observation of channel infilling across different portions of the sand trap.

**Figure 66. Calculated Morphology Change with Sand Trap Infilling Cross Sections (Post 2014 Dredge).**

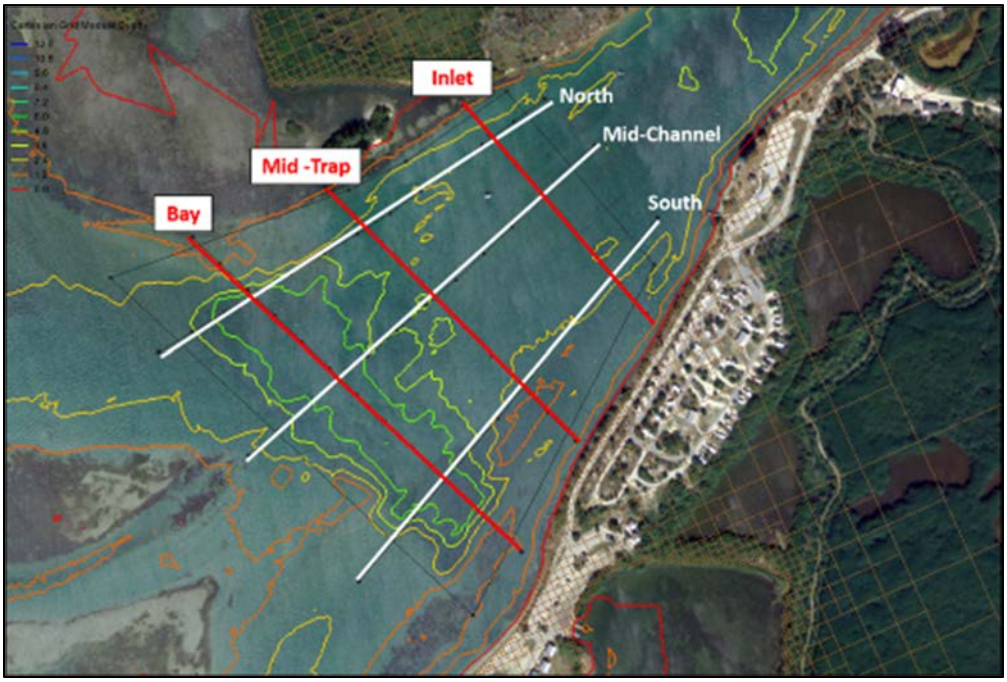


**Figure 67. Sand Trap Infilling Cross Sections with Bottom Topography Contours (Aerial Image: LABINS, 2004).**

The following series of plots detail the calculated channel infilling across various portions of the sand trap. Figure 68 and Figure 69 are the cross-channel arcs while Figure 70 and Figure 71 are along channel cross sections. For brevity, the mid channel and mid trap cross sections are presented in the appendices.

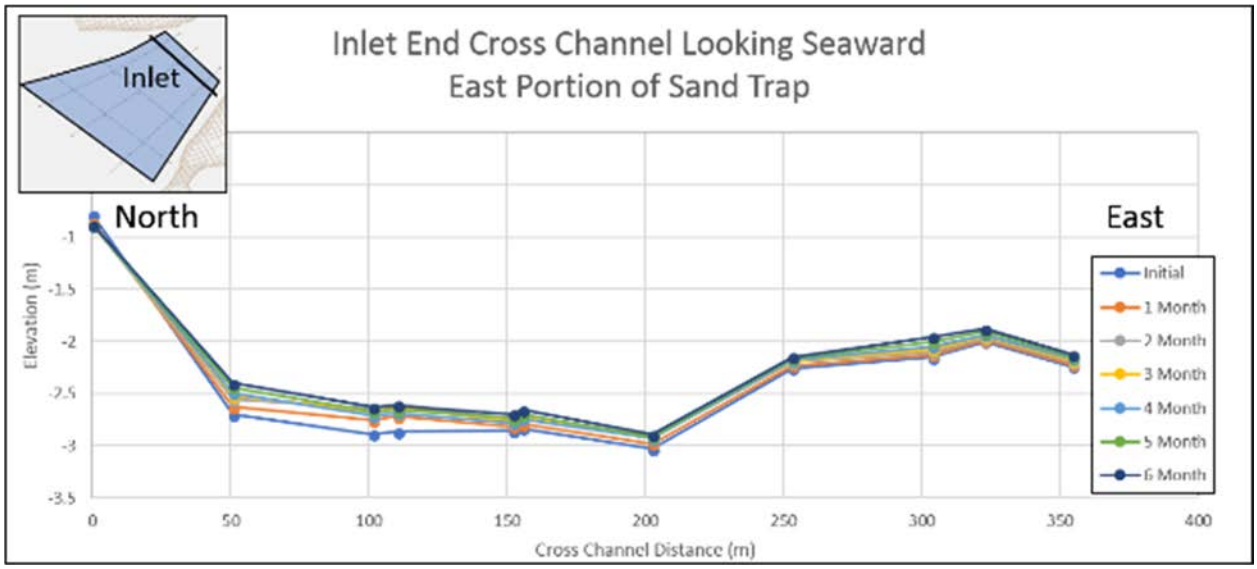


**Figure 68. Channel Infilling: Inlet End Cross Section.**

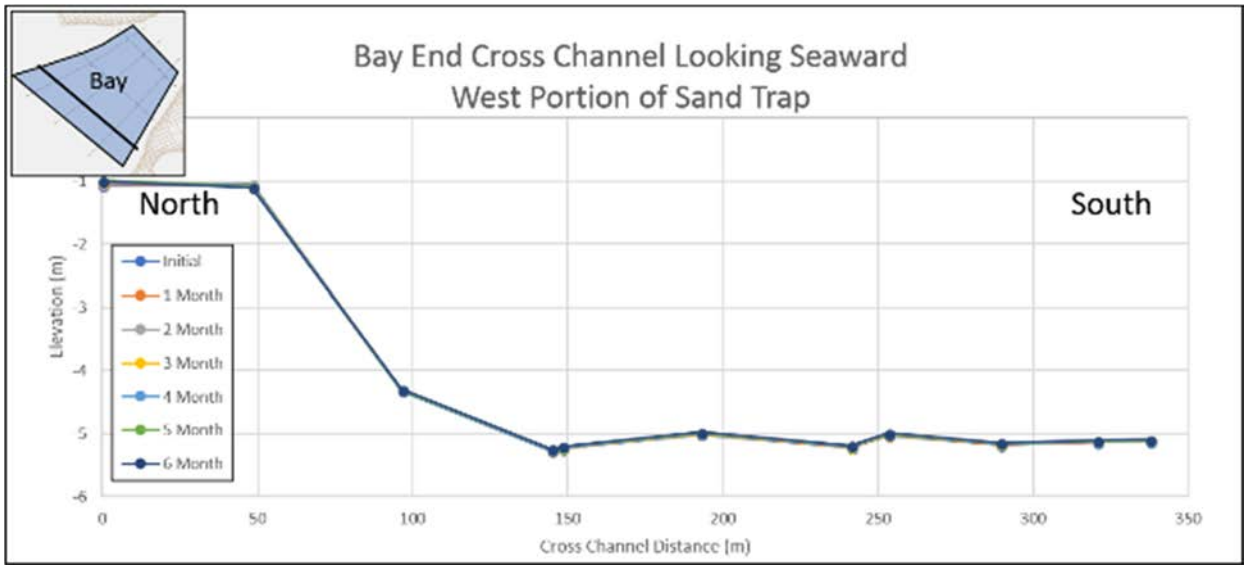


**Figure 69. Channel Infilling: Bay End Cross Section.**

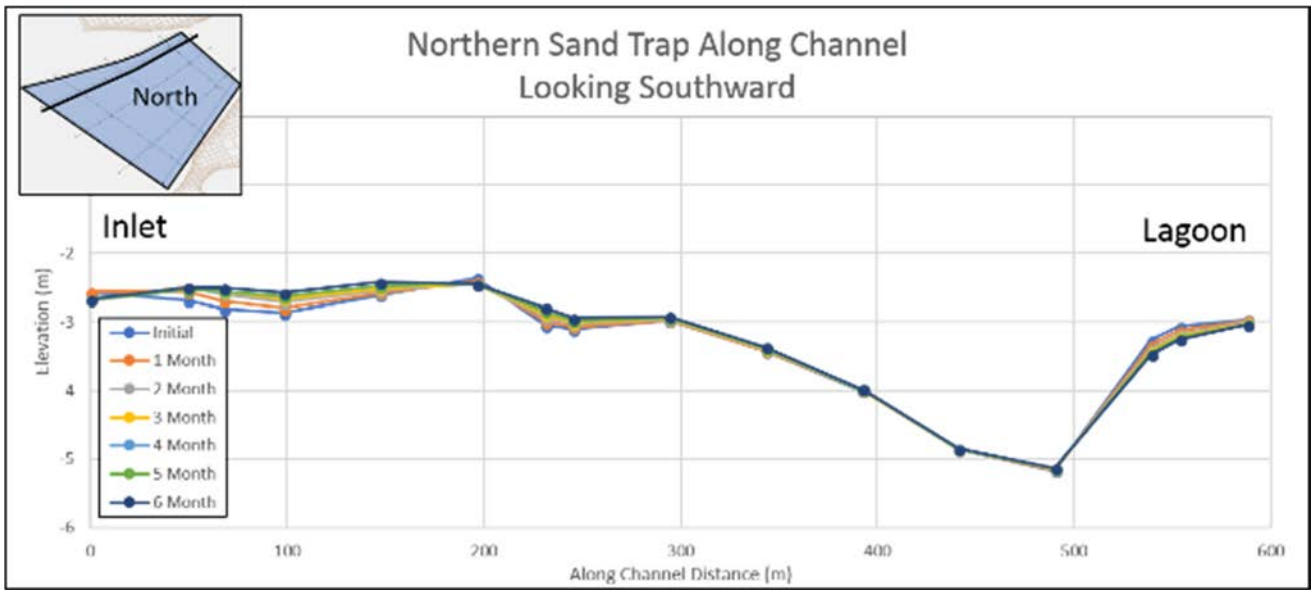


**Figure 70. Channel Infilling: North Sand Trap Along Channel.**

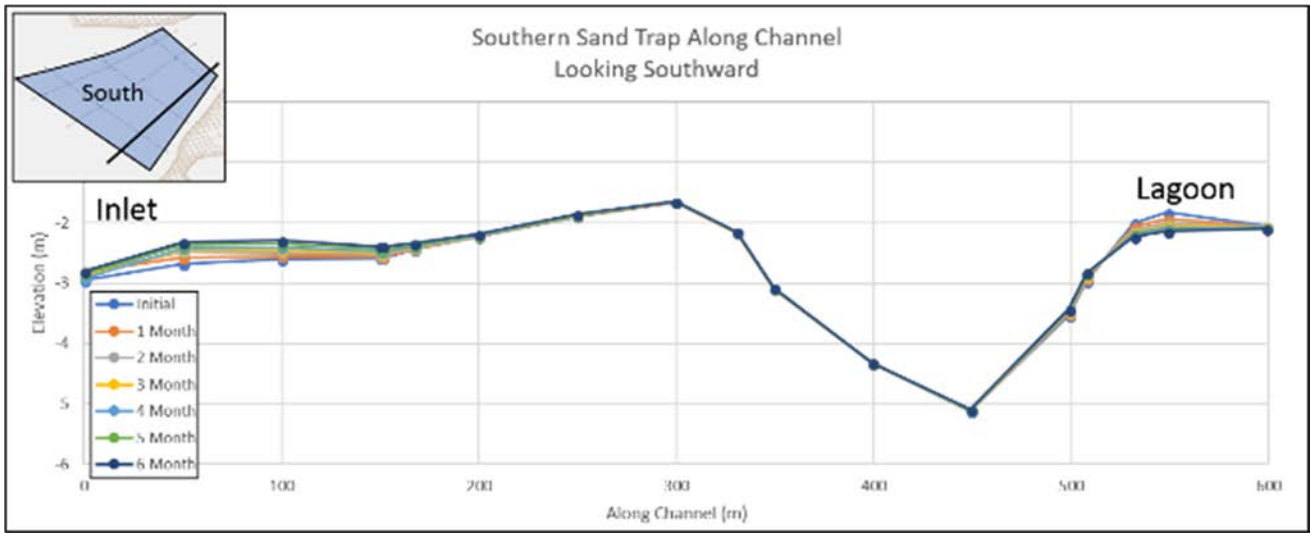


**Figure 71. Channel Infilling: Southern Portion of Sand Trap.**

The cross channel and along channel plots explicitly demonstrate the channel infilling and compliments the morphology change plot in Figure 66. The cross-channel profiles indicate that most of the deposition of sediment occurs on the inlet and mid sand trap sections where very little change is observed in the western portions of the sand trap. Similar behavior is observed in the along channel profiles however the western end of the along channel profiles extend into the flood shoal lobes which do show deposition throughout the simulation period. To illustrate this

behavior further, Figure 72 presents the cross-channel infilling spatially across the sand trap and Figure 73 presents the along channel transects.

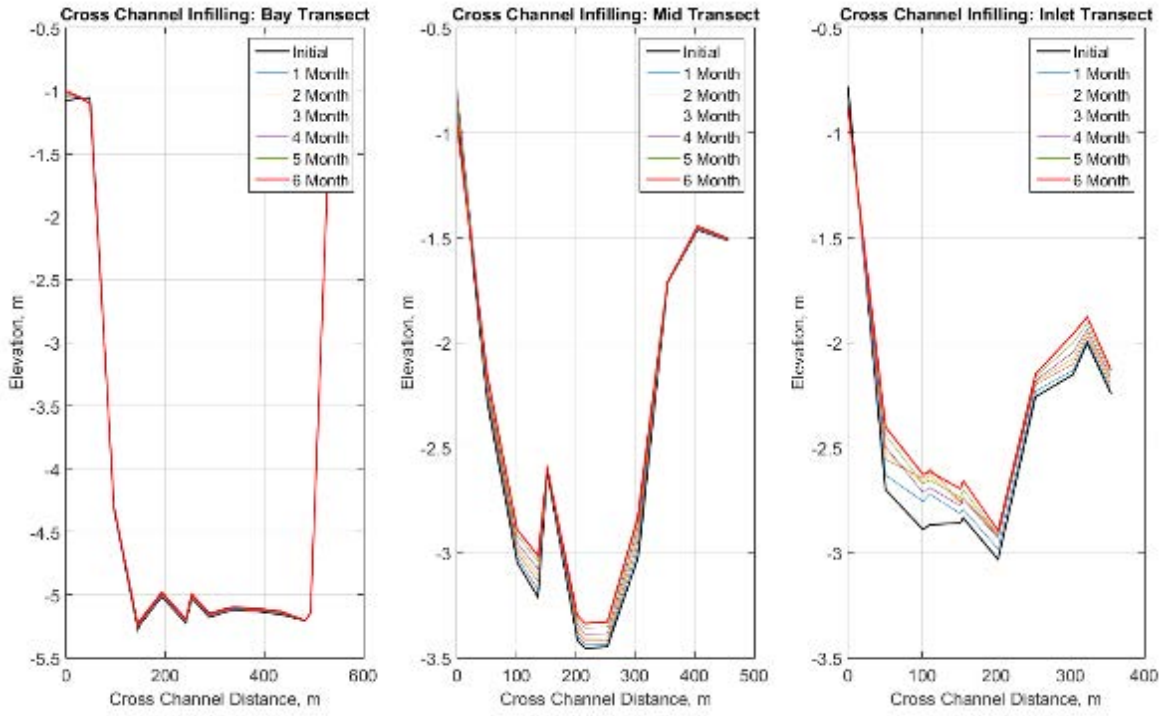


**Figure 72. Cross Channel Infilling Variation across Sand Trap.**

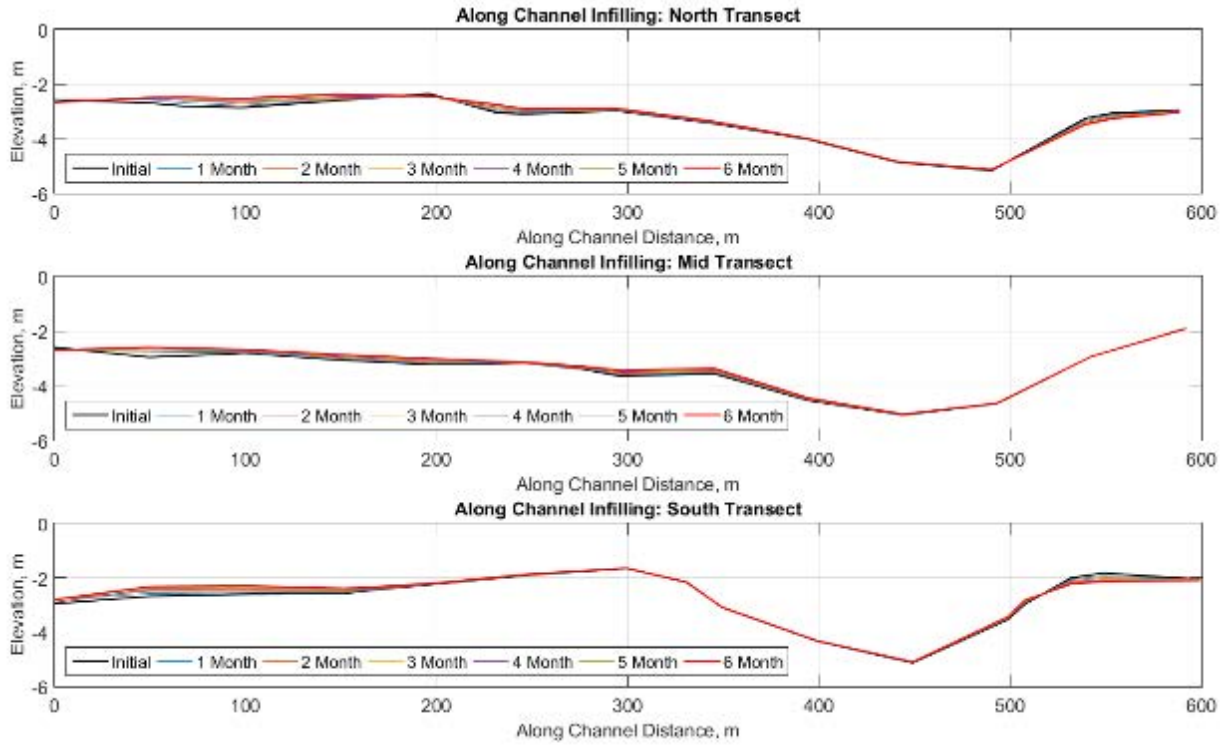


**Figure 73. Along Channel Infilling Variation across Sand Trap.**

A direct comparison of computed channel bottom topography changes to measured cannot be performed. The bottom topography from 2014 representing a post dredge condition was used with the 2017 model forcing conditions. This allowed for a comparison between immediately post dredge to present day bottom topography which is at the end of the proposed dredging cycle.

When the measured topography is compared between the 2014 Post Dredge (June) and Winter 2017, measured infilling is confined to the dredged portions of the sand trap region on the western ends of the sand trap area. At the time of this report, the dredge template is not available digitally therefore, the dredged portions of the area must be inferred by depth contours and morphology change. Selected transects are presented in Figure 74 and Figure 75 demonstrating the sediment deposition occurring primarily in the western (Lagoon) side of the sand trap. Figure 76 presents a comparison between calculated morphology change for the Winter 2017 simulation period compared with measured morphology change between the Winter 2017 bottom topography surface and the Post Dredge June 2014 bottom topography.

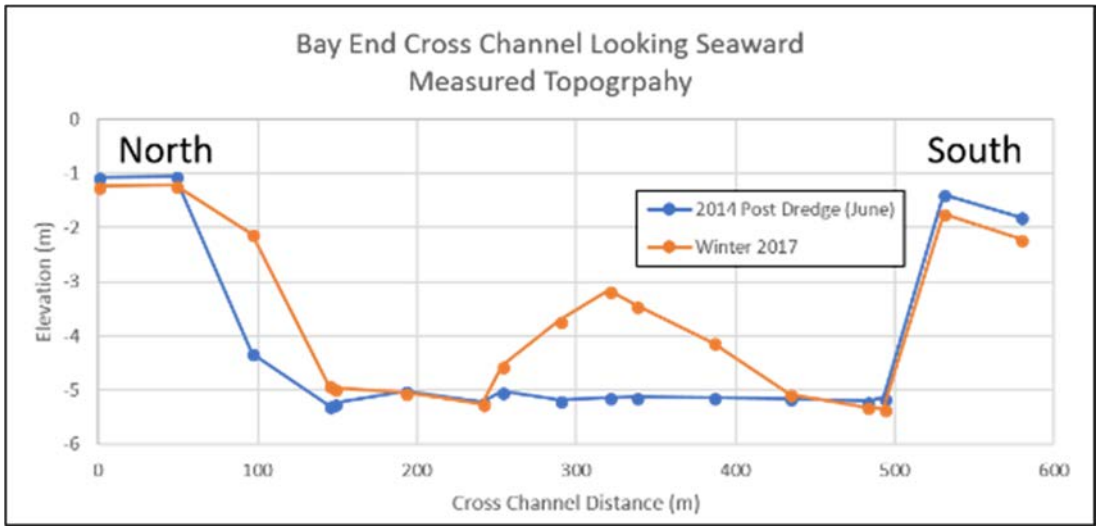


**Figure 74. Measured Topography: Bay End Cross Channel.**

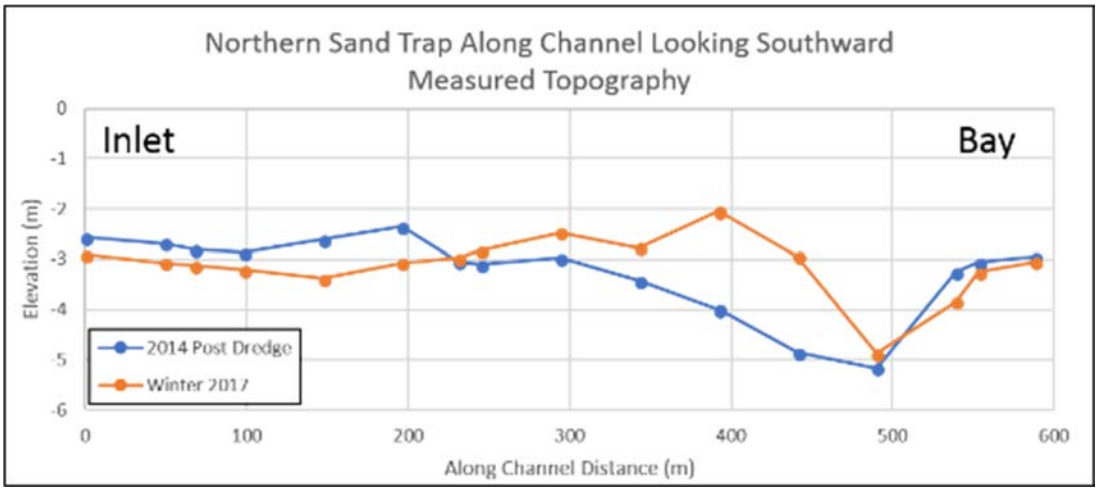


**Figure 75. Measured Topography: North Sand Trap Along Channel.**

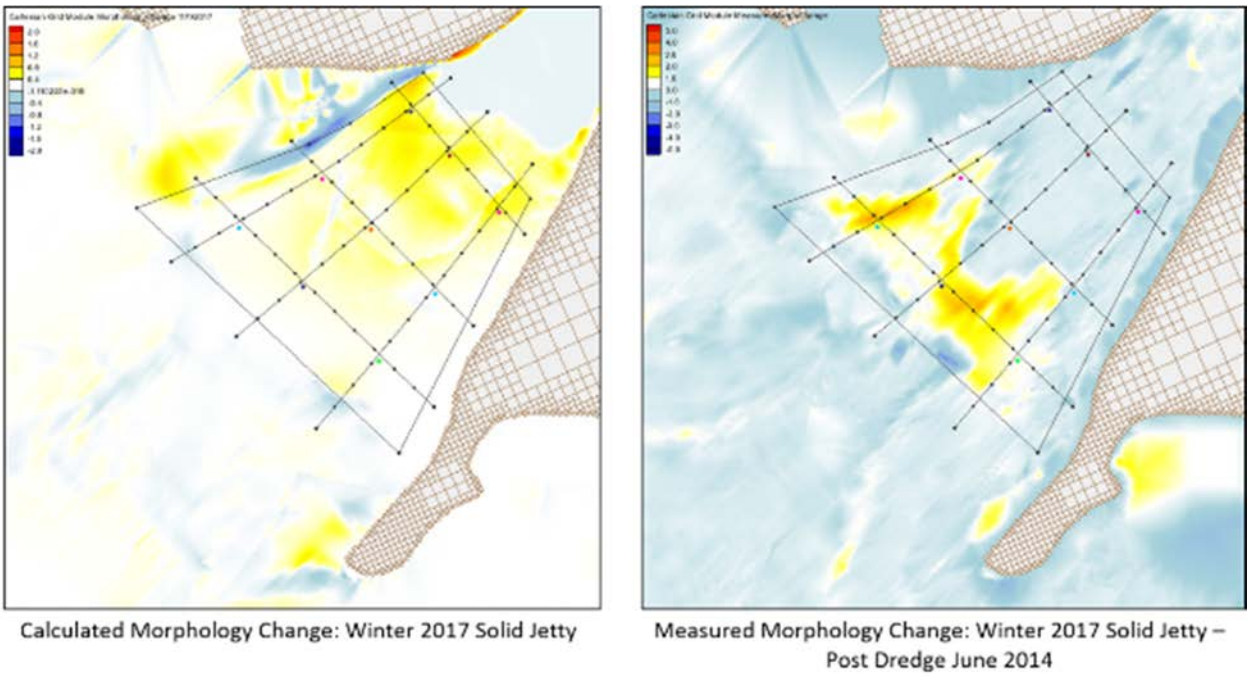


**Figure 76. Comparison between Calculated (left) and Measured (right) Morphology Change over Sand Trap [Winter2017 - Post Dredge 2014].**

The model is predicting the sedimentation occurring at the inlet end of the sand trap area rather than in reality, closer to the flood shoal area and confined to the dredge template. This indicates that the model needs to be further calibrated for flow through the inlet itself. This can be achieved by a more complete representation of the bridge support structure and further experimentation with roughness factors to better represent the hard bottom that characterizes the inlet throat. The morphologic interpretation is that the model is slowing the currents down too quickly upon exiting the hydraulic influence of the confined channel causing the sediment to fall out of suspension too early. Upon investigation into the current magnitudes and direction, the speeds are reasonable for an inlet of this hydraulic and geometric configuration. However, no flow data exists for current speeds through the inlet throat so calibration would need to be driven by the measured morphology change rather than hydrodynamics. Traditionally, model calibration is performed in sequence beginning with water surface elevation, hydrodynamics (wave magnitude and direction, current speed and direction) and finally, sediment transport and/or morphology change. It should also be noted that this comparison spans several years and represent different season conditions which can also contribute to differences in observed

morphology. This comparison is merely intended for a gross representation of preferential sediment deposition within the sand trap.

Computed Channel Infilling Rates

The computed rates of change elucidate variability in sedimentation rates with changes in flow forcing throughout the simulation period. The 2017 model forcing includes Hurricane Irma in the simulation period. This allows for the opportunity to observe sedimentation rates during more quiescent periods (May through August) and more energetic periods (September through October).

As anticipated in any morphological model run, higher rates of sedimentation are observed at the beginning of the run. This is due to the model smoothing out any rapid changes in bottom topography as the model comes to a numeric equilibrium. Colloquially, this can be referred to as “model spin up”. Computed sedimentation rates for each transect node are presented in the following tables. The first month is included for completeness. Values are presented as net change and independent of direction (shoaling or erosion) to observe variability in change throughout the simulation period.

Table 15 and

Table 16 present the monthly depth changes for Inlet End and Mid Trap cross sections. The Bay End cross section results are presented in the Model Appendices for reference since most of the depth changes occur on the eastern portions of the sand trap (Figures77 through Figure 82)Table 17 and

Table 18 are the calculated monthly depth change for the North and Mid along channel transects respectively. Each value represents a node along the transect. Sedimentation across each transect is presented in the following graphs. The direction of observation is indicated in each title with compass or feature indicated on either end of the cross section

**Table 15. Inlet End Sand Trap Calculated Monthly Depth Change.**

| Calculated Monthly Depth Change – Inlet End Cross Channel | | | | | |
|---|---|---|---|---|---|
| **May** | **June** | **July** | **August** | **September** | **October** |
| **1 Month** | **2 Month** | **3 Month** | **4 Month** | **5 Month** | **6 Month** |
| 0.07 | 0.02 | 0.00 | 0.00 | 0.00 | 0.00 |
| 0.07 | 0.08 | 0.04 | 0.02 | 0.06 | 0.04 |
| 0.14 | 0.11 | 0.02 | 0.04 | 0.04 | 0.04 |
| 0.15 | 0.12 | 0.03 | 0.06 | 0.03 | 0.04 |
| 0.04 | 0.06 | 0.01 | 0.01 | 0.04 | 0.04 |
| 0.04 | 0.06 | 0.00 | 0.01 | 0.04 | 0.04 |
| 0.05 | 0.06 | 0.01 | 0.02 | 0.02 | 0.02 |
| 0.03 | 0.03 | 0.01 | 0.01 | 0.02 | 0.01 |
| 0.02 | 0.03 | 0.03 | 0.03 | 0.04 | 0.04 |
| 0.01 | 0.02 | 0.02 | 0.02 | 0.03 | 0.03 |
| 0.02 | 0.02 | 0.02 | 0.02 | 0.02 | 0.02 |

**Table 16. Mid Sand Trap Calculated Monthly Depth Change.**

| Calculated Monthly Depth Change – Mid Trap Cross Channel | | | | | |
|---|---|---|---|---|---|
| **May** | **June** | **July** | **August** | **September** | **October** |
| **1 Month** | **2 Month** | **3 Month** | **4 Month** | **5 Month** | **6 Month** |
| 0.03 | 0.02 | 0.02 | 0.01 | 0.08 | 0.09 |
| 0.02 | 0.02 | 0.02 | 0.02 | 0.03 | 0.02 |
| 0.02 | 0.02 | 0.02 | 0.02 | 0.03 | 0.03 |
| 0.04 | 0.04 | 0.03 | 0.03 | 0.04 | 0.02 |
| 0.01 | 0.01 | 0.00 | 0.00 | 0.00 | 0.00 |
| 0.02 | 0.02 | 0.02 | 0.02 | 0.03 | 0.02 |
| 0.02 | 0.02 | 0.02 | 0.02 | 0.03 | 0.02 |
| 0.01 | 0.02 | 0.02 | 0.02 | 0.03 | 0.03 |
| 0.04 | 0.04 | 0.03 | 0.03 | 0.03 | 0.02 |
| 0.05 | 0.04 | 0.03 | 0.03 | 0.03 | 0.02 |
| 0.00 | 0.00 | 0.00 | 0.00 | 0.00 | 0.00 |
| 0.00 | 0.00 | 0.00 | 0.00 | 0.00 | 0.00 |
| 0.00 | 0.00 | 0.00 | 0.00 | 0.00 | 0.00 |

**Table 17. North Sand Trap Calculated Monthly Depth Change.**

| Calculated Monthly Depth Change - North Along Channel | | | | | |
|---|---|---|---|---|---|
| **May** | **June** | **July** | **August** | **September** | **October** |
| **1 Month** | **2 Month** | **3 Month** | **4 Month** | **5 Month** | **6 Month** |
| 0.01 | 0.10 | 0.10 | 0.10 | 0.10 | 0.10 |
| 0.13 | 0.20 | 0.18 | 0.16 | 0.19 | 0.19 |
| 0.11 | 0.21 | 0.24 | 0.25 | 0.30 | 0.32 |
| 0.07 | 0.15 | 0.20 | 0.23 | 0.29 | 0.34 |
| 0.03 | 0.06 | 0.10 | 0.14 | 0.19 | 0.24 |
| 0.05 | 0.08 | 0.09 | 0.09 | 0.09 | 0.09 |
| 0.06 | 0.11 | 0.16 | 0.21 | 0.26 | 0.30 |
| 0.03 | 0.07 | 0.10 | 0.13 | 0.17 | 0.20 |
| 0.01 | 0.02 | 0.03 | 0.05 | 0.07 | 0.08 |
| 0.01 | 0.02 | 0.03 | 0.04 | 0.06 | 0.08 |
| 0.00 | 0.01 | 0.01 | 0.01 | 0.02 | 0.03 |
| 0.00 | 0.01 | 0.01 | 0.01 | 0.02 | 0.03 |
| 0.00 | 0.01 | 0.01 | 0.01 | 0.02 | 0.02 |
| 0.01 | 0.02 | 0.02 | 0.03 | 0.04 | 0.05 |
| 0.07 | 0.12 | 0.17 | 0.20 | 0.21 | 0.22 |
| 0.06 | 0.11 | 0.14 | 0.17 | 0.19 | 0.21 |
| 0.02 | 0.04 | 0.06 | 0.07 | 0.08 | 0.09 |

**Table 18. Mid Sand Trap Calculated Monthly Depth Change.**

| Calculated Monthly Depth Change - Mid Channel | | | | | |
|---|---|---|---|---|---|
| **May** | **June** | **July** | **August** | **September** | **October** |
| **1 Month** | **2 Month** | **3 Month** | **4 Month** | **5 Month** | **6 Month** |
| 0.05 | 0.10 | 0.10 | 0.10 | 0.10 | 0.10 |
| 0.21 | 0.30 | 0.24 | 0.21 | 0.29 | 0.36 |
| 0.03 | 0.09 | 0.09 | 0.08 | 0.12 | 0.16 |
| 0.02 | 0.07 | 0.07 | 0.06 | 0.10 | 0.14 |
| 0.02 | 0.07 | 0.07 | 0.07 | 0.10 | 0.14 |
| 0.03 | 0.07 | 0.11 | 0.13 | 0.17 | 0.20 |
| 0.03 | 0.07 | 0.11 | 0.14 | 0.19 | 0.22 |
| 0.02 | 0.02 | 0.02 | 0.01 | 0.02 | 0.03 |
| 0.01 | 0.03 | 0.04 | 0.05 | 0.08 | 0.10 |
| 0.04 | 0.08 | 0.11 | 0.15 | 0.19 | 0.22 |
| 0.03 | 0.06 | 0.09 | 0.12 | 0.16 | 0.19 |
| 0.01 | 0.03 | 0.04 | 0.05 | 0.08 | 0.09 |
| 0.00 | 0.01 | 0.01 | 0.02 | 0.03 | 0.03 |
| 0.00 | 0.01 | 0.01 | 0.02 | 0.02 | 0.03 |
| 0.00 | 0.00 | 0.00 | 0.01 | 0.01 | 0.01 |
| 0.00 | 0.00 | 0.00 | 0.00 | 0.00 | 0.00 |
| 0.00 | 0.00 | 0.00 | 0.00 | 0.01 | 0.01 |

Current speeds across the sand trap vary with maximum speeds occurring on the inlet end of the trap with a decrease to approximately half at the lagoon side of the area. Descriptive statistics were developed for each observation node and presented in

Table 19.

**Table 19. Descriptive Statistics of Current Magnitude within Sand Trap.**

| | Bay North | Mid North | Inlet North |
|---|---|---|---|
| **Max** | 0.424 | 0.493 | 0.644 |
| **Min** | 0.424 | 0.002 | 0.004 |
| **Avg** | 0.154 | 0.201 | 0.258 |
| | **Bay Mid** | **Mid** | **Inlet Mid** |
| **Max** | 0.305 | 0.537 | 0.680 |
| **Min** | 0.001 | 0.002 | 0.002 |
| **Avg** | 0.108 | 0.216 | 0.281 |
| | **Bay South** | **Mid South** | **Inlet South** |
| **Max** | 0.206 | 0.389 | 0.592 |
| **Min** | 0.002 | 0.003 | 0.004 |
| **Avg** | 0.081 | 0.153 | 0.237 |

## 9.0 Conclusions and Recommendations

The annual update of the State of Sebastian Inlet includes five major areas of work; 1) an update of the analysis of volume contained in the sand reservoirs of the inlet system, 2) analysis of the sand budget based on the results of the sand volume analysis, 3) analysis of morphologic changes within the inlet system, 4) an update of the shoreline change analysis, and 5) numerical modeling analysis of hurricane impacts sand infilling patterns of the sand trap.

- Similar to the volumetric analysis described in previous state of the inlet reports, most inlet sand reservoirs are in a long-term dynamic equilibrium characterized by occasional large seasonal changes in volume superimposed on longer term trends of a lower order of magnitude.
- Examination of coastal sea level changes and sand volume between 2006 and 2018 revealed two important processes.
  - It can be demonstrated that the Sebastian Inlet sand reservoirs and the beach and shoreface areas both to the north and to the south of the inlet undergo periods of regional sand volume losses and periods of and volume gains.
  - Sand volume gains and losses cover the entire region rather than being inversely linked to gains or losses in adjacent subsections.

- Examples are sand volume gains that peaked in 2010 and again in 2016 were preceded by periods of regional sand volume losses.

- When the sea level record measured at Sebastian Inlet is examined over the 12-year period between 2006 and 2018, it can be demonstrated that periods of increasing cumulative sand volume losses correspond to periods of rising sea level
- Periods of falling sea level correspond to periods of cumulative sand volume gains and lower cumulative sand volume losses.
- The sea level record for late 2017 and the first 5 months of 2018 indicates that another period of rising sea level is beginning. This indicates a potential for an upcoming period of increased loss of sand volume
- The dynamic equilibrium and trends of sand volume changes within the inlet sand reservoirs associated with Sebastian Inlet are also reflected in sediment budget calculations.
- The sand budget for the Sebastian Inlet region is reported at three-time scales, including a longer time scale of 10 years, a time scale of 5 years, and a shorter time scale of 3 years.

- The most useful time scale is considered to be 10 years since it integrates over seasonal sand volume changes that mask longer term trends.
- Over the time period of 2007-2018, the benefits of sand by-passing from the sand trap and beach fill placement projects to the south of the inlet can be shown to directly offset sand volume gains within the inlet.
- The impacts of rising and falling sea level are more apparent in the 5-year and 3 years and budgets analyses presented in this report.
- Similar to the sand volume analysis, the results of shoreline mapping from survey data and aerial imagery vary considerably by time scale.
- Over the 10-year time scale from 2008 to 2017, shoreline changes south of the inlet reflect the position of beach fill placement in 2007, 2011, 2012 and 2014, along with periods of regional sand volume gains and losses
- Over the most recent period of analysis, the influence of sand placement from the sand trap excavation during the spring of 2014, along with the benefits of a recent 2-year period of falling sea level can be seen in sand volume gains reduced sand volume losses between 2013 and 2017 and in the comparison of the 2013 to 2017 shoreline positions.

**Acknowledgments:**

The project team acknowledges the Sebastian Inlet District Commissioners, the District Executive Director Marty Smithson and James Grey for their support.

**10 .0 References**

Brehin, F.G. and G.A. Zarillo. 2010. Morphodynamic Evolution and Wave Modeling of the Entrance Bar Surfing Break "Monster Hole": Sebastian Inlet, FL. 7th International Surfing Reef Symposium 2010, Sydney, Australia.

Buttolph. A.M., Reed, C.W., Kraus, N.C., Ono, N., Larson, M., Camenen, B., Hanson, H., Wamsley, T., and Zundel, A.K. 2006. Two-dimensional depth-averaged circulation model CMS-M2D: Version 3, Report 2, Sediment transport and morphology change. *ERDC/CHL TR-06-09*, U.S. Army Engineer Research and Development Center, Vicksburg, Mississippi.

Camenen, B., and M., Larson. 2007. A Total Load Formula for the Nearshore. Proceedings Coastal Sediments '07 Conference, ASCE Press, Reston, VA, 56-67.

Crowell, M., S.P. Leatherman, and M.K., Buckley. 1993. Erosion Rate Analysis: Long Termversus Short Term Data. Shore and Beach, 61 (2):13-20.

Dean, R. Dalrymple, R. (2003) Coastal Processes with Engineering Applications, Cambridge University Press. Cambridge, UK.

Dolan, R., M.S. Fenster, and S.J. Holme. 1991. Temporal analysis of shoreline recession and accretion. Journal of Coastal Research, 7(3):723-744.

USACE. 1994. Engineering Manual for Hydrographic Surveys EM 1110-2-1003 Change 1 (http://www.asace.army.mil) Accessed: October 2010.

Hoeke, R. K. G.A. Zarillo, and M. Synder. 2001. A GIS Based Tool for Extracting ShorelinePositions from Aerial Imagery (BeachTools).*ERDC/CHL CHETN-IV-37*, U.S. Army Engineer Research and Development Center, Vicksburg, MS.

Land Boundary Information System (LABINS) http://www.labins.org/index.cfm

Lin, L., H. Mase, F. Yamada, and Z. Demirbilek. 2006. Wave-Action Balance EquationDiffraction (WABED) model: Tests of wave diffraction and reflection at inlets. ERDC/CHL CHETN-III-73. Vicksburg, MS: U.S. Army Engineer Research and Development Center.

Lin, L., Demirbilik, Z., Mase, H., Zheng, J., Yamada, F. (2008) "CMS-Wave: A Nearshore Spectral Wave Process Model for Coastal Inlets and Navigation Projects" TR-08-13,

Engineer Research and Development Center, Coastal and Hydraulics Laboratory, Vicksburg, MS.

Morton, R. A. 2002. Factors controlling storm impacts on coastal barriers and beaches – Apreliminary basis for real-time forecasting: Journal of Coastal Research (18):486-501.

National Oceanic and Atmospheric Agency (2018) National Weather Service, Environmental Modeling Center, NOAA WaveWatch III. http://polar.ncep.noaa.gov/waves/index2.shtml

NOAA National Geodetic Survey (NGS). Coastal Relief Model Offshore Data Sets. (http://www.ngs.noaa.gov) Accessed: October 2010.

Rosati, J.D., Carlson, B. D., Davis, J. E., and T. D., Smith. 2001. "The Corps of Engineers'National Regional Sediment Management Demonstration Program," ERDC/CHL CHETN-XIV-1, U.S. Army Engineer Research and Development Center, Vicksburg, MS.

Rosati, J.D. and N.C., Kraus. 1999. "Formulation of sediment budgets at inlets," CoastalEngineering Technical Note IV-15, U.S. Army Engineer Waterways Experiment Station,Vicksburg, MS.

Rosati, J.D. and N. C. Kraus. 2001. Sediment Budget Analysis System (SBAS). ERDC/CHL. CHETN- XIV-3. U.S. Army Engineering Research and Development Center. Vicksburg, MS.

Ruggiero, P., D, Reid, Kaminsky, G. and J. Allan. 2003. Assessing Shoreline Change TrendsAlong U.S. Pacific Northwest Beaches. July 22 to 26, 2007, Proceedings of Coastal Zone 07, Portland, Oregon.

Sanchez, A., Lin, L, Demirbilek, Z., Beck, T., Brown, M., Li, H., Rosati, J., Wu, W., Reed, C., Zundel, A., 2012. *in review*, Coastal Modeling System User Manual, ERDC/CHL.

Sanchez, A., Lin, L., Demirbilek, Z., Beck, T. M., Brown, M., Li, H.. Zundel, A. (2013). *Coastal Modeling System User Manual*. Retrieved from Vicksburg, MS.:

Sanchez, A., Wu, W., Li, H.., Brown, M., Reed, C., Rosati, J., Demirbilek, Z. 2014 Coastal Modeling System: Mathematical Formulations and Numerical Methods, ERDC/CHL TR-14-Vicksburg, MS.

Tolman, 2010: WAVEWATCH III (R) development best practices Ver. 0.1. NOAA / NWS / NCEP / MMAB Technical Note 286, 19 pp

U.S Army Corps of Engineers. 2015. SBEACH – Storm-induced BEAch CHange Model. Available Online: [http://chl.erdc.usace.army.mil/chl.aspx?p=s&a=Software;31]. Last Accessed: March 3rd, 2015.

U.S. Army Corps of Engineers. 2002. Coastal Engineering Manual. Engineer Manual 1110-2-1100, U.S. Army Corps of Engineers, Washington, D.C. (in 6 volumes).

Wang, P., Kraus, N.C., David, R.A. 1998. Total Longshore Sediment Transport Rate in the Surf Zone: Field Measurements and Empirical Predictions. *Journal of Coastal Research*, 14(1), 269 – 282. Royal Palm Beach (Florida), ISSN0749 – 0208.

Wu, W., A. Sanchez, and M. Zhang. 2010. An Implicit 2-D Depth-Averaged Finite-Volume Model of Flow and Sediment Transport in Coastal Waters. June 30 – July 5, 2010, 32nd International Conference on Coastal Engineering (ICCE 2010) Shanghai, China.

Zarillo, G.A. and The Florida Tech Coastal Processes Research Group. 2007. State of Sebastian Inlet Report: An Assessment of Inlet Morphologic Processes, Historical Shoreline Changes, and Regional Sediment Budget, *Technical Report 2007-1*, Sebastian Inlet Tax District, FL.

Zarillo, G.A., Brehin, F.G., and TheFlorida Tech Coastal Processes Research Group. 2009. State of the Inlet Report: An Assessment of Inlet Morphologic Processes, Historical Shoreline Changes, Local Sediment Budget and Beach Fill Performance. Sebastian Inlet Tax District, FL.

Zarillo, G.A., Brehin, F.G, 2010. State of the Inlet Report: An Assessment of Inlet Morphologic Processes, Historical Shoreline Changes, Local Sediment Budget and Beach Fill Performance. Sebastian Inlet Tax District, FL.

Zarillo, G.A. and Bishop, J. 2008. Geophysical Survey of Potential Sand Resources Sebastian Inlet, Florida. Prepared for the Sebastian Inlet Tax District, 29p.

Zarillo, G.A. and Brehin, F.G. 2008. Wave Hind Cast Project Report. Submitted to the Sebastian Inlet Tax District, 18p.

Zarillo, G. A., et. al. "A New Method for Effective Beach Fill Design," *Coastal Zone '85*, 1985.

## 11.0 Model Appendices

Individual Channel Infilling Transects

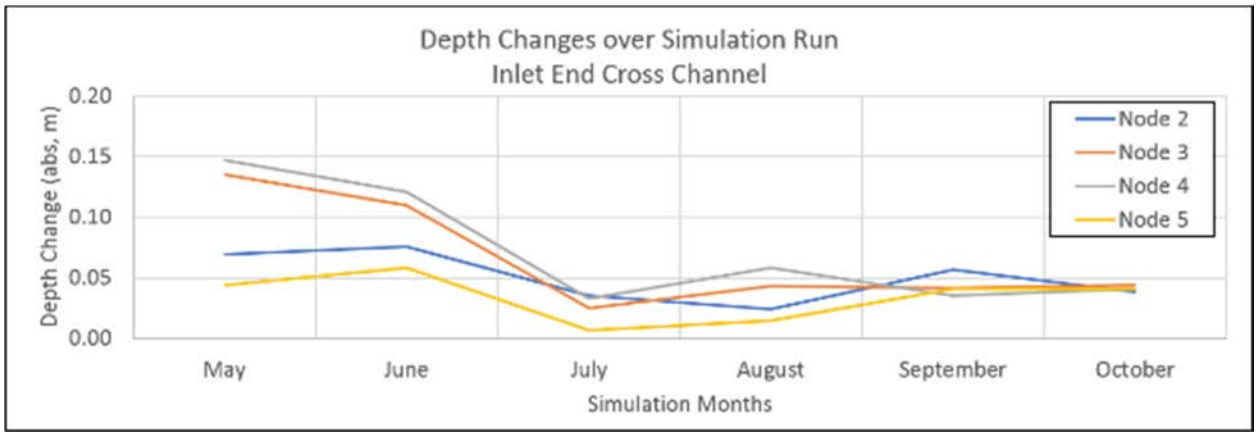


**Figure 77. Depth Changes through Simulation Run: Inlet End Cross Channel.**

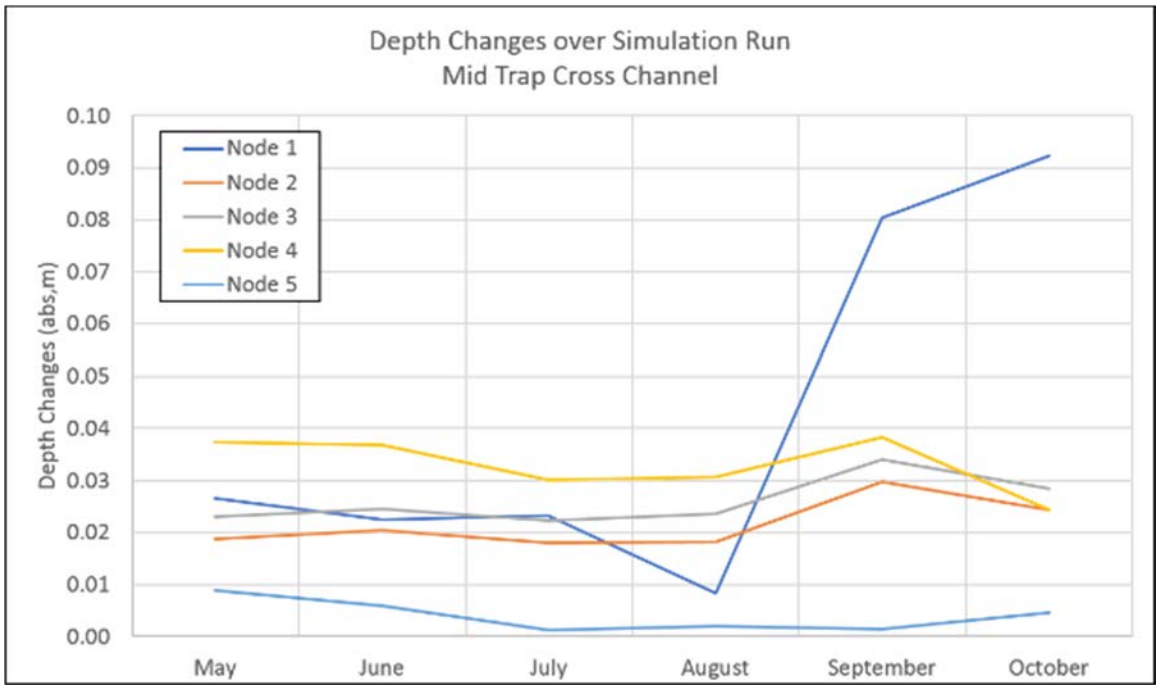


**Figure 78. Depth Changes through Simulation Run: Mid Trap Cross Channel.**

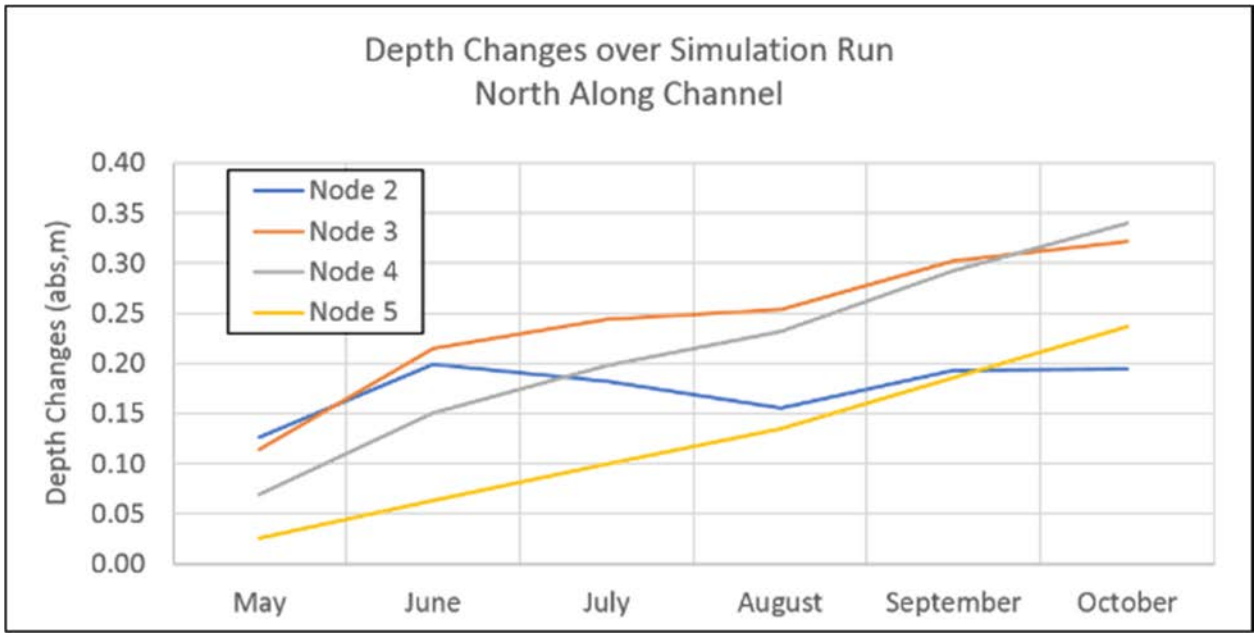


**Figure 79. Depth Changes through Simulation Run: North Along Channel.**

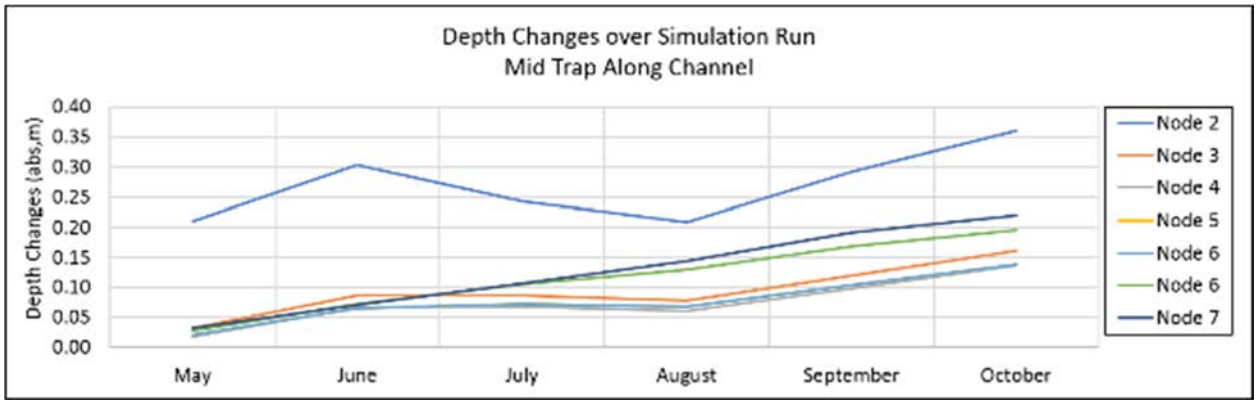


**Figure 80. Depth Changes through Simulation Run: Mid Trap Along Channel. Computed Current Field at Sand Trap.**

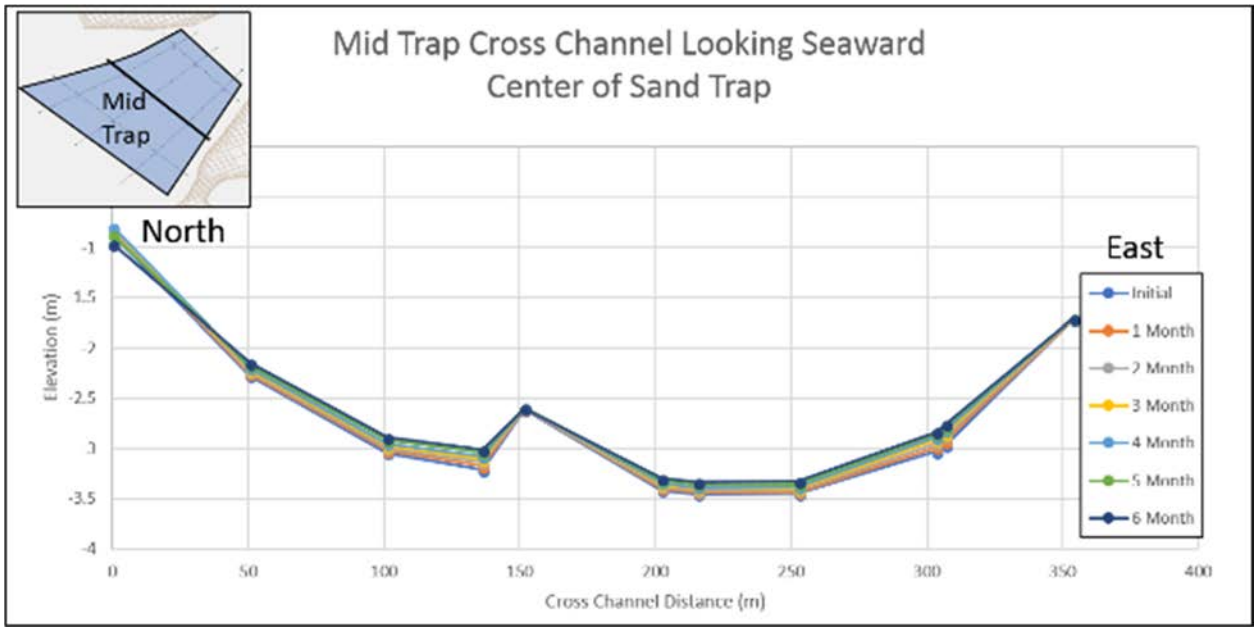


**Figure 81. Channel Infilling: Mid Cross Section.**

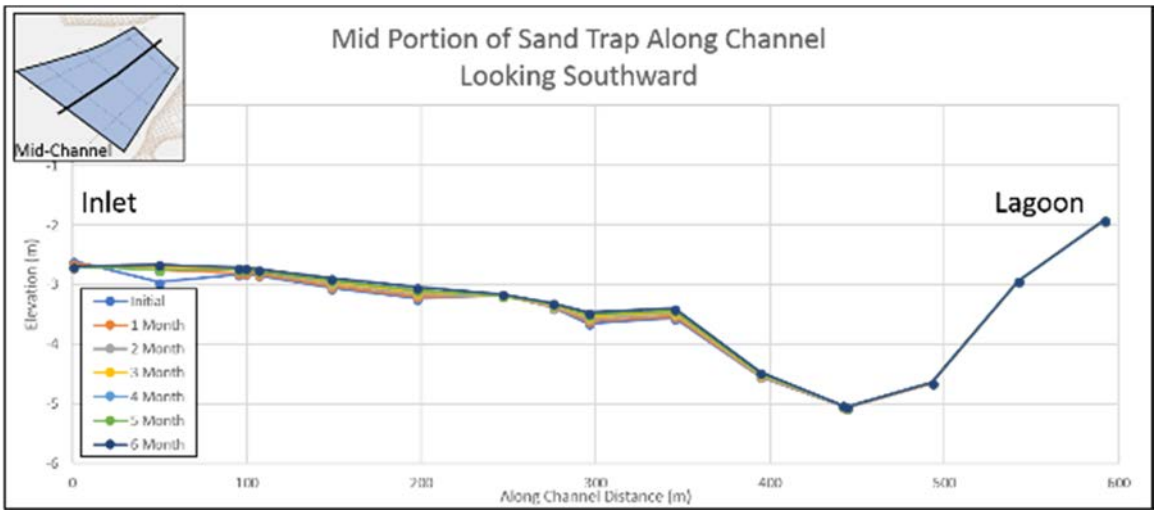


**Figure 82. Channel Infilling: Mid Portion of Sand Trap Along Channel.**

Calculated Monthly Elevation Change

**Table 20. Bay End Calculated Monthly Depth Change**

| Calculated Monthly Depth Change – Bay End Cross Channel | | | | | |
|---|---|---|---|---|---|
| **May** | **June** | **July** | **August** | **September** | **October** |
| **1 Month** | **2 Month** | **3 Month** | **4 Month** | **5 Month** | **6 Month** |
| 0.03 | 0.02 | 0.01 | 0.01 | 0.00 | 0.00 |
| 0.01 | 0.01 | 0.00 | 0.00 | 0.01 | 0.01 |
| 0.00 | 0.00 | 0.00 | 0.00 | 0.01 | 0.00 |
| 0.01 | 0.01 | 0.00 | 0.00 | 0.01 | 0.01 |
| 0.01 | 0.01 | 0.00 | 0.00 | 0.01 | 0.01 |
| 0.01 | 0.01 | 0.00 | 0.00 | 0.01 | 0.01 |
| 0.00 | 0.01 | 0.00 | 0.00 | 0.01 | 0.01 |
| 0.00 | 0.01 | 0.00 | 0.00 | 0.01 | 0.01 |
| 0.00 | 0.00 | 0.00 | 0.00 | 0.01 | 0.01 |
| 0.00 | 0.00 | 0.00 | 0.00 | 0.01 | 0.01 |
| 0.00 | 0.00 | 0.00 | 0.00 | 0.01 | 0.01 |